

**WestminsterResearch**

<http://www.westminster.ac.uk/westminsterresearch>

**Deiminated Proteins in Extracellular Vesicles and Serum of Llama  
(Lama glama) - Novel Insights into Camelid Immunity  
Criscitiello, M.F., Kraev, I. and Lange, S.**

NOTICE: this is the authors' version of a work that was accepted for publication in Molecular Immunology. Changes resulting from the publishing process, such as peer review, editing, corrections, structural formatting, and other quality control mechanisms may not be reflected in this document. Changes may have been made to this work since it was submitted for publication. A definitive version was subsequently published in Molecular Immunology, 117, pp. 37-53, 2020.

The final definitive version in Molecular Immunology is available online at:

<https://dx.doi.org/10.1016/j.molimm.2019.10.017>

© 2020. This manuscript version is made available under the CC-BY-NC-ND 4.0 license

<https://creativecommons.org/licenses/by-nc-nd/4.0/>

---

The WestminsterResearch online digital archive at the University of Westminster aims to make the research output of the University available to a wider audience. Copyright and Moral Rights remain with the authors and/or copyright owners.

---

Whilst further distribution of specific materials from within this archive is forbidden, you may freely distribute the URL of WestminsterResearch: (<http://westminsterresearch.wmin.ac.uk/>).

In case of abuse or copyright appearing without permission e-mail [repository@westminster.ac.uk](mailto:repository@westminster.ac.uk)

1                   **Deiminated Proteins in Extracellular Vesicles and Serum of Llama (*Lama glama*)**  
2                   **- Novel Insights into Camelid Immunity**

3  
4  
5                   Michael F. Criscitiello<sup>a,b</sup>, Igor Kraev<sup>c</sup>, Sigrun Lange<sup>d\*</sup>  
6

7  
8                   <sup>a</sup>*Comparative Immunogenetics Laboratory, Department of Veterinary Pathobiology, College of*  
9                   *Veterinary Medicine and Biomedical Sciences, Texas A&M University, College Station, TX 77843, USA.*

10  
11                   <sup>b</sup>*Department of Microbial Pathogenesis and Immunology, College of Medicine, Texas A&M Health*  
12                   *Science Center, Texas A&M University, College Station, TX 77843, USA, mcriscitiello@cvm.tamu.edu.*

13                   <sup>c</sup>*School of Life, Health and Chemical Sciences, The Open University, Walton Hall, MK7 6AA, UK;*  
14                   *igor.kraev@open.ac.uk.*

15  
16                   <sup>d</sup>*Tissue Architecture and Regeneration Research Group, School of Life Sciences, University of*  
17                   *Westminster, London W1W 6UW, UK; email: S.Lange@westminster.ac.uk*

18  
19                   \*Corresponding author: [S.Lange@westminster.ac.uk](mailto:S.Lange@westminster.ac.uk)  
20  
21  
22

23 **Abstract**

24 Peptidylarginine deiminases (PADs) are phylogenetically conserved calcium-dependent enzymes  
25 which post-translationally convert arginine into citrulline in target proteins in an irreversible manner,  
26 causing functional and structural changes in target proteins. Protein deimination causes generation of  
27 neo-epitopes, affects gene regulation and also allows for protein moonlighting. Furthermore, PADs  
28 have been found to be a phylogenetically conserved regulator for extracellular vesicle (EVs) release.  
29 EVs are found in most body fluids and participate in cellular communication via transfer of cargo  
30 proteins and genetic material. In this study, post-translationally deiminated proteins in serum and  
31 serum-EVs are described for the first time in camelids, using the llama (*Lama glama* L. 1758) as a  
32 model animal. We report a poly-dispersed population of llama serum EVs, positive for phylogenetically  
33 conserved EV-specific markers and characterised by TEM. In serum, 103 deiminated proteins were  
34 overall identified, including key immune and metabolic mediators including complement components,  
35 immunoglobulin-based nanobodies, adiponectin and heat shock proteins. In serum, 60 deiminated  
36 proteins were identified that were not in EVs, and 25 deiminated proteins were found to be unique to  
37 EVs, with 43 shared deiminated protein hits between both serum and EVs. Deiminated histone H3, a  
38 marker of neutrophil extracellular trap formation, was also detected in llama serum. PAD homologues  
39 were identified in llama serum by Western blotting, via cross reaction with human PAD antibodies,  
40 and detected at an expected 70 kDa size. This is the first report of deiminated proteins in serum and  
41 EVs of a camelid species, highlighting a hitherto unrecognized post-translational modification in key  
42 immune and metabolic proteins in camelids, which may be translatable to and inform a range of  
43 human metabolic and inflammatory pathologies.

44

45 **Key words:** Peptidylarginine deiminases (PADs); protein deimination; llama (*Lama glama*);  
46 extracellular vesicles (EVs); innate immunity; adaptive immunity; metabolism, complement;  
47 nanobodies; immunoglobulin; adiponectin; histone.

48

49 **Highlights**

- 50
- Deiminated proteins are identified for the first time in a camelid species
  - Extracellular vesicles (EVs) are characterised in llama serum based on nanoparticle tracking analysis, protein-specific EV markers and transmission electron microscopy
  - Key immune, metabolic and nuclear proteins are deiminated in llama serum and EVs
  - Comparative studies on deimination may inform inflammatory and metabolic diseases
- 51  
52  
53  
54

55

56

## 57 **Introduction**

58 Lamoids, or llamas, belong to a family of camelids which are economically important livestock and  
59 have developed complex features and immunological traits related to their habitat (Wu et al., 2014;  
60 Saadeldin et al., 2018a). The llama (*Lama glama*), Bactrian camel (*Camelus bactrianus*), dromedary  
61 (*Camelus dromedarius*) and alpaca (*Vicugna pacos*) differ in their habitat. The Bactrian camel and  
62 dromedary are adapted to arid-desert-adapted environments, alpacas to plateaus, and the llama to  
63 higher altitudes. Llamas are historically found in the Andean highlands, specifically the Altiplano of  
64 southeast Perú and western Bolivia, as well as in Chile and Argentina, which has the third highest  
65 population of llamas (Wu et al., 2014). The domesticated llama is closely related to two extant wild  
66 South American camelids, the vicuña (*Vicugna vicugna*) and guanaco (*Lama guanicoe*). Previous  
67 genomic studies have revealed a range of specific adaptations in camelids relating to fat and water  
68 metabolism, osmoregulation, blood glucose level regulation, stress responses to heat, aridity, as well  
69 as to intense ultraviolet radiation and dust (Wu et al., 2014). Furthermore, a particularly important  
70 feature in camelid immunity is the production of small, homodimeric heavy chain-only, antibodies  
71 (HCABs) which are of great value for the biomedical industry (Henry et al., 2019).

72 Peptidylarginine deiminases (PADs) are phylogenetically conserved calcium-dependent enzymes  
73 which post-translationally convert arginine into citrulline in target proteins in an irreversible manner.  
74 This can cause functional and structural changes in target proteins (Vossenaar, 2003; György et al.,  
75 2006; Wang and Wang, 2013; Bicker and Thompson, 2013). Structures most prone to deimination are  
76 beta-sheets and intrinsically disordered proteins, while the position of the arginine is also important;  
77 arginines sitting next to aspartic acid residues are most prone to citrullination, arginines next to  
78 glutamic acid residues are rarely citrullinated and those flanked by proline are poorly citrullinated  
79 (Nomura 1992; Tarsca et al., 1996; György et al., 2006). Protein deimination can affect gene regulation,  
80 cause generation of neoepitopes (Witalison et al., 2015; Lange et al., 2017) and may also allow for  
81 protein moonlighting, an evolutionary acquired phenomenon facilitating proteins to exhibit several  
82 physiologically relevant functions within one polypeptide chain (Henderson et al., 2014; Jeffrey, 2018;  
83 Magnadottir et al., 2018a). PADs have been identified throughout phylogeny from bacteria to  
84 mammals, with 5 tissue specific PAD isozymes in mammals, 3 in chicken, 1 in bony fish and arginine  
85 deiminase homologues in bacteria (Vossenaar et al., 2003; Rebl et al., 2010; Magnadottir 2018a,  
86 Magnadottir et al., 2019a; Kosgodage et al., 2019). While studies on PADs in relation to human  
87 pathophysiology, including cancer, autoimmune and neurodegenerative diseases (Wang and Wang,  
88 2013; Witalison et al., 2015; Lange et al., 2017; Kosgodage et al., 2017 & 2018) and CNS regeneration  
89 (Lange et al., 2011 and 2014) exist, relatively little phylogenetic research has been carried out on PADs  
90 in relation to normal physiology and evolutionary acquired adaptations of the immune system. Recent

91 comparative studies focussing on roles for PADs in teleost fish have identified post-translational  
92 deimination in key proteins of innate, adaptive and mucosal immunity (Magnadottir et al., 2018a;  
93 Magnadottir et al., 2018b; Magnadottir et al., 2019a; Magnadottir et al., 2019b). A recent study in  
94 shark also revealed novel insights into this post-translational modification in relation to key immune  
95 factors, including shark immunoglobulins (Criscitello et al., 2019). As the camelid family has developed  
96 unusual small immunoglobulins similar as to shark through convergent evolution, indicating common  
97 factors between shark and camelid immunity, we felt that an investigation of post-translationally  
98 deiminated proteins in camelids was warranted.

99 As PADs have been identified to be a key regulator of extracellular (EV)-release, a mechanism that has  
100 been found to be phylogenetically conserved from bacteria to mammals (Kholia et al., 2015;  
101 Kosgodage et al., 2017; Kosgodage et al., 2018; Gavinho et al., 2019; Kosgodage et al., 2019), the  
102 characterisation of EVs in camelids is of further interest. Extracellular vesicles (EVs) are found in most  
103 body fluids and participate in cellular communication via transfer of cargo proteins and genetic  
104 material (Inal et al., 2013; Colombo et al., 2014; Lange et al., 2017; Turchinovich et al., 2019; Vagner  
105 et al., 2019). EVs in body fluids, including serum, can also be useful biomarkers to reflect health status  
106 (Hessvik and Llorente, 2018; Ramirez et al., 2018). Previous work on EVs has hitherto mainly been in  
107 the context of human pathologies, while recently comparative studies are growing (Iliev et al., 2018;  
108 Yang et al., 2015; Magnadottir et al., 2019b; Criscitiello et al., 2019; Gavinho et al., 2019; Kosgodage  
109 et al., 2019). Few studies have been performed on EVs in camelids but therapeutic effects of EVs  
110 isolated from camel milk have been identified in halting cancer progression (Badawy et al., 2018). A  
111 recent study in shark identified for the first time deiminated small immunoglobulin proteins as part of  
112 EV cargo (Criscitello et al., 2019). Due to the link between camelid and shark immunity through  
113 convergent evolution including the unusual immunoglobulin structure of small heavy chain-only Ig's,  
114 a comparative study on EVs and deiminated EV cargo in a camelid species may provide further insights  
115 into shared immunological traits. Camelids have an unusual Ig repertoire and a large diversity of  
116 functional nanobodies has been identified in the llama (Harmsen & De Haard, 2007; Deschaght et al.,  
117 2017). This has made camelids an important source for small immunoglobulins that can be used for  
118 immunotherapy purposes, including for tumour targeting (van Lith et al., 2016), as well as for assessing  
119 cancer metastasis (Ramos-Gomes et al., 2018). As these nanobodies can also penetrate the blood-  
120 brain barrier (Širochmanová et al., 2018) they are of great value for a range of therapeutic treatment  
121 applications, including for brain cancers (Iqbal et al. 2010). Furthermore, as the camelid family has  
122 acquired unique metabolic features, they are also of interest as a model species for informing  
123 metabolic diseases.

124 In the current study we assessed post-translationally deiminated proteins in llama serum and serum-  
125 derived EVs, and report for the first time EV-mediated export of deiminated key immune, metabolic  
126 and nuclear proteins in serum of a camelid species.

## 127 **Materials and Methods**

128

### 129 **Animals and sampling**

130 Llama (*Lama glama* L. 1758) serum was shared from excess blood collected in routine health checks  
131 of a resident male llama at the Texas A&M Winnie Carter Wildlife Center. Blood collected from the  
132 jugular vein of this 21 year old llama was allowed to clot at room temperature for 2 h before serum  
133 was collected by centrifuging at 300 *g* for 10 min. Serum was aliquoted and immediately frozen at -80  
134 °C until further use.

135

### 136 **Extracellular vesicle (EV) isolation and nanoparticle tracking analysis (NTA)**

137 EVs were isolated by step-wise centrifugation according to established protocols using  
138 ultracentrifugation and the recommendations of MISEV2018 (the minimal information for studies of  
139 extracellular vesicles 2018; Théry et al., 2018). Llama serum was diluted 1:5 in ultrafiltered (using a  
140 0.22 µm filter) Dulbecco's PBS (DPBS, 100 µl serum added to 400 µl DPBS) and then centrifuged at  
141 4,000 *g* for 30 min at 4 °C for removal of cells and cell debris. The supernatant was collected and  
142 centrifuged at 100,000 *g* for 1 h at 4 °C. The pellet was then resuspended in DPBS and washed again  
143 at 100,000 *g* for 1 h at 4 °C. The resulting EV-enriched pellet was resuspended in 100 µl DPBS, diluted  
144 1/100 in DPBS and analysed by NTA, based on Brownian motion of particles in suspension, using the  
145 NanoSight NS300 system (Malvern, U.K.). The NanoSight was used in conjunction with a syringe pump  
146 to ensure continuous flow of the sample, with approximately 40-60 particles per frame and videos  
147 were recorded for 5 x 90 sec. The replicate histograms generated from the recordings were averaged.

148

### 149 **Transmission electron microscopy (TEM)**

150 EVs were isolated from serum as described above, the EV pellets were fixed with 2.5 % glutaraldehyde  
151 in 100 mM sodium cacodylate buffer (pH 7.0) for 1 h at 4 °C, resuspended in 100 mM sodium  
152 cacodylate buffer (pH 7.0), placed on to a grid with a glow discharged carbon support film, stained  
153 with 2 % aqueous uranyl acetate (Sigma-Aldrich) and thereafter viewed in TEM. Imaging was  
154 performed using a JEOL JEM 1400 transmission electron microscope (JEOL, Japan) operated at 80 kV  
155 at a magnification of 80,000 to 100,000. Digital images were recorded using an AMT XR60 CCD camera  
156 (Deben, UK).

157

158 **Western blotting**

159 Llama serum and EV isolates (an EV pellet derived from 100 µl serum, reconstituted in 100 µl DPBS  
160 after isolation and purification) were diluted 1:1 in 2x Laemmli sample buffer, boiled for 5 min at 100  
161 °C and separated by SDS-PAGE on 4-20 % gradient TGX gels (BioRad U.K.). Approximately 5 µg protein  
162 was loaded per lane and transferred to nitrocellulose membranes using semi-dry Western blotting.  
163 Blocking of membranes was performed in 5 % BSA in TBS-T for 1 h at room temperature (RT) and  
164 incubation with primary antibodies, diluted in TBS-T, was carried out at 4 °C overnight (F95 MABN328,  
165 Merck, 1/1000; PAD2 ab50257, Abcam, 1/1000; PAD3 ab50246, 1/1000; PAD4 ab50247, 1/1000; citH3  
166 ab5103, 1/1000; CD63 ab216130, 1/1000; Flot-1 ab41927, 1/2000). The membranes were washed in  
167 TBS-T for 3 x 10 min at RT and thereafter incubated in the corresponding secondary antibody (anti-  
168 rabbit IgG BioRad or anti-mouse IgM BioRad, diluted 1/4000 in TBS-T) for 1 h at RT. Membranes were  
169 washed for 6 x 10 min in TBS-T and visualisation performed using electrochemiluminescence (ECL) and  
170 the UVP BioDoc-ITTM System (Thermo Fisher Scientific, U.K.).

171

172 **Immunoprecipitation and identification of deiminated proteins in llama serum and EVs**

173 For isolation of total deiminated proteins from llama serum and serum derived EVs, the Catch and  
174 Release immunoprecipitation kit (Merck, U.K.) was used together with the F95 pan-deimination  
175 antibody (MABN328, Merck), which has been developed against a deca-citrullinated peptide and  
176 specifically detects proteins modified by citrullination (Nicholas and Whitaker, 2002). For F95  
177 enrichment, 50 µl serum was used according to the manufacturer's instructions (Merck). For EVs, total  
178 protein was first extracted from EV-enriched pellets derived from 100 µl serum, using 100 µl  
179 radioimmunoprecipitation assay (RIPA) buffer, containing protease inhibitor cocktail (P8340, Sigma,  
180 U.K.), and shaken gently on ice for 2 h. Thereafter proteins were isolated from the EVs by  
181 centrifugation at 16,000 *g* for 30 min, collecting the supernatant containing the proteins.  
182 Immunoprecipitation was carried out according to the manufacturer's instructions (Merck), using a  
183 rotating platform overnight at 4 °C. The F95 bound proteins were eluted using denaturing elution  
184 buffer, according to the manufacturer's instructions (Merck). The F95 enriched eluates were then  
185 either analysed by Western blotting or by LC-MS/MS (Cambridge Proteomics, Cambridge, UK). For LC-  
186 MS/MS, the F95-enriched eluates were run 1 cm into a SDS-PAGE gel and the whole F95-enriched  
187 eluate was cut out as one band, whereafter it was processed for proteomic analysis (carried out by  
188 Cambridge Proteomics). Peak files were submitted to in-house Mascot (Matrix Science; Cambridge  
189 Proteomics). Databases used for protein identification (in house, Cambridge Proteomics UK) were as  
190 follows: Camelidae\_family\_20190613 (21429 sequences; 9086806 residues) and also specifically for  
191 llama: Lama\_glama\_20190613 (234 sequences; 52757 residues).

192 **Results**

193 **EV analysis in llama serum**

194 EVs from llama serum were characterised, following step-wise ultracentrifugation, by size exclusion  
195 using NTA, by morphological analysis using TEM and by Western blotting using EV-specific markers  
196 (Fig 1). A poly-dispersed population of EVs in the size range of 30 to 576 nm, with main peaks at 38,  
197 119, 167, 237, 323 and 403 nm was identified by NTA analysis (Fig. 1A). Western blotting confirmed  
198 that the llama serum EVs were positive for the EV-specific markers CD63 and Flotillin-1 (Fig 1B). TEM  
199 analysis confirmed a poly-dispersed EVs population (Fig. 1C).

200

201 **PAD and deiminated proteins in llama serum**

202 A cross-reaction with human PAD2, 3 and 4 isozyme specific antibodies was observed in llama serum  
203 by Western blotting, at an approximate 70-75 kDa size range as expected for mammalian PADs (Fig  
204 2A). Deiminated histone H3 was also detected in llama serum by Western blotting at the expected  
205 approximate 20 kDa size (Fig. 2A). Total deiminated proteins in llama serum-EVs were detected by  
206 Western blotting using the F95 pan-deimination antibody, revealing a range of proteins between 25-  
207 100 kDa in size (Fig. 2B). Deiminated proteins were also assessed by Western blotting after F95  
208 enrichment from llama serum and serum-derived EVs (Fig. 2C). Deiminated proteins from the F95  
209 enriched eluates were further identified by LC-MS/MS analysis. In llama serum, 103 hits for camelid  
210 proteins were identified, as listed in Table 1 and Supplementary Table 1. Overall, 43 of these  
211 deiminated protein hits were common to whole serum and serum-derived EVs, while 60 hits were  
212 specific for whole serum (Fig. 2D).

213

214 **Table 1. Deiminated proteins identified by F95 enrichment and LC-MS/MS in total serum of llama (*Lama***  
215 ***glama*).** Deiminated proteins were isolated by immunoprecipitation using the pan-deimination F95 antibody.  
216 The F95 enriched eluate was analysed by LC-MS/MS and peak list files were submitted to in-house Mascot.  
217 Peptide sequence hits scoring with *Lama glama* (LAMGL) are included as well as hits with other camelids  
218 (CAMFR=*Camelus ferus*; CAMDR=*Camelus dromedaries*; LAMGU=*Lama guanicoe*; VICPA=*Vicugna pacos*  
219 (Alpaca)). Hits with uncharacterized proteins are omitted in the list. For a full list of peptide sequences and m/z  
220 values see Supplementary Table 1. An asterix (\*) indicates that the protein hit is specific to whole serum only.

Protein name (*unique for serum)	Number of peptide sequences identified	Total score ( $p < 0.05$ ) <sup>†</sup>
*O97643_LAMGL <b><i>Fibrinogen A-alpha chain</i></b>	6	282
*P01973 HBA_LAMGL <b><i>Hemoglobin subunit alpha</i></b>	5	189
P68226 HBB_LAMGL <b><i>Hemoglobin subunit beta</i></b>	4	166
Q865W8_LAMGL <b><i>Beta actin</i></b>	4	109
AOA1W5VKM5_LAMGL <b><i>Anti-RON nanobody</i></b>	2	117
*AOA1W5VKM7_LAMGL	2	111

<b>Anti-RON nanobody</b>		
*A0A1W5VKR8_LAMGL <b>Anti-RON nanobody</b>	2	96
*A0A1W5VKQ9_LAMGL <b>Anti-RON nanobody</b>	1	66
S9XDK9_CAMFR <b>Complement C3-like protein</b>	34	1575
S9WI87_CAMFR <b>Serum albumin</b>	20	972
S9XAP9_CAMFR <b>Keratin, type I cytoskeletal 14-like protein</b>	9	522
S9Y6J1_CAMFR <b>Keratin, type II cytoskeletal 5 isoform 13-like protein</b>	11	502
*S9X688_CAMFR <b>Keratin 6A-like protein</b>	10	462
*S9YD43_CAMFR <b>Complement component 4A-like protein</b>	9	443
*S9Y253_CAMFR <b>Kininogen-2 isoform I</b>	8	380
*T0MII3_CAMFR <b>Alpha-2-macroglobulin-like protein</b>	7	371
S9XI90_CAMFR <b>Keratin, type II cytoskeletal 75-like isoform</b>	8	357
S9X494_CAMFR <b>Keratin, type I cytoskeletal 42</b>	6	285
S9XBS9_CAMFR <b>Ig gamma-3 chain C region</b>	6	263
*S9XY2_CAMFR <b>Hemopexin</b>	5	246
A0A075T9L1_CAMDR <b>Dipeptidylpeptidase 4</b>	4	174
S9XXW2_CAMFR <b>Fibrinogen beta chain</b>	3	172
*S9WDV3_CAMFR <b>Fibrinogen gamma chain isoform gamma-B</b>	3	169
*A0A1K0GY87_VICPA <b>Globin A1</b>	4	166
S9WB99_CAMFR <b>Histone H2B</b>	3	146
S9XNF8_CAMFR <b>Xaa-Pro dipeptidase</b>	3	142
*S9YS49_CAMFR <b>Putative E3 ubiquitin-protein ligase Roquin</b>	3	132
*S9YGW7_CAMFR <b>Heparin cofactor 2</b>	3	123
S9WPM4_CAMFR <b>Adiponectin</b>	3	115
A2V743_CAMDR <b>Beta actin</b>	4	109
*S9XP08_CAMFR <b>Inter-alpha-trypsin inhibitor heavy chain H1</b>	1 2	109
S9XM15_CAMFR <b>Ferritin</b>	2	
T0NNK2_CAMFR <b>L-lactate dehydrogenase</b>	1	93

S9X3E8_CAMFR <b>Ig kappa chain V-II region RPMI 6410-like protein</b>	1	90
AOA0A0PAR2_CAMDR <b>Heat shock protein 90</b>	2	88
*S9XYF2_CAMFR <b>Heat shock cognate protein HSP 90-beta-like isoform 3</b>	2	87
S9XHZ4_CAMFR <b>Phosphotriesterase-related protein</b>	1	83
S9XM68_CAMFR <b>Xaa-Pro dipeptidase isoform 3</b>	2	73
S9WT57_CAMFR <b>Tubulin beta chain</b>	2	73
*S9YV02_CAMFR <b>Non-specific protein-tyrosine kinase</b>	1	69
*S9XC57_CAMFR <b>Plasminogen</b>	1	63
*S9YL21_CAMFR <b>Apolipoprotein A-I</b>	2	62
*S9WKZ8_CAMFR <b>Inter-alpha-trypsin inhibitor heavy chain H4</b>	1	62
S9WIA5_CAMFR <b>Glutathione synthetase</b>	1	61
T0MHN9_CAMFR <b>Pyruvate kinase</b>	1	60
*S9Y4U4_CAMFR <b>Complement C1q subcomponent subunit C isoform 2</b>	1	58
S9WAX5_CAMFR <b>Unconventional myosin-Va isoform 2</b>	2	57
S9WVY1_CAMFR <b>Actinin, alpha 1 isoform 6-like protein</b>	1	56
S9XA40_CAMFR <b>Heat shock cognate protein</b>	1	55
*S9YFM0_CAMFR <b>Keratin, type II cytoskeletal 71</b>	1	52
AOA0U2KTX5_CAMDR <b>VHH5 (Fragment)</b>	1	52
S9XR87_CAMFR <b>Ig lambda chain C regions isoform 19-like protein</b>	1	50
S9WGH8_CAMFR <b>Lysozyme</b>	1	49
S9WMX2_CAMFR <b>Dystonin</b>	2	49
*S9X8K9_CAMFR <b>Transaldolase</b>	1	46
*TONM23_CAMFR <b>Rootletin</b>	2	45
S9W610_CAMFR <b>Ferritin</b>	1	45
S9WF34_CAMFR <b>Tubulin alpha chain</b>	1	43
*S9YSI7_CAMFR <b>Triosephosphate isomerase</b>	1	43
*S9XSQ6_CAMFR <b>Vitamin D-binding protein-like protein</b>	1	40
*S9YMC0_CAMFR	2	40

<b><i>Transcription factor 20 isoform 1</i></b>		
*S9Y636_CAMFR <b><i>Receptor-type tyrosine-protein phosphatase-like N</i></b>	1	39
*S9X6M4_CAMFR <b><i>Dyslexia-associated protein</i></b>	1	37
T0MH94_CAMFR <b><i>Rabenosyn-5-like protein</i></b>	1	36
S9WJW3_CAMFR <b><i>N6-adenosine-methyltransferase subunit</i></b>	1	35
*A8IY99_LAMGU <b><i>Gamma-fibrinogen</i></b>	1	35
S9WRI7_CAMFR <b><i>Nuclear receptor coactivator 5 isoform 3-like protein</i></b>	1	35
S9W421_CAMFR <b><i>Hemoglobin, epsilon 1</i></b>	1	35
*S9W711_CAMFR <b><i>Charged multivesicular body protein 4c</i></b>	1	34
*S9X089_CAMFR <b><i>Ig lambda chain V-III region LOI-like protein</i></b>	1	34
S9WUC8_CAMFR <b><i>Ig kappa chain V-II region RPMI 6410-like protein</i></b>	1	32
*S9WVI6_CAMFR <b><i>Complement C1q subcomponent subunit A</i></b>	1	32
*S9Y5S1_CAMFR <b><i>Transcriptional repressor NF-X1</i></b>	1	32
*S9YC53_CAMFR <b><i>Alpha-1-antitrypsin-like protein</i></b>	1	32
*S9Y3F6_CAMFR <b><i>Dual specificity testis-specific protein kinase 1</i></b>	1	31
S9WKI8_CAMFR <b><i>HEAT repeat-containing protein 7B1</i></b>	1	31
*S9WVS9_CAMFR <b><i>Peroxisome proliferator-activated receptor gamma coactivator-related protein 1</i></b>	1	29
*S9XVK5_CAMFR <b><i>Transthyretin</i></b>	1	29
*S9Y967_CAMFR <b><i>General transcription factor II, i isoform 4 isoform 1-like protein</i></b>	1	28
*T0MC04_CAMFR <b><i>Spermatogenesis-associated protein 2-like protein</i></b>	1	28
*S9YSZ6_CAMFR <b><i>Centromere protein J</i></b>	1	28

221 †Ions score is  $-10 \cdot \log(P)$ , where P is the probability that the observed match is a random event. Individual ions  
222 scores > 20 indicated identity or extensive homology ( $p < 0.05$ ). Protein scores were derived from ions scores as  
223 a non-probabilistic basis for ranking protein hits. Cut-off was set at Ions score 20.  
224

## 225 Identification of deiminated proteins in EVs from llama serum

226 Llama serum-derived EVs showed positive for deiminated proteins by Western blotting, using the pan-  
227 deimination F95 antibody (Fig. 2B). Deiminated proteins were further identified by F95 enrichment  
228 and LC-MS/MS analysis, revealing 68 deiminated protein hits in total for EVs, with 25 hits unique to  
229 EVs (not identified from serum). Peptide sequences of hits with camelid proteins and m/z values are

230 listed in Table 2 and Supplementary Table 2. Overlap with deiminated proteins identified in whole  
 231 llama serum and EVs is represented in the Venn diagram in Fig. 2D.

232

233 **Table 2. Deiminated proteins identified by F95 enrichment and LC-MS/MS in EVs isolated from serum of llama**  
 234 **(*Lama glama*)**. Deiminated proteins were isolated by immunoprecipitation using the pan-deimination F95  
 235 antibody, the F95 enriched eluate was analysed by LC-MS/MS and peak list files were submitted to Mascot.  
 236 Peptide sequence hits scoring with *L. glama* (LAMGL) are presented as well as hits with other camelids  
 237 (CAMFR=*Camelus ferus*; CAMDR=*Camelus dromedaries*; LAMGU=*Lama guanicoe*). Hits with uncharacterised  
 238 proteins are not listed. For a full list of peptide sequences and m/z values see Supplementary Table 2. An asterix  
 239 (\*) indicates that the protein hit is unique for EVs only.

<b>Protein name (*unique for EVs)</b>	<b>Number of peptide sequences identified</b>	<b>Total score (<math>p &lt; 0.05</math>)<sup>†</sup></b>
AOA1W5VKM5_LAMGL <b>Anti-RON nanobody</b>	2	164
Q865W8_LAMGL <b>Beta actin</b>	2	85
*S9XAP9_CAMFR <b>Keratin, type I cytoskeletal 14-like protein</b>	9	554
*S9X688_CAMFR <b>Keratin 6A-like protein</b>	10	496
S9Y6J1_CAMFR <b>Keratin, type II cytoskeletal 5 isoform 13-like protein</b>	10	438
S9WI87_CAMFR <b>Serum albumin</b>	9	430
*S9YN99_CAMFR <b>Keratin, type I cytoskeletal 17-like isoform</b>	6	417
*S9XI90_CAMFR <b>Keratin, type II cytoskeletal 75-like isoform</b>	6	318
S9X494_CAMFR <b>Keratin, type I cytoskeletal 42</b>	5	269
S9XBS9_CAMFR <b>Ig gamma-3 chain C region</b>	4	162
AOA075T9L1_CAMDR <b>Dipeptidylpeptidase 4</b>	3	153
S9X684_CAMFR <b>Keratin, type II cytoskeletal 8</b>	2	136
S9WB99_CAMFR <b>Histone H2B</b>	3	133
S9YQ51_CAMFR <b>Tubulin beta chain</b>	3	114
*S9WX81_CAMFR <b>Histone 1, H2ai isoform 3-like protein</b>	3	89
*S9X8G9_CAMFR <b>Desmoplakin</b>	2	88
A2V743_CAMDR <b>Beta actin</b>	2	85
AOA0A0PAR2_CAMDR <b>Heat shock protein 90</b>	2	85
S9XA40_CAMFR <b>Heat shock cognate protein</b>	1	85
T0NNK2_CAMFR <b>L-lactate dehydrogenase</b>	1	81
S9XNF8_CAMFR	2	74

<b><i>Xaa-Pro dipeptidase</i></b>		
T0MHN9_CAMFR	1	71
<b><i>Pyruvate kinase</i></b>		
S9WVY1_CAMFR	1	60
<b><i>Actinin, alpha 1 isoform 6-like protein</i></b>		
*A0A0E3Z5I3_CAMDR	1	59
<b><i>Superoxide dismutase</i></b>		
S9XHZ4_CAMFR	1	57
<b><i>Phosphotriesterase-related protein</i></b>		
S9W9Y4_CAMFR	1	57
<b><i>Ferritin</i></b>		
S9XR87_CAMFR	1	56
<b><i>Ig lambda chain C regions isoform 19-like protein</i></b>		
S9X3E8_CAMFR	1	50
<b><i>Ig kappa chain V-II region RPMI 6410-like protein</i></b>		
S9WAX5_CAMFR	2	49
<b><i>Unconventional myosin-Va isoform 2</i></b>		
S9WF34_CAMFR	1	44
<b><i>Tubulin alpha chain</i></b>		
*S9W806_CAMFR	2	43
<b><i>Filamin-A isoform 1</i></b>		
*S9X6X3_CAMFR	2	42
<b><i>Scaffold attachment factor B-like protein</i></b>		
T0MH94_CAMFR	1	40
<b><i>Rabenosyn-5-like protein</i></b>		
*S9Y0S0_CAMFR	1	39
<b><i>DNA-directed RNA polymerase subunit beta</i></b>		
S9WJW3_CAMFR	1	38
<b><i>N6-adenosine-methyltransferase subunit</i></b>		
S9XM68_CAMFR	1	38
<b><i>Xaa-Pro dipeptidase isoform 3</i></b>		
*S9YV02_CAMFR	1	38
<b><i>Non-specific protein-tyrosine kinase</i></b>		
S9WGH8_CAMFR	1	32
<b><i>Lysozyme</i></b>		
S9WRI7_CAMFR	1	32
<b><i>Nuclear receptor coactivator 5 isoform 3-like protein</i></b>		
S9W421_CAMFR	1	32
<b><i>Hemoglobin, epsilon 1</i></b>		
*S9WI71_CAMFR	1	32
<b><i>Metabotropic glutamate receptor 3</i></b>		
*S9WB50_CAMFR	1	31
<b><i>TSC22 domain family protein 3-like protein</i></b>		
S9WMX2_CAMFR	1	31
<b><i>Dystonin</i></b>		
S9WKI8_CAMFR	1	31
<b><i>HEAT repeat-containing protein 7B1</i></b>		
S9WIA5_CAMFR	1	31
<b><i>Glutathione synthetase</i></b>		
*S9XC05_CAMFR	1	31
<b><i>Telomere-associated protein RIF1 isoform 1</i></b>		
A0A0U2KTX5_CAMDR	1	30
<b><i>VHH5</i></b>		
*T0MGG7_CAMFR	1	30
<b><i>Nucleoredoxin</i></b>		

*S9XET3_CAMFR <b>Rac GTPase-activating protein 1</b>	1	30
S9XDK9_CAMFR <b>Complement C3-like protein</b>	1	30
*S9XMI2_CAMFR <b>Pseudopodium-enriched atypical kinase 1</b>	1	29
*S9Y3S9_CAMFR <b>Core histone macro-H2A.1 isoform 2</b>	1	29
S9XXW2_CAMFR <b>Fibrinogen beta chain</b>	1	29
*S9YGX6_CAMFR <b>PAS domain-containing serine/threonine-protein kinase</b>	1	29
*TONMU1_CAMFR <b>SH2 domain-containing protein 7</b>	1	28
*TOMIT6_CAMFR <b>Serine-tRNA ligase, mitochondrial</b>	1	28
*S9W449_CAMFR <b>Fc receptor-like protein 5</b>	1	28

240 †Ions score is  $-10 \cdot \log(P)$ , where P is the probability that the observed match is a random event. Individual ions  
241 scores > 22 indicated identity or extensive homology ( $p < 0.05$ ). Protein scores were derived from ions scores as  
242 a non-probabilistic basis for ranking protein hits. Cut-off was set at Ions score 20.  
243

## 244 Discussion

245 For the first time deiminated proteins are described in a camelid, using the llama (*Lama glama*) as a  
246 model species. Post-translational deimination was identified in key immune, nuclear and metabolic  
247 proteins. A llama PAD homologue was identified at an expected 70-75 kDa size similar as for human  
248 PADs by Western blotting via cross reaction with anti-human PAD2, PAD3 and PAD4 antibodies. PAD2  
249 is known to be the phylogenetically most conserved PAD form (Vossenaar et al., 2003; Magnadottir et  
250 al., 2018a) and has also been seen in shark (Criscitiello et al., 2019). Deiminated histone H3, a marker  
251 of neutrophil extracellular trap formation (NETosis), was also detected in llama serum by Western  
252 blotting and is described for the first time in a camelid species but was recently described in shark  
253 (Criscitiello et al., 2019). NETosis is driven by PADs (Li et al., 2010), is conserved throughout phylogeny  
254 and is important in innate immune defences against a range of pathogens including bacteria, viruses  
255 and helminths (Brinkmann et al., 2004; Branzk et al., 2014; Schönrich and Raftery, 2016). NETosis has  
256 also been associated with clearance of apoptotic cells and during tissue remodelling in teleosts  
257 (Magnadottir et al., 2018a; Magnadottir et al., 2019a). Furthermore, NETosis is linked to a range of  
258 autoimmune diseases, due to NET activation via neo-epitopes (O'Neil and Kaplan, 2019), which can  
259 also lead to organ damage (Lee et al., 2017). NETosis is also associated with cancer (Gonzalez-Aparicio  
260 and Alfaro, 2019) and neurodegenerative diseases (Pietronigro et al., 2017).

261 Further deiminated proteins identified in llama serum and serum-derived EVs by F95 enrichment and  
262 LC-MS/MS analysis included key proteins of camelid innate and adaptive immunity, nuclear proteins,  
263 as well as proteins involved in metabolic function. Using STRING (Search Tool for the Retrieval of

264 Interacting Genes/Proteins) analysis (<https://string-db.org/>) for protein-protein interaction, PPI  
265 enrichment value for deiminated proteins in whole llama serum was found to be  $p < 1.0e-16$  for 43  
266 deiminated proteins out of 103 identified in serum, which indicates that these proteins have more  
267 interactions among themselves than what would be expected for a random set of proteins of similar  
268 size, drawn from the genome (STRING analysis, see Fig. 3A). For deiminated proteins in 29 out of the  
269 68 deiminated EV cargo proteins, the PPI enrichment value was found to be  $p=0.0193$  (STRING  
270 analysis, see Fig. 4A). Such enrichment indicates that the proteins are at least partially biologically  
271 connected, as a group. As the camelid proteins are not present in the STRING database, corresponding  
272 protein homologues for human were chosen to create the protein-protein interaction networks  
273 shown in Figures 3 and 4. Out of the 103 camelid proteins identified as deiminated in serum, protein  
274 IDs for 43 were present for *Homo sapiens* to perform the assessment of protein-protein interactions  
275 and identification of main biological GO pathways (response to stress, response to wounding, oxygen  
276 transport, small molecule metabolic process, vesicle mediated transport and regulated exocytosis; Fig  
277 3B). For llama EVs, out of 68 proteins identified as deiminated, 29 corresponding protein homologues  
278 were found in the STRING database for *Homo sapiens* and were analysed highlighting main biological  
279 GO pathways (response to stress, cytoskeleton organisation and vesicle-mediated transport; Fig.4B).  
280 Deimination protein candidates identified here in llama serum and EVs, which are involved in immune,  
281 nuclear and metabolic functions, are further discussed below, including where appropriate in a  
282 comparative context with relevant human diseases. Proteins that have previously been identified as  
283 deiminated in other species are listed first.

284

285 **Nanobodies** are based on immunoglobulin single variable domains, derived from the variable domains  
286 of heavy chain-only antibodies, which occur naturally in camelids (Deschaght et al., 2017). In the llama  
287 the heavy chain-only antibodies are comprised of at least two subclasses (Henry et al., 2019). These  
288 types of homodimeric, light chain-less antibodies have evolved through convergent evolution (Brooks  
289 et al., 2018), in at least two groups (camelids and cartilaginous fish), and their variable binding domains  
290 ( $V_HH_5$ ) are of great value for therapeutic and diagnostic applications (Muyldermans, 2013; Cristiciello,  
291 2014; Steeland et al., 2016; Könning et al., 2018; Henry et al., 2019). Nanobodies can act against  
292 challenging targets such as small molecules and toxins (Wesolowskiet al., 2009; Bever et al., 2016),  
293 viruses (Wei et al., 2011; Hassiki et al., 2016; Vanlandschoot et al., 2011; Cohen, 2018), enzymes  
294 (Muyldermans, 2013), ion channels (Wei et al., 2011; Danquah et al., 2016) and G protein-coupled  
295 receptors GPCRs (Cromie et al., 2015). Llama nanobodies have been shown to tether to early  
296 endosomes and to mitochondria (Traub, 2019), be used for diagnostics (Shriver-Lake et al., 2018), be  
297 used for design of cancer immunotherapeutics (Hussack et al., 2018; Bannas and Koch-Nolte, 2018;

298 Rossotti et al., 2019) and have been approved for passive immunotherapy (Sheridan, 2019). Our  
299 current finding, that llama nanobodies can be post-translationally deiminated may shed some light on  
300 their observed structural variation which still remains to be fully explained as sequence alignment  
301 does not fully elucidate their diversity (Mitchell and Colwell, 2018). As a structurally analogous  
302 immunoglobulin in shark, new antigen receptor (NAR) (Greenberg et al., 1995; Barelle et al., 2009;  
303 Flajnik and Dooley, 2009; De Silva et al., 2019) was recently also found to be deiminated (Criscitiello  
304 et al., 2019), our current finding may provide novel insights into function of these immune proteins  
305 and be useful for refinement in therapeutic nanobody development. Llama single-chain antibodies  
306 were here found to be deimination candidates both in llama whole serum and in serum derived EVs,  
307 highlighting also their EV-mediated export.

308

309 **Ig proteins** were identified here as being deiminated in llama serum and in serum-derived EVs, scoring  
310 with Ig components from other camelids. Immunoglobulins (Ig) are key molecules in adaptive  
311 immunity but post-translational deimination of Ig's has hitherto received little attention. Deimination  
312 of the IgG Fc region in patients with bronchiectasis and RA has been identified (Hutchinson et al.,  
313 2017). Furthermore, deimination of Ig's in teleost fish was recently described (Magnadottir et al.,  
314 2019a), as well as in shark (Criscitiello et al., 2019). Given the increased focus on understanding of Ig  
315 diversity throughout phylogeny (Smith et al., 2012; Zhang et al., 2013; de los Rios et al., 2015; Zhang  
316 et al., 2016; Zhang et al., 2017; Stanfield et al., 2018) and the unique features of camelid  
317 immunoglobulins (Plasil et al., 2019), our current finding of deimination of llama Ig's highlights a novel  
318 concept that may further understanding of Ig diversity throughout evolution. Of additional interest is  
319 the finding that some deiminated Ig proteins were also found to be exported in EVs.

320

321 **Complement components** identified to be deiminated in llama serum included C3, C4 and C1q, while  
322 only C3 was identified to be deiminated in serum derived EVs. Complement component C3 plays a  
323 central role in all pathways of complement activation and can also be directly activated by self- and  
324 non-self surfaces via the alternative pathway without a recognition molecule (Dodds and Law, 1998;  
325 Dodds, 2002). In camelids, the alternative and classical pathway haemolytic activity of serum has been  
326 assessed in the dromedary camel with respect to age and gender (Olaho-Mukani et al., 1995a and b).  
327 Hitherto little is known about roles for post-translational deimination of complement components  
328 throughout phylogeny. In teleost fish, C3 has been identified in serum in deiminated form  
329 (Magnadottir et al., 2019a) and also found to be deiminated in mucosal EVs of teleost fish  
330 (Magnadottir et al., 2019b), while post-translationally deiminated C3 was identified in shark total  
331 serum but not EVs (Criscitiello et al., 2019). Other complement components, including C4 and C1q,

332 which belong to the classical pathway of complement activation were here identified as deiminated  
333 in llama whole serum and some of those have also recently been reported to be deiminated in teleost  
334 fish (Magnadottir et al., 2019a). The C1q subcomponent can bind to the Fc region of immunoglobulins  
335 that are bound to antigen and activate the classical part of the complement pathway (Reid et al., 2002;  
336 Reid, 2018). Interestingly, an essential role for arginine in C1q has previously been suggested for C1q-  
337 IgG interaction (Kojouharova et al., 2004). C1q also serves as a potent pattern recognition molecule  
338 which recognises self, non-self and altered self-signals (Nayak et al., 2012; Reid, 2018) and may  
339 therefore also bind to deiminated neo-epitopes (Magnadottir et al., 2019a). The complement system  
340 has multifaceted roles. It forms part of the first line of immune defence against invading pathogens,  
341 acting in clearance of necrotic or apoptotic cells (Dodds and Law, 1998; Sunyer & Lambris, 1998;  
342 Fishelson et al., 2001; Carrol and Sim, 2011). Complement also has roles in regeneration (Del-Rio-  
343 Tsonis et al., 1998; Haynes et al., 2013) and tissue remodelling (Lange et al., 2004a; 2004b; Lange et  
344 al., 2005; Lange et al., 2006). Furthermore, C1 is also implicated in multiple non-complement functions  
345 including binding of apoptotic cells, cleavage of nuclear antigens and cleavage of MHC class I (Lu and  
346 Kishore, 2017). Post-translational deimination of complement components may possibly influence  
347 their function including cleavage ability, binding, deposition and generation of the convertase.

348

349 ***Apolipoprotein A-I*** is primarily involved in lipid metabolism where conformational plasticity and  
350 flexibility are regarded as key structural features (Arciello et al., 2016). Apo A-I is associated with  
351 regulation of mitochondrial function and bioenergetics (White et al., 2017). Furthermore, Apo A-I has  
352 been shown to have a regulatory role in the complement system by affecting membrane attach  
353 complex (MAC) assembly and thus the final lytic pathway (Hamilton et al., 1993; Jenne et al., 1991;  
354 French et al., 1994). Given the diverse roles of Apo A-I, the current finding of deiminated forms in  
355 serum may be of quite some relevance and has previously been identified in teleost fish (Magnadottir  
356 et al., 2019a). Apo A-I was here found to be deiminated in whole llama serum only.

357

358 ***Serum albumin*** is a major acidic plasma protein in vertebrates and serves as a transport molecule for  
359 fatty acids, bilirubin, steroids, amino acids and copper, as well as having roles in maintaining the colloid  
360 osmotic pressure of blood (Peters, 1996). In camelids, total albumin levels have been assessed, for  
361 example in relation to reproductive efficiency (El-Malky et al., 2018) and as biomarkers of oxidative  
362 stress (El-Deeb and Buczinski, 2016). While albumin has been identified as a glycoprotein in some  
363 species (Metcalf et al., 2007) investigation of post-translational deimination has been limited, but was  
364 recently identified in teleost fish (Magnadottir et al., 2019a). Serum albumin was identified as  
365 deiminated in both whole llama serum and EVs.

366

367 **Hemopexin** is a scavenger protein of haemoglobin and a predominant heme binding protein, which  
368 contributes to heme homeostasis (Smith and McCulloh, 2015; Immenschuh et al., 2017). Hemopexin  
369 also associates with high density lipoproteins (HDL), influencing their inflammatory properties (Mehta  
370 and Reddy, 2015). Hemopexin is a plasma glycoprotein that has been previously identified as a  
371 deimination candidate in teleost fish (Magnadottir et al., 2019a) and shark (Criscitiello et al., 2019).  
372 Here, hemopexin was found deiminated in whole llama serum only.

373

374 **Inter-alpha-trypsin inhibitor** (heavy chain H1) belongs to the serpin family of proteins, which have  
375 protease-inhibitory functions and are involved in diverse physiological and pathological processes  
376 including fertilisation, ovulation, coagulation, inflammation, as well as tumorigenesis, metastasis and  
377 dementia (Zhuo and Kimata, 2008; Weidle et al., 2018). Inter-alpha-trypsin inhibitor is synthesised in  
378 the liver, circulates in the blood and has two chains, a light and heavy chain, whereof the heavy-chain  
379 (ITIH) includes a von Willebrand domain and can interact with the extracellular matrix (Bost et al.,  
380 1998). ITIH is downregulated in tumours via methylation and ITIH2 is strongly reduced in invasive  
381 cancers (Hamm et al., 2008). While ITIH was recently identified as a deimination candidate in teleost  
382 fish (Magnadottir et al., 2019a) further studies on the regulation of ITIH2 via post-translational  
383 deimination have not been carried out. ITIH was here identified as deiminated in whole llama serum  
384 only.

385

386 **Fibrinogen** is a glycoprotein, synthesised in liver (Tennent et al., 2007) and forms part of the acute  
387 phase response as part of the coagulation cascade (Tiscia and Margaglione, 2018). In camelids,  
388 fibrinogen is a biomarker for stress and infection (Greunz et al., 2018; El-Bahr and El-Deeb, 2016; El-  
389 Deeb and Buczinski, 2016). Impaired mechanism of fibrinogen formation and fibrin polymerization are  
390 implicated with various pathologies including coagulopathies and ischemic stroke (Weisel and  
391 Litvinov, 2013), while acquired fibrinogen disorders can be associated with cancer, liver disease or  
392 post-translational modifications (Besser and MacDonald, 2016). Fibrinogen is indeed a known  
393 deimination candidate and this post-translational modification contributes to its antigenicity in  
394 autoimmune diseases (Hida et al., 2004; Muller and Radic, 2015; Blachère et al., 2017). Fibrinogen was  
395 here identified as deiminated both in whole llama serum and EVs.

396

397 **Tubulin beta-chain** participates in cytoskeletal rearrangement and its deimination has previously been  
398 linked to EV release (Kholia et al., 2015). Deimination of tubulin may therefore be crucial for facilitating

399 EV-mediated processes in homeostasis, immune responses and in relation to pathologies. Here,  
400 tubulin was identified as deiminated in both whole llama serum and EVs.

401

402 **Histone H2B** was identified as being deiminated in both llama serum and EVs and in addition, Histone  
403 1 (H2ai isoform 3-like protein) and core histone macro-H2A.1 isoform 2 were identified as deiminated  
404 in EVs only. Histones undergo various posttranslational modifications that affect gene regulation and  
405 can also act in concert (Latham et al., 2007; Bird, 2007). In addition to acetylation, phosphorylation  
406 and ubiquitination, histones are known to undergo deimination, including H2B (Sohn et al., 2015) and  
407 H2A (Hagiwara et al., 2005), as identified in this study in llama. Other histones that are known to  
408 undergo deimination include H3 and H4 (Chen et al., 2014; Kosgodage et al., 2018).

409

410 **Heat shock protein 90** (Hsp90) was here found to be deiminated both in llama whole serum and EVs.  
411 HSP90 has been described in camelid (Saeed et al., 2015). Hsp90 is a phylogenetically highly conserved  
412 chaperone protein involved in protein folding, stabilisation of proteins against heat stress, and aids in  
413 protein degradation (Buchner 1999; Picard, 2002). Hsp90 also stabilizes a number of proteins required  
414 for tumour growth and is therefore important in anti-cancer drug investigations (Goetz et al., 2003).  
415 Hsp90 is responsible for most of the ATPase activity of the proteasome (Imai et al., 2003) and has an  
416 ATP binding region, which also is the main binding site of drugs (Chiosis et al., 2006). In camelids,  
417 Hsp90 has been related to adaptive tolerance of camel somatic cells to acute and chronic heat shock  
418 (up to 20 hours at 45 degrees Celsius), which is lethal to many mammalian cells (Saadeldin et al.,  
419 2018b). Hsp90 has previously been described to be post-translationally deiminated in rheumatoid  
420 arthritis, allowing deimination-induced shifts in protein structure to generate cryptic epitopes capable  
421 of bypassing B cell tolerance (Travers et al., 2016). It is of some interest to find that Hsp90 is also found  
422 deiminated in llama serum, further highlighting protein moonlighting functions of Hsp90 in  
423 physiological and pathophysiological context via post-translational deimination. In addition, finding  
424 post-translational deimination of the same protein throughout phylogeny also supports translational  
425 value between species to further understanding of this post-translational modification in human  
426 pathologies.

427

428 The following deimination protein candidates identified in the current study in llama serum and  
429 serum-EVs have to our knowledge not been previously reported as deiminated:

430

431 **Alpha 2-macroglobulin** is closely related to other thioester containing proteins, such as complement  
432 proteins C3, C4 and C5 (Sottrup-Jensen et al., 1987; Davies and Sim, 1981). Alpha-2-M is

433 phylogenetically conserved from arthropods to mammals and found at high levels in mammalian  
434 plasma. Alpha-2-M forms part of the innate immune system and clears active proteases from tissue  
435 fluids (Armstrong and Quigley, 1999). Here, Alpha-2-M was found deiminated in whole llama serum  
436 only and has not reported as deiminated before, to our knowledge.

437

438 **Adiponectin** is the most abundant secreted adipokine with pleiotrophic roles in physiological and  
439 pathophysiological processes (Fiaschi, 2019). It has received considerable interest in the field of  
440 metabolic and obesity research (Frankenberg et al., 2017; Spracklen et al., 2019), as well as in diabetes  
441 (Yamauchi et al., 2003), due to its key function in regulating glucose (Yamauchi et al., 2002).  
442 Adiponectin is furthermore linked to longevity (Chen et al., 2019), regenerative functions (Fiaschi et  
443 al., 2014) and has roles in myopathies, such as Duchenne muscular dystrophy and collagen VI-related  
444 myopathies (Gamberi et al., 2019). Adiponectin is also implicated in a range of cancers, often in  
445 relation to obesity (Parida et al., 2019). Furthermore, adiponectin plays roles in reproduction, embryo  
446 pre-implantation and embryonic development (Barbe et al., 2019). Due to the range of functions in  
447 relation to key pathophysiologies there is great interest in drug development for modulating  
448 adiponectin signalling (Fiaschi, 2019). Given the unique metabolic adaptive features of camelids, the  
449 identification of post-translational deimination of this key metabolic protein may be of some interest.  
450 Recent studies in rheumatoid arthritis made a correlation between inflammation, autoantibodies and  
451 adiponectin levels (Hughes-Austin et al., 2018; Liu et al., 2019), while adiponectin itself has not been  
452 previously identified to be deiminated to our knowledge. Post-translational deimination may be a  
453 hitherto unrecognized mechanism for adiponectin, also in humans, to adapt moonlighting functions  
454 via changes in protein folding and therefore interaction with other proteins. Adiponectin is a small 244  
455 aa protein (NP\_001171271.1) in humans and contains 2 unfolded regions and 7 arginine sites, while  
456 camel adiponectin has 8 arginine sites. These could be subjected to PAD-mediated deimination and  
457 therefore modulate adiponectin folding and function, depending on which arginine is deiminated.  
458 Here, deiminated adiponectin was identified in whole llama serum only.

459

460 **Dystonin** is a plakin-family adhesion junction plaque protein and was here identified as deiminated in  
461 both llama serum and EVs. Dystonin, along with XVII collagen, form hemidesmosomes and both  
462 proteins are autoantigens believed to be responsible for the Type II hypersensitivity pathologic in the  
463 pruritic skin disease bullous pemphigoid (Bağcı et al., 2017; Basseri et al., 2018). Dystonin has also  
464 been linked to Sjögren's syndrome and linked to a hypermethylation status (Gonzalez et al., 2011),  
465 but post-translational deimination of dystonin has not been previously described to our knowledge,

466 although deimination is associated with a range of autoimmune diseases, including Sjögren's  
467 syndrome (Konsta et al., 2014; Selmi et al., 2015).

468

469 ***Xaa-Pro dipeptidase***, also known as prolidase, is an enzyme that in humans is encoded by the PEPD  
470 gene. Post-translational modifications of prolidase regulate its enzymatic abilities. Deficiency in  
471 prolidase leads to a rare, severe autosomal recessive disorder (prolidase deficiency) that causes many  
472 chronic, debilitating health conditions in humans (Viglio et al., 2006). These phenotypic symptoms  
473 vary and may include skin ulcerations, mental retardation, splenomegaly, recurrent infections,  
474 photosensitivity, hyperkeratosis, and unusual facial appearance. Furthermore, prolidase activity was  
475 found to be abnormal compared to healthy levels in various medical conditions including: bipolar  
476 disorder, breast cancer, endometrial cancer, keloid scar formation, erectile dysfunction, liver disease,  
477 lung cancer, hypertension, melanoma, and chronic pancreatitis (Kitchener et al., 2012). In some  
478 cancers with increased levels of prolidase activity, such as melanoma, the differential expression of  
479 prolidase and its substrate specificity for dipeptides with proline at the carboxyl end suggests the  
480 potential of prolidase in becoming a viable, selective endogenous enzyme target for proline prodrugs  
481 (Mittal et al., 2005). Serum prolidase enzyme activity is also currently being explored as a biomarker  
482 for diseases including chronic hepatitis B and liver fibrosis (Duygu et al., 2013; Sen et al., 2014; Stanfliet  
483 et al., 2015). Phosphorylation of prolidase has been shown to increase its activity while  
484 dephosphorylation leads to a decrease in enzyme activity. Post-translational deimination of prolidase  
485 has not been described before to our knowledge and may add to understanding of how this enzyme  
486 is regulated. Prolidase was here identified as deiminated in both llama serum and EVs.

487

488 ***Dipeptidylpeptidase 4*** (DPP4, also known as CD26) was here identified to be deiminated in both llama  
489 whole serum and EVs. DPP4 controls glucose homeostasis and has complex roles in inflammation and  
490 homeostasis, including in liver cytokine expression, while its activity in plasma has been shown to  
491 correlate with body weight and fat mass (Varin et al., 2019). Interestingly, in camel milk, DPP4  
492 inhibitory peptides have been identified and suggested to play roles in the regulation of glycaemia in  
493 humans (Nongonierma et al., 2018). Furthermore, roles for DPP4 in cancer have been found to relate  
494 to its post-translational processing of chemokines, thereby limiting lymphocyte migration to sites of  
495 inflammation and tumours (Barreira da Silva et al., 2015). As the success of antitumour immune  
496 responses depends on the infiltration of solid tumours by effector T cells, a process which is guided by  
497 chemokines, DPP4 inhibitors have been suggested as a strategy to enhance tumour immunotherapy  
498 (Barreira da Silva et al., 2015). Furthermore, serum DPP4 activity levels in primary HIV infection were  
499 found to be significantly decreased and to correlate with inflammation and HIV-induced intestinal

500 damage (Ploquin et al., 2018). Middle East respiratory syndrome coronavirus (MERS-CoV) has been  
501 found to utilize dipeptidyl peptidase 4 (DPP4) as an entry receptor, via glycosylated sites (Peck et al.,  
502 2017). Therefore the identification of DPP4 as a deimination candidate may be of some relevance as  
503 such post-translational modification can affect DPP4 structure and function, allowing for moonlighting  
504 functions which may vary in pathological compared to pathophysiological milieus.

505

506 ***E3 ubiquitin-protein ligase Roquin***, belongs to the Roquins which are a family of highly conserved  
507 RNA-binding proteins involved in ubiquination, are crucial for T-cell-dependent B-cell responses  
508 (Athanasopoulos et al., 2016) and play important roles in modulating T-cell activity (Akef and Muljo,  
509 2018). Roquins repress constitutive decay elements containing mRNAs and play a critical role in RNA  
510 homeostasis and immunological self-tolerance (Zhang et al., 2015; Essig et al., 2018; Mino and  
511 Takeuchi, 2018). Roquin plays multifaceted roles both in the generation of a homeostatic immune  
512 response, as well as during chronic inflammation and autoimmunity (Schaefer and Klein, 2016; Lee et  
513 al., 2019). While roquin causes post-translational ubiquination of target proteins, post-translational  
514 deimination of roquin itself may modulate its function and is described here for the first time. Roquin  
515 was here identified as deiminated in whole llama serum only.

516

517 ***Serine-tRNA ligase, mitochondrial*** was here identified as a deimination candidate protein in llama EVs  
518 only. It has been linked to HUPRA syndrome which is a rare mitochondrial disease characterized by  
519 hyperuricemia, pulmonary hypertension, renal failure in infancy and alkalosis (Rivera et al., 2013). It  
520 has furthermore been linked to progressive spastic paresis (Linnankivi et al., 2016). Post-translational  
521 deimination of this mitochondrial protein has not been described before to our knowledge.

522

523 ***Nucleoredoxin*** (Nrx) was here identified to be deiminated in EVs only. It is an oxidoreductase of the  
524 thioredoxin family of proteins with numerous functions in the redox regulation of metabolic pathways,  
525 cellular morphology, and signal transduction (Urbainsky et al., 2018). Nrx has been shown to inhibit  
526 Wnt-beta-catenin signalling (Funato et al., 2006) and is linked to Ca<sup>2+</sup>-mediated mitochondrial reactive  
527 oxygen species metabolism (Rharass et al., 2014). Nrx has furthermore been identified as an  
528 epigenetic cancer marker related to the oxidative status of human blood (Schöttker et al., 2015), but  
529 hitherto not been described as deiminated.

530

531 ***Dyslexia-associated protein*** was here identified to be deiminated in total serum of llama. It is  
532 associated with developmental dyslexia (Levecque et al., 2009) and has been shown to have roles in  
533 cell-cell interactions and signalling and neuronal migration (Velayos-Baeza et al., 2008), as well as in

534 axon guidance (Poon et al., 2011). Dyslexia-associated protein has previously been found to follow the  
535 classical clathrin-mediated endocytosis pathway and its surface expression seems regulated by  
536 endocytosis, indicating that the internalization and recycling of the protein may be involved in fine-  
537 tuning its role in neuronal migration (Levecque et al., 2009). It has been described to be highly  
538 glycosylated in different mammalian cell lines (Velayos-Baeza et al., 2008), while deimination has not  
539 been described before.

540

541 **Metabotropic glutamate receptor 3** was identified here as deiminated in llama EVs only. It has, like  
542 other components of the glutamatergic system, a widespread distribution outside the central nervous  
543 system (CNS) and has been linked to regulation of the brain-gut axis (Julio-Pieper et al., 2013). It has  
544 also been linked to pain (Acher and Goudet, 2015) and psychotic disorders (Matrisciano et al., 2015).  
545 The group III mGlu receptors have been described in human stomach and colon, revealing a huge  
546 potential for these receptors in the treatment of peripheral disorders, including gastrointestinal  
547 dysfunction (Julio-Pieper et al., 2013). As post-translational deimination has not been described  
548 before in this receptor, but may well affect its tertiary structure, our current finding may be of some  
549 relevance in relation to strategies for developing antagonistic probes (Wenthur et al., 2012). Such  
550 pharmacological tools originally designed for mGlu receptors in the CNS may also be directed towards  
551 new disease targets in the periphery. Ulcerative colitis and Crohn's disease are potential targets, as  
552 irritable bowel diseases can be co-morbid with anxiety and depression (Julio-Pieper et al., 2013).

553

554 **Glutathione synthetase** (GSS) was here identified to be deiminated in both llama whole serum and  
555 EVs. GSS is the second enzyme in the glutathione (GSH) biosynthesis pathway involved in homeostasis  
556 and cellular maintenance and also acts as a potent antioxidant (Njålsson & Norgren, 2005). In  
557 camelids, glutathione peroxidase, which also belongs to the GSH biosynthesis pathway and is a potent  
558 anti-oxidant, has been identified as a seminal plasma fertility biomarker (Waheed et al., 2015).  
559 Furthermore, camel milk has been shown to boost glutathione and total anti-oxidant capacity in sera  
560 and exudates in animal studies (Arab et al., 2017). In a diabetic mouse model, the activities of GSH,  
561 alongside glucose insulin and ROS levels, were restored after camel whey protein treatment (Sayed et  
562 al., 2017). In humans, GSS deficiency is an autosomal recessive disorder with varyingly severe clinical  
563 manifestations that include metabolic acidosis, hemolytic anemia, hyperbilirubinemia, neurological  
564 disorders and sepsis (Guney Varal et al., 2019). Deimination of GSS identified here has not been  
565 assessed before and may possibly affect the GSH biosynthesis pathway and such post-translational  
566 regulation remains to be further investigated.

567

568 **Rootletin**, also known as ciliary rootlet coiled-coil protein (CROCC), is a protein that is required for  
569 centrosome cohesion and is therefore important in mitosis (Bahe et al., 2005; Graser et al., 2007). It  
570 was identified here as deiminated in whole llama serum only. Rootletin has been shown to be  
571 phosphorylated and to have the ability to form centriole-associated fibers, suggesting a dynamic  
572 model for centrosome cohesion based on entangling filaments (Bahe et al., 2005). Deletion of rootletin  
573 in mouse models causes photoreceptor degeneration and impaired mucociliary clearance, supporting  
574 its key function in rootlet structures (Yang et al., 2005). Post-translational deimination of rootletin, as  
575 identified here, may possibly facilitate its dynamic functions.

576

577 **Centromere protein J** is a highly conserved and ubiquitously expressed centrosomal protein,  
578 involved in microtubule disassembly and plays a structural role in the maintenance of centrosome  
579 integrity, genome stability and normal spindle morphology during cell division (Tang et al., 2009;  
580 McIntyre, 2012). It was here identified as deiminated in whole llama serum only. Knockout mouse  
581 models targeting the gene encoding this protein have phenotypes of impaired glucose tolerance,  
582 hypoalbuminemia and increased micronuclei, indicative of genomic instability (Gerdin 2010). In  
583 humans, it is associated with primary autosomal recessive microcephaly (Gul et al., 2006) and the  
584 microcephalic primordial dwarfism disorder Seckel syndrome (Al-Dosari et al., 2010; McIntyre et al.,  
585 2012). Deimination has not been described before in this protein to our knowledge.

586

587 **Telomere-associated protein RIF1 isoform 1** is involved in the repair of double-strand DNA breaks in  
588 response to DNA damage (Silverman et al., 2004; Escribano-Díaz et al., 2013; Drané et al., 2017) and  
589 protects telomeres (Fontana et al., 2018). It was identified here as deiminated in EVs only. RIF1 has  
590 been associated with cancer via activation of human telomerase reverse transcriptase expression (Liu  
591 et al., 2018). It is also required for immunoglobulin class-switch recombination during the germinal  
592 centre reaction for humoral antibody immunity (Di Virgilio et al., 2013). RIF1 is involved in telomere  
593 homeostasis and was recently found to be post-translationally S-acylated, identifying a novel  
594 posttranslational modification regulating DNA repair (Fontana et al., 2019). Post-translational  
595 deimination has hitherto not been described.

596

597 **Rabenosyn-5-like protein** was here identified as a deimination protein candidate in both llama whole  
598 serum and EVs. It acts in early endocytic membrane fusion and membrane trafficking of recycling  
599 endosomes (Naslavsky et al., 2004; Rai et al., 2017). It plays a role in the lysosomal trafficking of  
600 CTSD/cathepsin D from the Golgi to lysosomes and also promotes the recycling of transferrin directly  
601 from early endosomes to the plasma membrane (Navaroli et al., 2012). Rabenosyn-5-like protein also

602 binds phospholipid vesicles and plays roles in regulating protein sorting and recycling to the plasma  
603 membrane (Nielsen et al., 2000; de Renzis et al., 2002; Naslavsky et al., 2004). Rabenosyn-5 was  
604 recently identified as an upregulated urinary biomarker associated with malignant upper  
605 gastrointestinal cancer (Husi et al., 2019) and found to be increased in diabetic kidney disease  
606 (Dumont et al., 2017). Rabenosyn-5 has been shown to be phosphorylated, regulating its recruitment  
607 to membranes (Macé et al., 2005). Post-translational deimination has hitherto not been described. .

608

609 ***Spermatogenesis-associated protein 2 (SPATA2)*** was here identified as deiminated in whole llama  
610 serum only. It is expressed in testis and to a lesser extent in spleen, thymus, and prostate (Graziotto  
611 et al., 1999). SPATA2 has been identified as a bridging factor that regulates TNF-alpha-induced  
612 necroptosis and is instrumental for TNF-induced cell death (Elliott et al., 2016; Kupka et al., 2016;  
613 Schlicher et al., 2016; Wagner et al., 2016; Schlicher et al., 2017). SPATA2 ensures normal secretory  
614 function of Sertoli cells (Zhao et al., 2017) and has recently been identified as a novel predictor in  
615 ovarian cancer outcome (Wieser et al., 2019). While SPATA2 has been linked to ubiquitination (Schlicher  
616 et al., 2016), post-translational deimination has not been investigated.

617

618 ***Vitamin D-binding protein (VDBP)*** belongs to the albumin gene family, together with human serum  
619 albumin and alpha-fetoprotein. It is a multifaceted protein mainly produced in the liver, where its  
620 regulation is influenced by estrogen, glucocorticoids and inflammatory cytokines (Bikle and Schwartz,  
621 2019). It is secreted into the blood circulation and is able to bind the various forms of vitamin D  
622 including ergocalciferol (vitamin D<sub>2</sub>) and cholecalciferol (vitamin D<sub>3</sub>), the 25-hydroxylated forms  
623 (calcifediol), and the active hormonal product 1,25-dihydroxyvitamin D (calcitriol) (Verboven et al.,  
624 2002; Norman, 2008). It transports vitamin D metabolites between skin, liver and kidney, and then on  
625 to various target tissues (Norman, 2008). VDBP is a macrophage activating factor (MAF) and has been  
626 tested as an anti-cancer agent via activation of macrophages against cancer cells (Yamamoto et al.,  
627 2008). Some association has also been made between polymorphisms of VDBP and the risk of  
628 coronary artery disease (Tarighi et al., 2017). Post-translational modifications (which still remain to be  
629 identified) of VDBP have been associated with multiple sclerosis (MS) (Perga et al., 2015), while  
630 protein deimination is well known to be associated with MS (Moscarello et al., 2013). VDBP has  
631 previously been identified to be glycosylated (Kilpatrick & Phinney, 2017) but was here identified as a  
632 deimination candidate in whole llama serum only. Post-translational deimination may contribute to  
633 various functions of VDBP in physiological as well as pathophysiological processes.

634

635 ***Pseudopodium-enriched atypical kinase 1*** (PEAK1) was here identified as deiminated in EVs only. It is  
636 a tyrosine kinase and scaffold protein that transmits integrin-mediated extracellular matrix (ECM)  
637 signals to facilitate cell movement and growth. While aberrant expression of PEAK1 has been linked  
638 to cancer progression, its normal physiological role in vertebrate biology is still relatively unknown.  
639 Deletion of the PEAK1 gene in zebrafish, mice and human endothelial cells (ECs) induced severe  
640 defects in new blood vessel formation due to deficiencies in EC proliferation, survival and migration.  
641 PEAK1 seems therefore to play roles in modulation of cell adhesion and growth factor cues from the  
642 extracellular environment necessary for new vessel formation during vertebrate development and  
643 cancer (Wang et al., 2018). PEAK1 has not been described as deiminated before.

644

645 ***Desmoplakin*** was here identified to be deiminated in llama EVs only. Desmoplakin is a unique and  
646 critical component of desmosomal cell-cell junctions and involved in integrity of the cytoskeletal  
647 intermediate filament network (Bendrick et al., 2019). It has been shown to be required for epidermal  
648 integrity and morphogenesis in the *Xenopus laevis* embryo (Bharathan and Dickinson, 2019) and novel  
649 roles in coordination of cell migration were recently established (Bendrick et al., 2019). Mutations in  
650 desmoplakin have been linked to multiple allergies, severe dermatitis and metabolic wasting (SAM)  
651 syndrome (Liang et al., 2019). It is also linked to Carvajal syndrome, involving altered skin and hair  
652 abnormalities, and heart diseases (Yermakovich et al., 2018), including cardiomyopathies (Reichl et  
653 al., 2018; Chen et al., 2019). Desmosomal proteins have been shown to have both tumour-promoting  
654 and tumour-suppressive functions, depending of cancer types and can regulate cell proliferation,  
655 differentiation, migration, apoptosis, and impact treatment sensitivity in different types of cancers  
656 (Zhou et al., 2017). As the roles of desmosomal proteins in cancer and metastasis are not fully  
657 understood, the identification of deiminated desmoplakin in llama EVs here, and not described before,  
658 may be of some interest and add to understanding of diverse functional ability via such post-  
659 translational modification.

660

661 ***TSC22 domain family protein 3***, also called glucocorticoid-induced leucine zipper protein (GILZ), was  
662 here identified as a deimination candidate in llama EVs only. It is a glucocorticoid-responsive molecule  
663 involved in immune regulation and glucocorticoid actions. Its interactions with signal transduction  
664 pathways, many of which are operative in RA and other inflammatory diseases, suggest that it is a key  
665 endogenous regulator of the immune response including a key glucocorticoid-induced regulator of  
666 inflammation in rheumatoid arthritis (RA) (Beaulieu & Morand, 2011). GILZ is a small, 135-amino acid  
667 protein with anti-inflammatory properties and has been shown to inhibit NF- $\kappa$ B and MAPK pathways  
668 (Bereshchenko et al., 2019; Ricci et al., 2019). It has also been shown to be induced in response to

669 hypoxia by a HIF1 $\alpha$ -dependent mechanism and in response to cholesterol starvation, leading to  
670 downstream shedding of procoagulant EVs in ovarian cancer (Koizume et al., 2019). Post-translational  
671 deimination of GILZ has not been described before but may indeed affect its multifaceted functions,  
672 including in inflammation and cancer.

673

674 In the current study we report deiminated proteins in llama serum and serum-derived EVs. Due to the  
675 fact that the llama genome is not yet fully annotated, the hits identified here may underestimate the  
676 amount of deiminated proteins present in llama serum and EVs. Therefore a wider protein-hit analysis  
677 was carried out including other members of the camelid family, using known sequences from *Camelus*  
678 *ferus*, *Camelus dromedaries*, *Lama guanicoe* and *Vicugna pacos*. Deimination of key immune factors  
679 of innate and adaptive immunity and key metabolic proteins is identified here for the first time in a  
680 camelid species, highlighting putative protein moonlighting functions via post-translational  
681 deimination. It must be noted that in relation to previously observed increases of deiminated proteins  
682 with age (Ding et al., 2017), the llama used in this study would be considered relatively old at 21 years  
683 of age, as typical llama lifespans are 15 to 25 years, with some individuals surviving 30 years or more.  
684 Our findings presented here furthermore complement expanding research in the comparative EV  
685 research field. Previous studies on the camel urinary proteome revealed enriched proteins from EVs  
686 and relevance to stress and immune responses as well as antimicrobial activities (Alhaider et al., 2012).  
687 Research on EVs is a relatively new field in comparative immunology and to our knowledge; this is the  
688 first description of EVs in serum of a camelid species. Previous studies on EVs in camelids focussed on  
689 EVs in camel milk, which were shown to have anti-cancerous properties (Badawy et al., 2018). As  
690 PADs have been identified to play major roles in the regulation of EV release (Kholia et al., 2015;  
691 Kosgodage et al., 2017 and 2018), including in host-pathogen interactions (Gavinho et al., 2019), such  
692 EV-mediated communication may be of great relevance also for addressing diverse zoonotic diseases  
693 identified in camels (El-Alfy et al., 2019; Zhu et al., 2019).

694

695 In continuation of the current pilot study, the assessment of changes in deiminated proteins in camelid  
696 serum, and their lateral transfer via EVs, will be of great interest to assess animal health in response  
697 to infection and environmental stress. Our findings will further current understanding of the roles for  
698 EVs, PADs and posttranslational deimination throughout phylogeny and in relation to adaption to a  
699 range of, including extreme, environments. Furthermore, novel identification of post-translational  
700 deimination in key proteins of metabolism and immunity may reveal hitherto unrecognized  
701 moonlighting function of these proteins throughout phylogeny, in relation to physiological and  
702 pathological processes, as well as being translational to and informing inflammatory and metabolic

703 diseases. PAD-mediated contribution to protein moonlighting and in EV-mediated communication in  
704 response to physiological and pathophysiological changes remains therefore a field of further studies.

705

## 706 **Conclusion**

707 This is the first report of deiminated proteins in serum and serum-EVs of a camelid species, using the  
708 llama as a model animal. Our findings highlight a hitherto unrecognized post-translational  
709 modification in key immune and metabolic proteins in camelids, which may be translatable to and  
710 inform a range of human metabolic and inflammatory pathologies.

711

## 712 **Acknowledgements**

713 The authors would like to thank Yagnesh Umrana and Michael Deery at the Cambridge Centre for  
714 Proteomics for the LC-MS/MS analysis, as well as Alice Blue-McLendon of Texas A&M University's  
715 Winnie Carter Wildlife Center for sharing llama serum. This study was funded in part by a University  
716 of Westminster start-up grant to SL and U.S. National Science Foundation grant IOS-1656870 to MFC.  
717 Thanks are due to The Guy Foundation for funding the purchase of equipment utilised in this work.

718

## 719 **Credit Author Statement**

720 **MFC:** Resources; Funding acquisition; Validation; Writing - review & editing.

721 **IK:** Formal analysis; Resources; Validation; Visualization.

722 **SL:** Conceptualization; Data curation; Formal analysis; Funding acquisition; Investigation;  
723 Methodology; Project administration; Resources; Validation; Visualization; Writing -original draft;  
724 Writing - review & editing.

725

## 726 **References**

727 Acher, F., Goudet, C., 2015. Therapeutic potential of group III metabotropic glutamate receptor ligands  
728 in pain. *Curr. Opin. Pharmacol.* 20, 64-72.

729

730 Akef, A., Muljo, S.A., 2018. How T cells go rogue in the absence of Roquins. *Noncoding RNA Investig.*  
731 2, pii: 20.

732

733 Al-Dosari, M.S., Shaheen, R., Colak, D., Alkuraya, F.S., 2010. Novel CENPJ mutation causes Seckel  
734 syndrome. *J. Medical Genetics.* 47 (6), 411-4.

735

736 Alhaider, A.A., Bayoumy, N., Argo, E., Gader, A.G., Stead, D.A., 2012. Survey of the camel urinary  
737 proteome by shotgun proteomics using a multiple database search strategy. *Proteomics.* 12(22), 3403-  
738 6.

739

740 Arab, H.H., Salama, S.A., Abdelghany, T.M., Omar, H.A., Arafa, E.A., Alrobaian, M.M., Maghrabi, I.A.,  
741 2017. Camel Milk Attenuates Rheumatoid Arthritis Via Inhibition of Mitogen Activated Protein Kinase  
742 Pathway. *Cell Physiol Biochem.* 43(2), 540-552.  
743  
744 Arciello, A., Piccoli, R., Monti, D.M., 2016. Apolipoprotein A-I: the dual face of a protein. *FEBS Lett.*  
745 590(23) (2016), 4171-4179.  
746  
747 Armstrong, P. B., Quigley, J.P., 1999. Alpha2-macroglobulin: an evolutionarily conserved arm of the  
748 innate immune system. *Dev. Comp. Immunol.* 23, 375.  
749  
750 Athanasopoulos, V., Ramiscal, R.R., Vinuesa, C.G., 2016. ROQUIN signalling pathways in innate and  
751 adaptive immunity. *Eur. J. Immunol.* 46(5), 1082-90.  
752  
753 Badawy, A.A., El-Magd, M.A., ALSadrah, S.A., 2018. Therapeutic Effect of Camel Milk and Its Exosomes  
754 on MCF7 Cells In Vitro and In Vivo. *Integr Cancer Ther.* 17(4), 1235-1246.  
755  
756 Bağcı, I.S., Horváth, O.N., Ruzicka, T., Sárdy, M., 2017. Bullous pemphigoid. *Autoimmun Rev.* 16(5),  
757 445-455.  
758  
759 Bahe, S., Stierhof, Y.D., Wilkinson, C.J., Leiss, F., Nigg, E.A., 2005. Rootletin forms centriole-associated  
760 filaments and functions in centrosome cohesion. *J Cell Biol.* 171(1), 27-33.  
761  
762 Bannas, P., Koch-Nolte, F., 2018. Perspectives for the Development of CD38-Specific Heavy Chain  
763 Antibodies as Therapeutics for Multiple Myeloma. *Front. Immunol.* 9, 2559.  
764  
765 Bharathan NK, Dickinson AJG., 2019. Desmoplakin is required for epidermal integrity and  
766 morphogenesis in the *Xenopus laevis* embryo. *Dev Biol.*, 450(2),115-131.  
767  
768 Barbe, A., Bongrani, A., Mellouk, N., Estienne, A., Kurowska, P., Grandhay, J., Elfassy, Y., Levy, R., Rak,  
769 A., Froment, P., et al., 2019. Mechanisms of adiponectin action in fertility: An overview from  
770 gametogenesis to gestation in humans and animal models in normal and pathological conditions. *Int.*  
771 *J. Mol. Sci.* 20, 1526.  
772  
773 Barelle, C., Gill, D.S., Charlton, K., 2009. Shark novel antigen receptors--the next generation of biologic  
774 therapeutics? *Adv Exp Med Biol.* 655, 49-62.  
775  
776 Barreira da Silva, R., Laird, M.E., Yatim, N., Fiette, L., Ingersoll, M.A., Albert, M.L., 2015.  
777 Dipeptidylpeptidase 4 inhibition enhances lymphocyte trafficking, improving both naturally occurring  
778 tumor immunity and immunotherapy. *Nat Immunol.* 16(8), 850-8.  
779  
780 Basseri, S., Ly, T.Y., Hull, P.R. J., 2018. Dyshidrotic Bullous Pemphigoid: Case Report and Review of  
781 Literature. *Cutan Med Surg.* 22(6), 614-617.  
782  
783 Beaulieu, E., Morand, E.F., 2011. Role of GILZ in immune regulation, glucocorticoid actions and  
784 rheumatoid arthritis. *Nat Rev Rheumatol.* 7(6), 340-8.  
785  
786 Bendrick, J.L., Eldredge, L.A., Williams, E.I., Haight, N.B., Dubash, A.D., 2019. Desmoplakin Harnesses  
787 Rho GTPase and p38 Mitogen-Activated Protein Kinase Signaling to Coordinate Cellular Migration. *J.*  
788 *Invest. Dermatol.* 139(6), 1227-1236.  
789

790 Bereshchenko, O., Migliorati, G., Bruscoli, S., Riccardi, C., 2019. Glucocorticoid-Induced Leucine Zipper:  
791 A Novel Anti-inflammatory Molecule. *Front Pharmacol.*,10, 308.  
792

793 Besser, M.W., MacDonald, S.G., 2016. Acquired hypofibrinogenemia: Current perspectives. *J. Blood*  
794 *Med.* 7, 217–225.  
795

796 Bever, C.S., Dong, J-X., Vasylieva, N., Barnych, B., Cui, Y., Xu, Z-L., et al., 2016. VHH antibodies:  
797 emerging reagents for the analysis of environmental chemicals. *Anal Bioanal Chem* 408, 5985–6002.  
798

799 Bicker, K.L., Thompson, P.R., 2013. The protein arginine deiminases: Structure, function, inhibition,  
800 and disease. *Biopolymers.* 99(2), 155-63.  
801

802 Bird, A., 2007. Perceptions of epigenetics. *Nature* 447, 396–398.  
803

804 Bikle, D.D., Schwartz, J., 2019. Vitamin D Binding Protein, Total and Free Vitamin D Levels in Different  
805 Physiological and Pathophysiological Conditions. *Front Endocrinol (Lausanne).* 10, 317.  
806

807 Blachère, N.E., Parveen, S., Frank, M.O., Dill, B.D., Molina, H., Orange, D.E., 2017. High-Titer  
808 Rheumatoid Arthritis Antibodies Preferentially Bind Fibrinogen Citrullinated by Peptidylarginine  
809 Deiminase 4. *Arthritis Rheumatol.* 69(5), 986-995.  
810

811 Bost, F., Diarra-Mehrpour, M., Martin, J.P., 1998. Inter-alpha-trypsin inhibitor proteoglycan family – a  
812 group of proteins binding and stabilizing the extracellular matrix. *Eur. J. Biochem.* 252, 339-346.  
813

814 Branzk, N., Lubojemska, A., Hardison, S.E., Wang, Q., Gutierrez, M.G., Brown, G.D., Papayannopoulos,  
815 V., 2014. Neutrophils sense microbe size and selectively release neutrophil extracellular traps in  
816 response to large pathogens. *Nat. Immunol.* 15(11), 1017-25.  
817

818 Brinkmann, V., Reichard, U., Goosmann, C., Fauler, B., Uhlemann, Y., Weiss, D.S., Weinrauch, Y.,  
819 Zychlinsky, A., 2004. Neutrophil extracellular traps kill bacteria. *Science.* 303, 1532–1535.  
820

821 Brooks, C.L., Rossotti, M.A., Henry, K.A., 2018. Immunological Functions and Evolutionary Emergence  
822 of Heavy-Chain Antibodies. *Trends Immunol.* 39(12), 956-960.  
823

824 Buchner J., 1999. Hsp90 & Co. - a holding for folding. *Trends Biochem. Sci.* 24 (4), 136–41.  
825

826 Carroll, M.V., Sim, R.B., 2011. Complement in health and disease. *Adv. Drug Deliv. Rev.* 63(12), 965-  
827 75.  
828

829 Chen, R., Kang, R., Fan, X.-G., Tang, D., 2014. Release and activity of histone in diseases. *Cell Death Dis.*  
830 5, e1370.  
831

832 Chen, Y.L., Tao, J., Zhao, P.J., Tang, W., Xu, J.P., Zhang, K.Q., Zou, C.G., 2019. Adiponectin receptor  
833 PAQR-2 signaling senses low temperature to promote *C. elegans* longevity by regulating autophagy.  
834 *Nat Commun.* 10(1), 2602.  
835

836 Chen, L., Song, J., Chen, X., Chen, K., Ren, J., Zhang, N., Rao, M., Hu, Z., Zhang, Y., Gu, M., Zhao, H.,  
837 Tang, H., Yang, Z., Hu, S., 2019. A novel genotype-based clinicopathology classification of  
838 arrhythmogenic cardiomyopathy provides novel insights into disease progression. *Eur Heart J.* 40(21),  
839 1690-1703.  
840

841 Chiosis, G., Caldas Lopes, E., Solit, D., 2006. Heat shock protein-90 inhibitors: a chronicle from  
842 geldanamycin to today's agents. *Curr Opin Investig Drugs*. 7 (6), 534–41.

843

844 Cohen, J., 2018. Llama antibodies inspire gene spray to prevent all flus. *Science*. 362(6414), 511.

845

846 Colombo, M., Raposo, G., Théry, C., 2014. Biogenesis, secretion, and intercellular interactions of  
847 exosomes and other extracellular vesicles. *Annu. Rev. Cell Dev. Biol.* 30, 255–289.

848

849 Criscitiello, M.F., 2014. What the shark immune system can and cannot provide for the expanding  
850 design landscape of immunotherapy. *Expert Opin Drug Discov.* 9(7), 725-39.

851

852 Criscitiello, M.F., Kraev, I., Lange, S., 2019. Deiminated proteins in extracellular vesicles and plasma of  
853 nurse shark (*Ginglymostoma cirratum*) - Novel insights into shark immunity. *Fish Shellfish Immunol.*  
854 92, 249-255.

855

856 Cromie, K.D., Van Heeke, G., Boutton, C., 2015. Nanobodies and their use in GPCR drug discovery. *Curr*  
857 *Top Med Chem* 15, 2543–57.

858

859 Danquah, W., Meyer-Schwesinger, C., Rissiek, B., Pinto, C., Serracant-Prat, A., Amadi, M., et al., 2016.  
860 Nanobodies that block gating of the P2X7 ion channel ameliorate inflammation. *Sci Transl Med.* 8,  
861 366ra162.

862

863 Davies, S.G., Sim, R.B., 1981. Intramolecular general acid catalysis in the binding reactions of alpha 2-  
864 macroglobulin and complement components C3 and C4. *Biosci Rep.* 1(6), 461-8.

865

866 de los Rios, M., Criscitiello, M.F., Smider, V.V., 2015. Structural and genetic diversity in antibody  
867 repertoires from diverse species. *Curr Opin Struct Biol.* 33, 27-41.

868

869 de Renzis, S., Sönnichsen, B., Zerial, M., 2002. Divalent Rab effectors regulate the sub-compartmental  
870 organization and sorting of early endosomes. *Nat Cell Biol.* 4(2), 124-33.

871

872 De Silva, D.P.N., Tan, E., Mizuno, N., Hosoya, S., Reza, M.S., Watabe, S., Kinoshita, S., Asakawa, S.,  
873 2019. Transcriptomic analysis of immunoglobulin novel antigen receptor (IgNAR) heavy chain constant  
874 domains of brownbanded bamboo shark (*Chiloscyllium punctatum*). *Fish Shellfish Immunol.* 84, 370-  
875 376.

876

877 Del Rio-Tsonis, K., Tsonis, P.A., Zarkadis, I.K., Tsagas, A.G., Lambris, J.D., 1998. Expression of the third  
878 component of complement, C3, in regenerating limb blastema cells of urodeles. *J. Immunol.* 161(12),  
879 6819-24.

880

881 Deschaght, P., Vintém, A.P., Logghe, M., Conde, M., Felix, D., Mensink, R., Gonçalves, J., Audiens, J.,  
882 Bruynooghe, Y., Figueiredo, R., Ramos, D., Tanghe, R., Teixeira, D., Van de Ven, L., Stortelers, C.,  
883 Dombrecht, B., 2017. Large Diversity of Functional Nanobodies from a Camelid Immune Library  
884 Revealed by an Alternative Analysis of Next-Generation Sequencing Data. *Front Immunol.* 8, 420.

885

886 Ding D., Enriquez-Algeciras M., Bhattacharya S.K., Bonilha V.L. 2017. Protein Deimination in Aging and  
887 Age-Related Diseases with Ocular Manifestations. In: Nicholas A., Bhattacharya S., Thompson P. (eds)  
888 Protein Deimination in Human Health and Disease. Springer, Cham.

889

890 Di Virgilio, M., Callen, E., Yamane, A., Zhang, W., Jankovic, M., Gitlin, A.D., Feldhahn, N., Resch, W.,  
891 Oliveira, T.Y., Chait, B.T., Nussenzweig, A., Casellas, R., Robbiani, D.F, Nussenzweig, M.C., 2013. Rif1

892 prevents resection of DNA breaks and promotes immunoglobulin class switching. *Science*. 339(6120),  
893 711-5.

894

895 Dodds, A.W., 2002. Which came first, the lectin/classical pathway or the alternative pathway of  
896 complement? *Immunobiology*. 205(4-5), 340-54.

897

898 Dodds, A.W., Law, S.K., 1998. The phylogeny and evolution of the thioester bond-containing proteins  
899 C3, C4 and alpha 2-macroglobulin. *Immunol. Rev.* 166, 15-26.

900

901 Drané, P., Brault, M.E., Cui, G., Meghani, K., Chaubey, S., Detappe, A., Parnandi, N., He, Y., Zheng, X.F.,  
902 Botuyan, M.V., Kalousi, A., Yewdell, W.T., Münch, C., Harper, J.W., Chaudhuri, J., Soutoglou, E., Mer,  
903 G., Chowdhury, D., 2017. TIRR regulates 53BP1 by masking its histone methyl-lysine binding function.  
904 *Nature*. 543(7644), 211-216.

905

906 Dumont, V., Tolvanen, T.A., Kuusela, S., Wang, H., Nyman, T.A., Lindfors, S., Tienari, J., Nisen, H.,  
907 Suetsugu, S., Plomann, M., Kawachi, H., Lehtonen, S., 2017. PACSIN2 accelerates nephrin trafficking  
908 and is up-regulated in diabetic kidney disease. *FASEB J.* 31(9) (2017), 3978-3990.

909

910 Duygu, F., Aksoy, N., Cicek, A.C., Butun, I., Unlu, S., 2013. Does prolidase indicate worsening of  
911 hepatitis B infection?. *Journal of Clinical Laboratory Analysis*. 27 (5), 398–401.

912

913 El-Alfy, E.S., Abu-Elwafa, S., Abbas, I., Al-Araby, M., Al-Kappany, Y., Umeda, K., Nishikawa, Y., 2019.  
914 Molecular screening approach to identify protozoan and trichostrongylid parasites infecting one-  
915 humped camels (*Camelus dromedarius*). *Acta Trop.* 197, 105060.

916

917 El-Bahr, S.M., El-Deeb, W.M., 2016. *Trypanosoma evansi* in naturally infected dromedary camels: lipid  
918 profile, oxidative stress parameters, acute phase proteins and proinflammatory cytokines.  
919 *Parasitology*. 143(4) (2016), 518-22.

920

921 El-Deeb, W.M., Buczinski, S., 2015. The diagnostic and prognostic importance of oxidative stress  
922 biomarkers and acute phase proteins in Urinary Tract Infection (UTI) in camels. *PeerJ*. 3, e1363.

923

924 El-Malky, O.M., Mostafa, T.H., Abd El-Salaam, A.M., Ayyat, M.S., 2018. Effect of reproductive disorders  
925 on productivity and reproductive efficiency of dromedary she-camels in relation to cytokine  
926 concentration. *Trop Anim Health Prod.* 50(5), 1079-1087.

927

928 Elliott, P.R., Leske, D., Hrdinka, M., Bagola, K., Fiil, B.K., McLaughlin, S.H., Wagstaff, J., Volkmar, N.,  
929 Christianson, J.C., Kessler, B.M., Freund, S.M., Komander, D., Gyrd-Hansen, M., 2016. SPATA2 Links  
930 CYLD to LUBAC, Activates CYLD, and Controls LUBAC Signaling. *Mol Cell*. 63(6), 990-1005.

931

932 Escribano-Díaz, C., Orthwein, A., Fradet-Turcotte, A., Xing, M., Young, J.T., Tkáč, J., Cook, M.A.,  
933 Rosebrock, A.P., Munro, M., Canny, M.D., Xu, D., Durocher, D., 2013. A cell cycle-dependent regulatory  
934 circuit composed of 53BP1-RIF1 and BRCA1-CtIP controls DNA repair pathway choice. *Mol Cell*. 49(5),  
935 872-83.

936

937 Essig, K., Kronbeck, N., Guimaraes, J.C., Lohs, C., Schlundt, A., Hoffmann, A., Behrens, G., Brenner, S.,  
938 Kowalska, J., Lopez-Rodriguez, C., Jemielity, J., Holtmann, H., Reiche, K., Hackermüller, J., Sattler, M.,  
939 Zavolan, M., Heissmeyer, V., 2018. Roquin targets mRNAs in a 3'-UTR-specific manner by different  
940 modes of regulation. *Nat Commun*. 9(1), 3810.

941

942 Fishelson, Z., Attali, G., Mevorach, D., 2001. Complement and apoptosis. *Mol. Immunol.* 38(2-3), 207-  
943 19.  
944  
945 Fiaschi, T., 2019. Mechanisms of Adiponectin Action. *Int J Mol Sci.* 20(12), pii, E2894.  
946  
947 Fiaschi, T., Magherini, F., Gamberi, T., Modesti, P.A., Modesti, A., 2014. Adiponectin as a tissue  
948 regenerating hormone: More than a metabolic function. *Cell. Mol. Life Sci.*, 71, 1917–1925.  
949  
950 Flajnik, M.F., Dooley, H., 2009. The generation and selection of single-domain, v region libraries from  
951 nurse sharks. *Methods Mol Biol.* 562, 71-82.  
952  
953 Fontana, G.A., Reinert, J.K., Thomä, N.H., Rass, U., 2018. Shepherding DNA ends: Rif1 protects  
954 telomeres and chromosome breaks. *Microb Cell.* 5(7), 327-343.  
955  
956 Fontana, G.A., Hess, D., Reinert, J.K., Mattarocci, S., Falquet, B., Klein, D., Shore, D., Thomä, N.H., Rass,  
957 U., 2019. Rif1 S-acylation mediates DNA double-strand break repair at the inner nuclear membrane.  
958 *Nat Commun.* 10(1), 2535.  
959  
960 Frankenberg, A.D.V., Reis, A.F., Gerchman, F., 2017. Relationships between adiponectin levels, the  
961 metabolic syndrome, and type 2 diabetes: a literature review. *Arch Endocrinol Metab.* 61(6), 614-622.  
962  
963 French, L.E., Wohlwend, A., Sappino, A.P., Tschopp, J., Schifferli, J.A., 1994. Human clusterin gene  
964 expression is confined to surviving cells during in vitro programmed cell death. *J. Clin. Invest.* 93(2),  
965 877-84.  
966  
967 Funato, Y., Michiue, T., Asashima, M., Miki, H., 2006. The thioredoxin-related redox-regulating protein  
968 nucleoredoxin inhibits Wnt-beta-catenin signalling through dishevelled. *Nat Cell Biol.* 8(5), 501-8.  
969  
970 Gamberi, T., Magherini, F., Fiaschi, T., 2019. Adiponectin in myopathies. *Int. J. Mol. Sci.* 20, 1544.  
971  
972 Gavinho, B, Rossi., IV, Evans-Osses, I., Lange, S., Ramirez, M.I., 2019. Peptidylarginine Deiminase  
973 inhibition abolishes the production of large extracellular vesicles from *Giardia intestinalis*, affecting  
974 host-pathogen interactions by hindering adhesion to host cells. *bioRxiv* 2019; 586438; doi:  
975 <https://doi.org/10.1101/586438>.  
976  
977 Gerdin, A.K., 2010. The Sanger Mouse Genetics Programme: High throughput characterisation of  
978 knockout mice. *Acta Ophthalmologica.* 88, 925–7.  
979  
980 Goetz, M.P., Toft, D.O., Ames, M.M., Erlichman, C., 2003. The Hsp90 chaperone complex as a novel  
981 target for cancer therapy. *Ann. Oncol.* 14 (8), 1169–76.  
982  
983 Gonzalez-Aparicio, M., Alfaro, C., 2019. Influence of Interleukin-8 and Neutrophil Extracellular Trap  
984 (NET) Formation in the Tumor Microenvironment: Is There a Pathogenic Role? *J Immunol Res.*2019,  
985 6252138.  
986  
987 Gonzalez, S., Aguilera, S., Alliende, C., Urzua, U., Quest, A. F., Herrera, L., Molina, C., Hermoso, M.,  
988 Ewert, P., Brito, M., Romo, R., Leyton, C., Pérez, P., González, M.J., 2011. Alterations in type I  
989 hemidesmosome components suggestive of epigenetic control in the salivary glands of patients with  
990 Sjögren’s syndrome. *Arthritis Rheum.* 63, 1106–1115.  
991

992 Graser, S., Stierhof, Y.D., Nigg, E.A., 2007. Cep68 and Cep215 (Cdk5rap2) are required for centrosome  
993 cohesion. *J Cell Sci.* 120 (24), 4321-31.  
994  
995 Graziotto, R., Foresta, C., Scannapieco, P., Zeilante, P., Russo, A., Negro, A., Salmaso, R., Onisto, M.,  
996 1999. cDNA cloning and characterization of PD1: a novel human testicular protein with different  
997 expressions in various testiculopathies. *Exp Cell Res.* 248(2), 620-6.  
998  
999 Greenberg, A.S., Avila, D., Hughes, M., Hughes, A., McKinney, E.C., Flajnik, M.F., 1995. A new antigen  
1000 receptor gene family that undergoes rearrangement and extensive somatic diversification in sharks.  
1001 *Nature.* 374(6518), 168-73.  
1002  
1003 Greunz, E.M., Krogh, A.K.H., Pieters, W., Ruiz, O.A., Bohner, J., Reckendorf, A., Monaco, D., Bertelsen,  
1004 M.F., 2018. THE ACUTE-PHASE AND HEMOSTATIC RESPONSE IN DROMEDARY CAMELS ( CAMELUS  
1005 DROMEDARIUS). *J Zoo Wildl Med.* 49(2), 361-370.  
1006  
1007 Gul, A, Hassan, M.J., Hussain, S., Raza, S.I., Chishti, M.S., Ahmad, W., 2006. A novel deletion mutation  
1008 in CENPJ gene in a Pakistani family with autosomal recessive primary microcephaly. *Journal of Human*  
1009 *Genetics.* 51 (9), 760–4.  
1010  
1011 Guney, Varal, I., Dogan, P., Gorukmez, O., Dorum, S., Akdag, A., 2019. Glutathione synthetase  
1012 deficiency: a novel mutation with femur agenesis. *Fetal Pediatr Pathol.* 14, 1-7.  
1013  
1014 György, B., Toth, E., Tarcsa, E., Falus, A., Buzas, E.I., 2006. Citrullination: a posttranslational  
1015 modification in health and disease. *Int. J. Biochem. Cell Biol.* 38, 1662–77.  
1016  
1017 Hagiwara, T., Hidaka, Y., Yamada, M., 2005. Deimination of histone H2A and H4 at arginine 3 in HL-60  
1018 granulocytes. *Biochemistry* 44, 5827–5834.  
1019  
1020 Hamilton, K.K., Zhao, J., Sims, P.J., 1993. Interaction between apolipoproteins A-I and A-II and the  
1021 membrane attack complex of complement. Affinity of the apoproteins for polymeric C9. *J. Biol. Chem.*  
1022 268(5), 3632-8.  
1023  
1024 Hamm, A., Veeck, J., Bektas, N., Wild, P.J., Hartmann, A., Hendrichs, U., Kristiansen, G., Werbowetski-  
1025 Ogilvie, T., Del Maestro, R., Knüchel, R., Dahl, E., 2008. Frequent expression loss of Inter- $\alpha$ -trypsin  
1026 inhibitor heavy chain (ITI $\text{H}$ ) genes in multiple human solid tumors: a systematic expression analysis.  
1027 *BMC Cancer.* 8, 25.  
1028  
1029 Harmsen, M.M., De Haard, H.J., 2007. Properties, production, and applications of camelid single-  
1030 domain antibody fragments. *Appl Microbiol Biotechnol.* 77(1), 13-22.  
1031  
1032 Hassiki, R., Labro, A.J., Benlasfar, Z., Vincke, C., Somia, M., El Ayeb, M., et al., 2016. Dromedary immune  
1033 response and specific Kv2.1 antibody generation using a specific immunization approach. *Int J Biol*  
1034 *Macromol* 93, 167–71.  
1035  
1036 Haynes, T., Luz-Madriral, A., Reis, E.S., Echeverri Ruiz, N.P., Grajales-Esquivel, E., Tzekou, A., Tsonis,  
1037 P.A., Lambris, J.D., Del Rio-Tsonis K., 2013. Complement anaphylatoxin C3a is a potent inducer of  
1038 embryonic chick retina regeneration. *Nat. Commun.* 4, 2312.  
1039  
1040 Henderson, B., Martin, A.C., 2014. Protein moonlighting: a new factor in biology and medicine.  
1041 *Biochem. Soc. Trans.* 42(6), 1671-8.  
1042

1043 Henry, K.A., van Faassen, H., Harcus, D., Marcil, A., Hill, J.J., Muyldermans, S., MacKenzie, C.R., 2019.  
1044 Llama peripheral B-cell populations producing conventional and heavy chain-only IgG subtypes are  
1045 phenotypically indistinguishable but immunogenetically distinct. *Immunogenetics*. 71(4), 307-320.  
1046  
1047 Hessvik, N.P., Llorente, A., 2018. Current knowledge on exosome biogenesis and release. *Cell Mol Life*  
1048 *Sci*. 75, 193-208.  
1049  
1050 Hida, S., Miura, N.N., Adachi, Y., Ohno, N., 2004. Influence of arginine deimination on antigenicity of  
1051 fibrinogen. *J. Autoimmun.* 23(2), 141-50.  
1052  
1053 Hughes-Austin, J.M., Deane, K.D., Giles, J.T., Derber, L.A., Zerbe, G.O., Dabelea, D.M., Sokolove, J.,  
1054 Robinson, W.H., Holers, V.M., Norris, J.M., 2018. Plasma adiponectin levels are associated with  
1055 circulating inflammatory cytokines in autoantibody positive first-degree relatives of rheumatoid  
1056 arthritis patients. *PLoS One*. 13(6), e0199578.  
1057  
1058 Husi, H., Fernandes, M., Skipworth, R.J., Miller, J., Cronshaw, A.D., Fearon, K.C.H., Ross, J.A., 2019.  
1059 Identification of diagnostic upper gastrointestinal cancer tissue type-specific urinary biomarkers.  
1060 *Biomed Rep*. 10(3), 165-174.  
1061  
1062 Hussack, G., Raphael, S., Lowden, M.J., Henry, K.A., 2018. Isolation and characterization of camelid  
1063 single-domain antibodies against HER2. *BMC Res Notes*. 11(1), 866.  
1064  
1065 Hutchinson, D., Clarke, A., Heesom, K., Murphy, D., Eggleton, P., 2017. Carbamylation/citrullination of  
1066 IgG Fc in bronchiectasis, established RA with bronchiectasis and RA smokers: a potential risk factor for  
1067 disease. *ERJ. Open Res*. 3(3), pii: 00018-2017.  
1068  
1069 Iliev, D., Strandskog, G., Nepal, A., Aspar, A., Olsen, R., Jørgensen, J., Wolfson, D., Ahluwalia, B.S.,  
1070 Handzhiyski, J., Mironova, R., 2018. Stimulation of exosome release by extracellular DNA is conserved  
1071 across multiple cell types. *FEBS J*. 285(16), 3114-3133.  
1072  
1073 Immenschuh, S., Vijayan, V., Janciauskiene, S., Gueler, F., 2017. Heme as a Target for Therapeutic  
1074 Interventions. *Front. Pharmacol*. 8 (2017), 146  
1075  
1076 Imai, J., Maruya, M., Yashiroda, H., Yahara, I., Tanaka, K., 2003. The molecular chaperone Hsp90 plays  
1077 a role in the assembly and maintenance of the 26S proteasome. *EMBO J*. 22 (14), 3557-67.  
1078  
1079 Inal, J.M., Ansa-Addo, E.A., Lange, S., 2013. Interplay of host-pathogen microvesicles and their role in  
1080 infectious disease. *Biochem Soc Trans*. 1;41(1), 258-62.  
1081  
1082 Iqbal, U., Trojahn, U., Albaghdadi, H., Zhang, J., O'Connor-McCourt, M., Stanimirovic, D., Tomanek, B.,  
1083 Sutherland, G., Abulrob, A., 2010. Kinetic analysis of novel mono- and multivalent VHH-fragments and  
1084 their application for molecular imaging of brain tumours. *Br J Pharmacol*. 160(4), 1016-28.  
1085  
1086 Jeffrey, C.J., 2018. Protein moonlighting: what is it, and why is it important? *Philos. Trans. R. Soc. Lond.*  
1087 *B. Biol. Sci*. 373(1738), pii 20160523.  
1088  
1089 Jenne, D.E., Lowin, B., Peitsch, M.C., Böttcher, A., Schmitz, G., Tschopp, J., 1991. Clusterin  
1090 (complement lysis inhibitor) forms a high density lipoprotein complex with apolipoprotein A-I in  
1091 human plasma. *J. Biol. Chem*. 266(17), 11030-6.  
1092

1093 Julio-Pieper, M., O'Connor, R.M., Dinan, T.G., Cryan, J.F., 2013. Regulation of the brain-gut axis by  
1094 group III metabotropic glutamate receptors. *Eur J Pharmacol.* 698(1-3), 19-30.  
1095  
1096 Kholia, S., Jorfi, S., Thompson, P.R., Causey, C.P., Nicholas, A.P., Inal, J., Lange, S., 2015. A Novel Role  
1097 for Peptidylarginine Deiminases (PADs) in Microvesicle Release: A Therapeutic Potential for PAD  
1098 Inhibitors to Sensitize Prostate Cancer Cells to Chemotherapy. *J Extracell Vesicles.* 4, 26192.  
1099  
1100 Kilpatrick, L.E., Phinney, K.W., 2017. Quantification of Total Vitamin-D-Binding Protein and the  
1101 Glycosylated Isoforms by Liquid Chromatography-Isotope Dilution Mass Spectrometry. *J Proteome*  
1102 *Res.* 16(11), 4185-4195.  
1103  
1104 Kitchener, R.L., Grunden, A.M., 2012. Prolidase function in proline metabolism and its medical and  
1105 biotechnological applications. *Journal of Applied Microbiology.* 113 (2), 233–47.  
1106  
1107 Koizume, S., Takahashi, T., Yoshihara, M., Nakamura, Y., Ruf, W., Takenaka, K., Miyagi, E., Miyagi, Y.,  
1108 2019. Cholesterol Starvation and Hypoxia Activate the FVII Gene via the SREBP1-GILZ Pathway in  
1109 Ovarian Cancer Cells to Produce Procoagulant Microvesicles. *Thromb Haemost.* 119(7), 1058-1071.  
1110  
1111 Kojouharova, M.S., Gadjeva, M.G., Tsacheva, I.G., Zlatarova, A., Roumenina, L.T., Tchorbadjieva, M.I.,  
1112 Atanasov, B.P., Waters, P., Urban, B.C., Sim, R.B., Reid, K.B., Kishore, U., 2004. Mutational analyses of  
1113 the recombinant globular regions of human C1q A, B, and C chains suggest an essential role for  
1114 arginine and histidine residues in the C1q-IgG interaction. *J. Immunol.* 172(7), 4351-8.  
1115  
1116 Könning, D., Zielonka, S., Grzeschik, J., Empting, M., Valldorf, B., Krah, S., Schröter, C., Sellmann, C.,  
1117 Hock, B., Kolmar, H., 2017. Camelid and shark single domain antibodies: structural features and  
1118 therapeutic potential. *Curr Opin Struct Biol.* 45, 10-16.  
1119  
1120 Konsta, O.D., Thabet, Y., Le Dantec, C., Brooks, W.H., Tzioufas, A.G., Pers, J.O., Renaudineau, Y., 2014.  
1121 The contribution of epigenetics in Sjögren's Syndrome. *Front Genet.* 5, 71.  
1122  
1123 Kosgodage, U.S., Trindade, R.P., Thompson, P.T., Inal, J.M., Lange, S., 2017.  
1124 Chloramide/Bisindolylmaleimide-I-Mediated Inhibition of Exosome and Microvesicle Release and  
1125 Enhanced Efficacy of Cancer Chemotherapy. *Int J Mol Sci.* 18(5), pii E1007.  
1126  
1127 Kosgodage, U.S., Onganer, P.U., Maclatchy, A., Nicholas, A.P., Inal, J.M., Lange, S., 2018.  
1128 Peptidylarginine Deiminases Post-translationally Deiminate Prohibitin and Modulate Extracellular  
1129 Vesicle Release and miRNAs 21 and 126 in Glioblastoma Multiforme. *Int J Mol Sci.* 20(1), pii E103.  
1130  
1131 Kosgodage, U.S., Matewele, P., Mastroianni, G., Kraev, I., Brotherton, D., Awamaria, B., Nicholas, A.P.,  
1132 Lange, S., Inal, J.M. 2019. Peptidylarginine Deiminase Inhibitors Reduce Bacterial Membrane Vesicle  
1133 Release and Sensitize Bacteria to Antibiotic Treatment. *Front. Cell. Infect. Microbiol.* 9, 227.  
1134  
1135 Kupka, S., De Miguel, D., Draber, P., Martino, L., Surinova, S., Rittinger, K., Walczak, H., 2016. SPATA2-  
1136 Mediated Binding of CYLD to HOIP Enables CYLD Recruitment to Signaling Complexes. *Cell Rep.* 16(9),  
1137 2271-80.  
1138  
1139 Lange, S., Bambir, S., Dodds, A.W., Magnadottir, B., 2004a. The ontogeny of complement component  
1140 C3 in Atlantic Cod (*Gadus morhua* L.)—an immunohistochemical study. *Fish Shellfish Immunol.* 16,  
1141 359-367.  
1142

1143 Lange, S., Bambir, S., Dodds, A.W., Magnadottir, B., 2004b. An immunohistochemical study on  
1144 complement component C3 in juvenile Atlantic halibut (*Hippoglossus hippoglossus* L.). *Dev. Comp.*  
1145 *Immunol.* 28(6), 593-601.  
1146  
1147 Lange, S., Dodds, A.W., Gudmundsdóttir, S., Bambir, S.H., Magnadottir, B., 2005. The ontogenic  
1148 transcription of complement component C3 and Apolipoprotein A-I tRNA in Atlantic cod (*Gadus*  
1149 *morhua* L.)--a role in development and homeostasis? *Dev. Comp. Immunol.* 29(12), 1065-77.  
1150  
1151 Lange, S., Bambir, S.H., Dodds, A.W., Bowden, T., Bricknell, I., Espelid, S., Magnadottir, B., 2006.  
1152 Complement component C3 transcription in Atlantic halibut (*Hippoglossus hippoglossus* L.) larvae.  
1153 *Fish Shellfish Immunol.* 20(3), 285-94.  
1154  
1155 Lange, S., Gögel, S., Leung, K.Y., Vernay, B., Nicholas, A.P., Causey, C.P., Thompson, P.R., Greene, N.D.,  
1156 Ferretti, P., 2011. Protein deiminases: new players in the developmentally regulated loss of neural  
1157 regenerative ability. *Dev. Biol.* 355(2), 205-14.  
1158  
1159 Lange, S., Rocha-Ferreira, E., Thei, L., Mawjee, P., Bennett, K., Thompson, P.R., Subramanian, V.,  
1160 Nicholas, A.P., Peebles, D., Hristova, M., Raivich, G., 2014. Peptidylarginine deiminases: novel drug  
1161 targets for prevention of neuronal damage following hypoxic ischemic insult (HI) in neonates. *J.*  
1162 *Neurochem.* 130(4), 555-62.  
1163  
1164 Lange, S., Gallagher, M., Kholia, S., Kosgodage, U.S., Hristova, M., Hardy, J., Inal, J.M., 2017.  
1165 Peptidylarginine Deiminases-Roles in Cancer and Neurodegeneration and Possible Avenues for  
1166 Therapeutic Intervention via Modulation of Exosome and Microvesicle (EMV) Release? *Int. J. Mol. Sci.*  
1167 18(6), pii E1196.  
1168  
1169 Latham, J.A., Dent, S.Y., 2007. Cross-regulation of histone modifications. *Nat. Struct. Mol. Biol.*, 14,  
1170 1017-1024.  
1171  
1172 Lee, KH, Kronbichler, A, Park, DD, Park, Y, Moon, H, Kim, H, Choi, JH, Choi, Y, Shim, S, Lyu, IS, et al.,  
1173 2017. Neutrophil extracellular traps (NETs) in autoimmune diseases: A comprehensive review.  
1174 *Autoimmun Rev.* 16(11):1160-1173.  
1175  
1176 Lee, S.Y., Lee, S.H., Seo, H.B., Ryu, J.G., Jung, K., Choi, J.W., Jhun, J., Park, J.S., Kwon, J.Y., Kwok, S.K.,  
1177 Youn, J., Park, S.H., Cho, M.L., 2019. Inhibition of IL-17 ameliorates systemic lupus erythematosus in  
1178 Roquinsan/san mice through regulating the balance of TFH cells, GC B cells, Treg and Breg. *Sci Rep.*  
1179 9(1), 5227.  
1180  
1181 Levecque, C., Velayos-Baeza, A., Holloway, Z.G., Monaco, A.P., 2009. The dyslexia-associated protein  
1182 KIAA0319 interacts with adaptor protein 2 and follows the classical clathrin-mediated endocytosis  
1183 pathway. *Am J Physiol Cell Physiol.* 297(1), C160-8  
1184  
1185 Li, P., Li, M., Lindberg, M.R., Kennett, M.J., Xiong, N., Wang, Y., 2010. PAD4 is essential for antibacterial  
1186 innate immunity mediated by neutrophil extracellular traps. *J. Exp. Med.* 207(9), 1853-62.  
1187  
1188 Liang, J., Li C., Zhang, Z., Ni, C., Yu, H., Li, M., Yao, Z., 2019. Severe dermatitis, multiple allergies and  
1189 metabolic wasting (SAM) syndrome caused by de novo mutation in the DSP gene misdiagnosed as  
1190 generalized pustular psoriasis and treatment of acitretin with gabapentin. *J Dermatol.* 2019 May 20.  
1191 doi: 10.1111/1346-8138.14925. [Epub ahead of print]  
1192

1193 Linnankivi, T., Neupane, N., Richter, U., Isohanni, P., Tynismaa, H., 2016. Splicing Defect in  
1194 Mitochondrial Seryl-tRNA Synthetase Gene Causes Progressive Spastic Paresis Instead of HUPRA  
1195 Syndrome. *Hum Mutat.* 37(9), 884-8.

1196

1197 Liu, Y.B., Mei, Y., Long, J., Zhang, Y., Hu, D.L., Zhou, H.H., 2018. RIF1 promotes human epithelial ovarian  
1198 cancer growth and progression via activating human telomerase reverse transcriptase expression. *J*  
1199 *Exp Clin Cancer Res.* 37(1), 182.

1200

1201 Liu, R, Zhao, P, Zhang, Q, Che, N, Xu, L, Qian, J, Tan, W, Zhang, M., 2019. Adiponectin promotes  
1202 fibroblast-like synoviocytes producing IL-6 to enhance T follicular helper cells response in rheumatoid  
1203 arthritis. *Clin Exp Rheumatol.* 2019 Apr 11. [Epub ahead of print]

1204

1205 Lu, J., Kishore, U., 2017. C1 Complex: An Adaptable Proteolytic Module for Complement and Non-  
1206 Complement Functions. *Front. Immunol.* 8, 592.

1207

1208 Macé, G., Miaczynska, M., Zerial, M., Nebreda, A.R., 2005. Phosphorylation of EEA1 by p38 MAP kinase  
1209 regulates mu opioid receptor endocytosis. *EMBO J.*, 24(18), 3235-46.

1210

1211 Magnadóttir, B., Hayes, P., Hristova, M., Bragason, B.P., Nicholas, A.P., Dodds, A.W., Gudmundsdóttir,  
1212 S., Lange, S., 2018a. Post-translational Protein Deimination in Cod (*Gadus morhua* L.) Ontogeny –  
1213 Novel Roles in Tissue Remodelling and Mucosal Immune Defences? *Dev. Comp. Immunol.* 87, 157-  
1214 170.

1215

1216 Magnadóttir, B., Hayes, P., Gísladóttir, B., Bragason, B.P., Hristova, M., Nicholas, A.P.,  
1217 Guðmundsdóttir, S., Lange, S., 2018b. Pentraxins CRP-I and CRP-II are post-translationally deiminated  
1218 and differ in tissue specificity in cod (*Gadus morhua* L.) ontogeny. *Dev. Comp. Immunol.* 87, 1-11.

1219

1220 Magnadóttir, B., Bragason, B.T., Bricknell, I.R., Bowden T., Nicholas, A.P., Hristova, M.,  
1221 Gudmundsdóttir, S., Dodds, A.W., Lange, S., 2019a. Peptidylarginine Deiminase and Deiminated  
1222 Proteins are detected throughout Early Halibut Ontogeny - Complement Components C3 and C4 are  
1223 post-translationally Deiminated in Halibut (*Hippoglossus hippoglossus* L.). *Dev Comp Immunol.* 92, 1-  
1224 19.

1225

1226 Magnadóttir, B., Kraev, I., Guðmundsdóttir, S., Dodds, A.W., Lange, S., 2019b Extracellular vesicles  
1227 from cod (*Gadus morhua* L.) mucus contain innate immune factors and deiminated protein cargo. *Dev*  
1228 *Comp Immunol.* 99, 103397.

1229

1230 McIntyre, R.E., Lakshminarasimhan Chavali, P., Ismail, O., Carragher, D.M., Sanchez-Andrade, G.,  
1231 Forment, J.V., et al., 2012. Disruption of mouse Cenpj, a regulator of centriole biogenesis, phenocopies  
1232 Seckel syndrome. *PLoS Genetics.* 8 (11), e1003022.

1233

1234 Matriciano, F., Panaccione, I., Grayson, D.R., Nicoletti, F., Guidotti, A., 2016. Metabotropic Glutamate  
1235 2/3 Receptors and Epigenetic Modifications in Psychotic Disorders: A Review. *Curr Neuropharmacol.*  
1236 14(1), 41-7.

1237

1238 Mehta, N.U., Reddy, S.T., 2015. Role of hemoglobin/heme scavenger protein hemopexin in  
1239 atherosclerosis and inflammatory diseases. *Curr. Opin. Lipidol.* 26(5), 384-7.

1240

1241 Metcalf, V.J., George, P.M., Brennan, S.O., 2007. Lungfish albumin is more similar to tetrapod than to  
1242 teleost albumins: purification and characterisation of albumin from the Australian lungfish,  
1243 *Neoceratodus forsteri*. *Comp. Biochem. Physiol. B Biochem. Mol. Biol.* 147(3), 428-37.

1244  
1245 Mino, T., Takeuchi, O., 2018. Post-transcriptional regulation of immune responses by RNA binding  
1246 proteins. *Proc Jpn Acad Ser B Phys Biol Sci.* 94(6), 248-258.  
1247  
1248 Mitchell, L.S., Colwell, L.J., 2018. Comparative analysis of nanobody sequence and structure data.  
1249 *Proteins.* 86(7), 697-706.  
1250  
1251 Mittal, S., Song, X., Vig, B.S., Landowski, C.P., Kim, I., Hilfinger, JM., Amidon, G.L., 2005. Prolidase, a  
1252 potential enzyme target for melanoma: design of proline-containing dipeptide-like prodrugs.  
1253 *Molecular Pharmaceutics.* 2 (1), 37-46.  
1254  
1255 Moscarello, M.A., Lei, H., Mastronardi, F.G., Winer, S., Tsui, H., Li, Z., Ackerley, C., Zhang, L., Raijmakers,  
1256 R., Wood, D.D., 2013. Inhibition of peptidyl-arginine deiminases reverses protein-hypercitrullination  
1257 and disease in mouse models of multiple sclerosis. *Dis Model Mech.* 6(2), 467-78.  
1258  
1259 Muller, S., Radic, M., 2015. Citrullinated Autoantigens: From Diagnostic Markers to Pathogenetic  
1260 Mechanisms. *Clin. Rev. Allergy Immunol.* 49(2), 232-9.  
1261  
1262 Muyldermans, S., 2013. Nanobodies: natural single-domain antibodies. *Annu Rev Biochem* 82, 775-  
1263 97.  
1264  
1265 Naslavsky N., Boehm M., Backlund PS Jr., Caplan, S., 2004. Rabenosyn-5 and EHD1 interact and  
1266 sequentially regulate protein recycling to the plasma membrane. *Mol Biol Cell.* 15(5), 2410-22.  
1267  
1268 Navaroli, D.M., Bellvé, K.D., Standley, C., Lifshitz, L.M., Cardia, J., Lambright, D., Leonard, D., Fogarty,  
1269 K.E., Corvera, S., 2012. Rabenosyn-5 defines the fate of the transferrin receptor following clathrin-  
1270 mediated endocytosis. *Proc Natl Acad Sci U S A.* 109(8), E471-80.  
1271  
1272 Nayak, A., Pednekar, L., Reid, K.B., Kishore, U., 2012. Complement and non-complement activating  
1273 functions of C1q: a prototypical innate immune molecule. *Innate Immun.* 18(2), 350-63.  
1274  
1275 Nicholas, A.P., Whitaker, J.N., 2002. Preparation of a monoclonal antibody to citrullinated epitopes:  
1276 its characterization and some applications to immunohistochemistry in human brain. *Glia* 37(4), 328-  
1277 36.  
1278  
1279 Nielsen, E., Christoforidis, S., Uttenweiler-Joseph, S., Miaczynska, M., Dewitte, F., Wilm, M., Hoflack,  
1280 B., Zerial, M., 2000. Rabenosyn-5, a novel Rab5 effector, is complexed with hVPS45 and recruited to  
1281 endosomes through a FYVE finger domain. *J Cell Biol.* 151(3), 601-12.  
1282  
1283 Njålsson, R., Norgren, S., 2005. Physiological and pathological aspects of GSH metabolism. *Acta*  
1284 *Paediatr.* 94 (2), 132-7.  
1285  
1286 Nomura, K., 1992. Specificity and mode of action of the muscle-type protein-arginine deiminase. *Arch.*  
1287 *Biochem. Biophys.* 293(2), 362-9.  
1288  
1289 Nongonierma, A.B., Paoletta, S., Mudgil, P., Maqsood, S., FitzGerald, R.J., 2018. Identification of novel  
1290 dipeptidyl peptidase IV (DPP-IV) inhibitory peptides in camel milk protein hydrolysates. *Food Chem.*  
1291 244, 340-348.  
1292  
1293 Norman, A.W., 2008. A vitamin D nutritional cornucopia: new insights concerning the serum 25-  
1294 hydroxyvitamin D status of the US population. *Am J Clin Nutr.* 88(6), 1455-6.

1295  
1296 Olaho-Mukani, W., Nyang'ao, J.N., Kimani, J.K., Omuse, J.K., 1995a. Studies on the haemolytic  
1297 complement of the dromedary camel (*Camelus dromedarius*). I. Classical pathway haemolytic activity  
1298 in serum. *Vet Immunol Immunopathol.* 46(3-4), 337-47.  
1299  
1300 Olaho-Mukani, W., Nyang'ao, J.N., Kimani, J.K., Omuse, J.K., 1995b. Studies on the haemolytic  
1301 complement of the dromedary camel (*Camelus dromedarius*). II. Alternate complement pathway  
1302 haemolytic activity in serum. *Vet Immunol Immunopathol.* 48(1-2), 169-76.  
1303  
1304 O'Neil, L.J., Kaplan, M.J., 2019. Neutrophils in Rheumatoid Arthritis: Breaking Immune Tolerance and  
1305 Fueling Disease. *Trends Mol Med.* 25(3):215-227.  
1306  
1307 Parida, S., Siddharth, S., Sharma, D., 2019. Adiponectin, obesity, and cancer: Clash of the bigwigs in  
1308 health and disease. *Int. J. Mol. Sci.* 20, 2519.  
1309  
1310 Peck, K.M., Scobey, T., Swanstrom, J., Jensen, K.L., Burch, C.L., Baric, R.S., Heise, M.T., 2017.  
1311 Permissivity of Dipeptidyl Peptidase 4 Orthologs to Middle East Respiratory Syndrome Coronavirus Is  
1312 Governed by Glycosylation and Other Complex Determinants. *J Virol.* 91(19), pii: e00534-17.  
1313  
1314 Perga, S., Giuliano Albo, A., Lis, K., Minari, N., Falvo, S., Marnetto, F., Caldano, M., Reviglione, R., et al.,  
1315 2015. Vitamin D Binding Protein Isoforms and Apolipoprotein E in Cerebrospinal Fluid as Prognostic  
1316 Biomarkers of Multiple Sclerosis. *PLoS One.* 10(6), e0129291.  
1317  
1318 Peters, T., Jr., 1996. All about albumin. *Biochemistry, Genetics, and Medical Applications.* Academic  
1319 Press, Inc, San Diego.  
1320  
1321 Picard, D., 2002. Heat-shock protein 90, a chaperone for folding and regulation. *Cell. Mol. Life Sci.* 59  
1322 (10), 1640–8.  
1323  
1324 Pietronigro, E.C., Della Bianca, V., Zenaro, E., Constantin, G., 2017. NETosis in Alzheimer's Disease.  
1325 *Front Immunol.* 8:211.  
1326  
1327 Plasil, M., Wijkmark, S., Elbers, J.P., Oppelt, J., Burger, P.A., Horin, P., 2019. The major  
1328 histocompatibility complex of Old World camelids: Class I and class I-related genes. *HLA.* 93(4), 203-  
1329 215.  
1330  
1331 Ploquin, M.J., Casrouge, A., Madec, Y., Noël, N., Jacquelin, B., Huot, N., Duffy, D., Jochems, S.P., Micci,  
1332 L., et al., 2018. Systemic DPP4 activity is reduced during primary HIV-1 infection and is associated with  
1333 intestinal RORC+ CD4+ cell levels: a surrogate marker candidate of HIV-induced intestinal damage. *J*  
1334 *Int AIDS Soc.* 21(7), e25144.  
1335  
1336 Poon, M.W., Tsang, W.H., Chan, S.O., Li, H.M., Ng, H.K., Waye, M.M., 2011. Dyslexia-associated  
1337 kiaa0319-like protein interacts with axon guidance receptor nogo receptor 1. *Cell Mol Neurobiol.*  
1338 31(1), 27-35.  
1339  
1340 Rai, A., Goody, R.S., Müller, M.P., 2017. Multivalency in Rab effector interactions. *Small GTPases.* 27,  
1341 1-7.  
1342  
1343 Ramirez, S.H., Andrews, A.M., Paul, D., Pachter, J.S., 2018. Extracellular vesicles: mediators and  
1344 biomarkers of pathology along CNS barriers. *Fluids Barriers CNS.* 15(1), 19.  
1345

1346 Ramos-Gomes, F., Bode, J., Sukhanova, A., Bozrova, S.V., Saccomano, M., Mitkovski, M., Krueger, J.E.,  
1347 Wege, A.K., Stuehmer, W., Samokhvalov, P.S., Baty, D., Chames, P., Nabiev, I., Alves, F., 2018. Single-  
1348 and two-photon imaging of human micrometastases and disseminated tumour cells with conjugates  
1349 of nanobodies and quantum dots. *Sci Rep.* 8(1), 4595.  
1350  
1351 Rebl, A., Köllner, B., Anders, E., Wimmers, K., Goldammer, T., 2010. Peptidylarginine deiminase gene  
1352 is differentially expressed in freshwater and brackish water rainbow trout. *Mol. Biol. Rep.* 37(5), 2333-  
1353 9.  
1354  
1355 Reichl, K., Kreykes, S.E., Martin, C.M., Shenoy, C., 2018. Desmoplakin Variant-Associated  
1356 Arrhythmic Cardiomyopathy Presenting as Acute Myocarditis. *Circ Genom Precis Med.* 11(12),  
1357 e002373.  
1358  
1359 Reid, K.B., Colomb, M., Petry, F., Loos, M., 2002. Complement component C1 and the collectins--first-  
1360 line defense molecules in innate and acquired immunity. *Trends Immunol.* 23(3), 115-7.  
1361  
1362 Reid, K.B.M., 2018. Complement Component C1q: Historical Perspective of a Functionally Versatile,  
1363 and Structurally Unusual, Serum Protein. *Front. Immunol.* 9, 764.  
1364  
1365 Rharass, T., Lemcke, H., Lantow, M., Kuznetsov, S.A., Weiss, D.G., Panáková, D., 2014. Ca<sup>2+</sup>-mediated  
1366 mitochondrial reactive oxygen species metabolism augments Wnt/ $\beta$ -catenin pathway activation to  
1367 facilitate cell differentiation. *J Biol Chem.* 289(40), 27937-51.  
1368  
1369 Ricci, E., Ronchetti, S., Gabrielli, E., Pericolini, E., Gentili, M., Roselletti, E., Vecchiarelli, A., Riccardi, C.,  
1370 2019. GILZ restrains neutrophil activation by inhibiting the MAPK pathway. *J Leukoc Biol.* 105(1), 187-  
1371 194.  
1372  
1373 Rivera, H., Martín-Hernández, E., Delmiro, A., García-Silva, M.T., Quijada-Fraile, P., Muley, R., Arenas,  
1374 J., Martín, M.A., Martínez-Azorín, F., 2013. A new mutation in the gene encoding mitochondrial seryl-  
1375 tRNA synthetase as a cause of HUPRA syndrome. *BMC Nephrol.* 14, 195.  
1376  
1377 Rossotti, M.A., Henry, K.A., van Faassen, H., Tanha, J., Callaghan, D., Hussack, G., Arbabi-Ghahroudi,  
1378 M., MacKenzie, C.R., 2019. Camelid single-domain antibodies raised by DNA immunization are potent  
1379 inhibitors of EGFR signaling. *Biochem J.* 476(1), 39-50.  
1380  
1381 Saeed, H., Shalaby, M., Embaby, A., Ismael, M., Pathan, A., Ataya, F., Alanazi, M., Bassiouny, K., 2015.  
1382 The Arabian camel *Camelus dromedarius* heat shock protein 90 $\alpha$ : cDNA cloning, characterization and  
1383 expression. *Int J Biol Macromol.* 81, 195-204.  
1384  
1385 Saadeldin, I.M., Abdel-Aziz Swelum, A., Alzahrani, F.A., Alowaimer, A.N., 2018a. The current  
1386 perspectives of dromedary camel stem cells research. *Int J Vet Sci Med.* 6(Suppl), S27-S30.  
1387  
1388 Saadeldin, I.M., Swelum, A.A., Elsafadi, M., Mahmood, A., Alfayez, M., Alowaimer, A.N., 2018b.  
1389 Differences between the tolerance of camel oocytes and cumulus cells to acute and chronic  
1390 hyperthermia. *J Therm Biol.* 74, 47-54.  
1391  
1392 Sayed, L.H., Badr, G., Omar, H.M., Abd, El-Rahim, A.M., Mahmoud, M.H., 2017. Camel whey protein  
1393 improves oxidative stress and histopathological alterations in lymphoid organs through Bcl-XL/Bax  
1394 expression in a streptozotocin-induced type 1 diabetic mouse model. *Biomed Pharmacother.* 88, 542-  
1395 552.  
1396

1397 Schaefer, J.S., Klein, J.R., 2016. Roquin--a multifunctional regulator of immune homeostasis. *Genes*  
1398 *Immun.* 17(2), 79-84.  
1399

1400 Schlicher, L., Wissler, M., Preiss, F., Brauns-Schubert, P., Jakob, C., Dumit, V., Borner, C., Dengjel, J.,  
1401 Maurer, U., 2016. SPATA2 promotes CYLD activity and regulates TNF-induced NF- $\kappa$ B signaling and cell  
1402 death. *EMBO Rep.* 17(10), 1485-1497.  
1403

1404 Schlicher L, Brauns-Schubert P, Schubert F, Maurer U. SPATA2: more than a missing link. *Cell Death*  
1405 *Differ.* 24(7) (2017), 1142-1147.  
1406

1407 Schönrich, G., Raftery, M.J., 2016. Neutrophil Extracellular Traps Go Viral. *Front. Immunol.* 7, 366.  
1408

1409 Schöttker, B., Zhang, Y., Heiss, J.A., Butterbach, K., Jansen, E.H., Bewerunge-Hudler, M., Saum, K.U.,  
1410 Holleccek, B., Brenner, H, 2015. Discovery of a novel epigenetic cancer marker related to the oxidative  
1411 status of human blood. *Genes Chromosomes Cancer.* 54(9), 583-94.  
1412

1413 Selmi, C., Cantarini, L., Kivity, S., Dagaan, A., Shovman, O., Zandman-Goddard, G., Perricone, C., Amital,  
1414 H., Toubi, E., Shoenfeld, Y., 2015. The 2014 ACR annual meeting: a bird's eye view of autoimmunity in  
1415 2015. *Autoimmun Rev.* 14(7), 622-32.  
1416

1417 Şen, V., Uluca, Ü., Ece, A., Kaplan, İ., Bozkurt, F., Aktar, F., Bağlı, S., Tekin ,R., 2014. Serum prolidase  
1418 activity and oxidant-antioxidant status in children with chronic hepatitis B virus infection. *Italian*  
1419 *Journal of Pediatrics.* 40 (1), 95.  
1420

1421 Sheridan, C., 2019. Llama-inspired antibody fragment approved for rare blood disorder. *Nat*  
1422 *Biotechnol.* 37(4), 33-334.  
1423

1424 Shriver-Lake, L.C., Liu, J.L., Zabetakis, D., Sugiharto, V.A., Lee, C.R., Defang, G.N., Wu, S.L., Anderson,  
1425 G.P., Goldman, E.R., 2018. Selection and Characterization of Anti-Dengue NS1 Single Domain  
1426 Antibodies. *Sci Rep.* 8(1), 18086.  
1427

1428 Silverman, J., Takai, H., Buonomo, S.B., Eisenhaber, F., de Lange, T., 2004. Human Rif1, ortholog of a  
1429 yeast telomeric protein, is regulated by ATM and 53BP1 and functions in the S-phase checkpoint.  
1430 *Genes Dev.* 18(17), 2108-19.  
1431

1432 Širochmanová, I., Čomor, Ľ., Káňová, E., Jiménez-Munguía, I.Tkáčová, Z., Bhide, M., 2018. Permeability  
1433 of the blood-brain barrier and transport of nanobodies across the blood-brain barrier. *Folia Veterinaria,*  
1434 62 (1), 59—66.  
1435

1436 Smith, L.E., Crouch, K., Cao, W., Müller, M.R., Wu, L., Steven, J., Lee, M., Liang, M., Flajnik, M.F., Shih,  
1437 H.H., Barelle, C.J., Paulsen, J., Gill, D.S., Dooley, H., 2012. Characterization of the immunoglobulin  
1438 repertoire of the spiny dogfish (*Squalus acanthias*). *Dev Comp Immunol.* 36(4), 665-79.  
1439

1440 Smith, A., McCulloh, R.J., 2015. Hemopexin and haptoglobin: allies against heme toxicity from  
1441 hemoglobin not contenders. *Front. Physiol.* 6, 187.  
1442

1443 Sohn, D.H., Rhodes, C., Onuma, K., Zhao, X., Sharpe, O., Gazitt, T., Shiao, R., Fert-Bober, J., Cheng, D.,  
1444 Lahey, L.J., et al., 2015. Local Joint inflammation and histone citrullination in a murine model of the  
1445 transition from preclinical autoimmunity to inflammatory arthritis. *Arthritis Rheumatol.* 67, 2877–  
1446 2887.  
1447

1448 Sottrup-Jensen, L., Stepanik, T.M., Kristensen, T., Lønblad, P.B., Jones, C.M., Wierzbicki, D.M.,  
1449 Magnusson, S., Domdey, H., Wetsel, R.A., Lundwall, A., et al., 1985. Common evolutionary origin of  
1450 alpha 2-macroglobulin and complement components C3 and C4. *Proc Natl Acad Sci U S A.* 82(1), 9-13.  
1451  
1452 Spracklen, C.N., Karaderi, T., Yaghootkar, H., Schurmann, C., Fine, R.S., et al., 2019. Exome-Derived  
1453 Adiponectin-Associated Variants Implicate Obesity and Lipid Biology. *Am J Hum Genet.* pii: S0002-  
1454 9297(19)30188-0.  
1455  
1456 Stanfliet, J.C., Locketz, M., Berman, P., Pillay, T.S., 2015. Evaluation of the utility of serum prolidase as  
1457 a marker for liver fibrosis. *J Clin Lab Anal.* 29(3), 208-13.  
1458  
1459 Stanfield, R.L., Haakenson, J., Deiss, T.C., Criscitiello, M.F., Wilson, I.A., Smider, V.V., 2018. The Unusual  
1460 Genetics and Biochemistry of Bovine Immunoglobulins. *Adv Immunol.* 137, 135-164.  
1461  
1462 Steeland, S., Vandembroucke, R.E., Libert, C., 2016. Nanobodies as therapeutics: big opportunities for  
1463 small antibodies. *Drug Discov Today* 21, 1076–113.  
1464  
1465 Sunyer, J.O., Lambris, J.D., 1998. Evolution and diversity of the complement system of poikilothermic  
1466 vertebrates. *Immunol. Rev.* 166, 39-57.  
1467  
1468 Tang, C.J., Fu, R.H., Wu, K.S., Hsu, W.B., Tang, T.K., 2009. CPAP is a cell-cycle regulated protein that  
1469 controls centriole length. *Nat Cell Biol* 11, 825–831.  
1470  
1471 Tarighi, S., Najafi, M., Hossein-Nezhad, A., Ghaedi, H., Meshkani, R., Moradi, N., Fadaei, R., Kazerouni,  
1472 F., Shanaki, M., 2017. Association Between Two Common Polymorphisms of Vitamin D Binding Protein  
1473 and the Risk of Coronary Artery Disease: A Case-control Study. *J Med Biochem.* 36(4), 349-357.  
1474  
1475 Tarcsa, E., Marekov, L.N., Mei, G., Melino, G., Lee, S.C., Steinert, P.M., 1996. Protein unfolding by  
1476 peptidylarginine deiminase. Substrate specificity and structural relationships of the natural substrates  
1477 trichohyalin and filaggrin. *J. Biol. Chem.* 271(48), 30709-16.  
1478  
1479 Tennent, G.A., Brennan, S.O., Stangou, A.J., O’Grady, J., Hawkins, P.N., Pepys, M.B., 2007. Human  
1480 plasma fibrinogen is synthesized in the liver. *Blood*, 109, 1971–1974.  
1481  
1482 Théry, C., Witwer, K.W., Aikawa, E., Alcaraz, M.J., Anderson, J.D., Andriantsitohaina, R., Antoniou, A.,  
1483 Arab, T., Archer, F., Atkin-Smith, G.K., et al., 2018. Minimal information for studies of extracellular  
1484 vesicles 2018 (MISEV2018): A position statement of the International Society for Extracellular Vesicles  
1485 and update of the MISEV2014 guidelines. *J. Extracell. Vesicles.* 7, 1535750.  
1486  
1487 Tiscia, G.L., Margaglione, M., 2018. Human Fibrinogen: Molecular and Genetic Aspects of Congenital  
1488 Disorders. *Int. J. Mol. Sci.* 19(6), pii: E1597.  
  
1489 Traub, L.M., 2019. A nanobody-based molecular toolkit provides new mechanistic insight into clathrin-  
1490 coat initiation. *Elife.* 8, pii: e41768.  
1491  
1492 Travers, T.S., Harlow, L., Rosas, I.O., Gochuico, B.R., Mikuls, T.R., Bhattacharya, S.K., Camacho, C.J.,  
1493 Ascherman, D.P., 2016. Extensive Citrullination Promotes Immunogenicity of HSP90 through Protein  
1494 Unfolding and Exposure of Cryptic Epitopes. *J Immunol.* 197(5), 1926-36.  
1495  
1496 Turchinovich, A., Drapkina, O., Tonevitsky, A., 2019. Transcriptome of Extracellular Vesicles: State-of-  
1497 the-Art. *Front Immunol.* 10, 202.  
1498

1499 Urbainsky, C., Nölker, R., Imber, M., Lübken, A., Mostertz, J., Hochgräfe, F., Godoy, J.R., Hanschmann,  
1500 EM, Lillig, C.H., 2018. Nucleoredoxin-Dependent Targets and Processes in Neuronal Cells. *Oxid Med*  
1501 *Cell Longev.* 2018, 4829872.  
1502  
1503 Vagner, T., Chin, A., Mariscal, J., Bannykh, S., Engman, D.M., Di Vizio, D., 2019. Protein Composition  
1504 Reflects Extracellular Vesicle Heterogeneity. *Proteomics*, e1800167.  
1505  
1506 Vanlandschoot, P., Stortelers, C., Beirnaert, E., Ibañez, L.I., Schepens, B., Depla, E., et al., 2011.  
1507 Nanobodies®: new ammunition to battle viruses. *Antiviral Res* 92, 389–407.  
1508  
1509 van Lith, S.A., Roodink, I., Verhoeff, J.J., Mäkinen, P.I., Lappalainen, J.P., Ylä-Herttuala, S., Raats, J., van  
1510 Wijk, E., Roepman, R., Letteboer, S.J., Verrijp, K., Leenders, W.P., 2016. In vivo phage display screening  
1511 for tumor vascular targets in glioblastoma identifies a llama nanobody against dynactin-1-p150Glued.  
1512 *Oncotarget.* 7(44), 71594-71607.  
1513  
1514 Varin, E.M., Mulvihill, E.E., Beaudry, J.L., Pujadas, G., Fuchs, S., Tanti, J.F., Fazio, S., Kaur, K., Cao, X.,  
1515 Baggio, L.L., Matthews, D., Campbell, J.E., Drucker, D.J., 2019. Circulating Levels of Soluble Dipeptidyl  
1516 Peptidase-4 Are Dissociated from Inflammation and Induced by Enzymatic DPP4 Inhibition. *Cell*  
1517 *Metab.* 29(2), 320-334.  
1518  
1519 Velayos-Baeza, A., Toma, C., Paracchini, S., Monaco, A.P., 2008. The dyslexia-associated gene  
1520 KIAA0319 encodes highly N- and O-glycosylated plasma membrane and secreted isoforms. *Hum Mol*  
1521 *Genet.* 17(6), 859-71.  
1522  
1523 Verboven, C., Rabijns, A., De Maeyer, M., Van Baelen, H., Bouillon, R., De Ranter, C., 2002. A structural  
1524 basis for the unique binding features of the human vitamin D-binding protein. *Nat Struct Biol.* 9(2),  
1525 131-6.  
1526  
1527 Viglio, S., Annovazzi, L., Conti, B., Genta, I., Perugini, P., Zanone, C., Casado, B., Cetta, G., Iadarola, P.,  
1528 2006. The role of emerging techniques in the investigation of prolidase deficiency: from diagnosis to  
1529 the development of a possible therapeutical approach. *Journal of Chromatography B.* 832 (1), 1–8.  
1530  
1531 Vossenaar, E.R., Zendman, A.J., van Venrooij, W.J., Pruijn, G.J., 2003. PAD, a growing family of  
1532 citrullinating enzymes: genes, features and involvement in disease. *Bioessays.* 25(11), 1106-18.  
1533  
1534 Wagner, S.A., Satpathy, S., Beli, P., Choudhary, C., 2016. SPATA2 links CYLD to the TNF- $\alpha$  receptor  
1535 signaling complex and modulates the receptor signaling outcomes. *EMBO J.* 35(17), 1868-84.  
1536  
1537 Waheed, M.M., Ghoneim, I.M., Alhaider, A.K., 2015. Seminal plasma and serum fertility biomarkers in  
1538 dromedary camels (*Camelus dromedarius*). *Theriogenology.* 83(4) 650-4.  
1539  
1540 Wang, S., Wang, Y. Peptidylarginine deiminases in citrullination, gene regulation, health and  
1541 pathogenesis. *Biochim. Biophys. Acta.* 1829(10) (2013), 1126-35.  
1542  
1543 Wang, H., Lapek, J., Fujimura, K., Strnadel, J., Liu, B., Gonzalez, D.J., Zhang, W., Watson, F., Yu, V., Liu,  
1544 C., Melo, C.M., Miller, Y.I., Elliott, K.C., Cheresch, D.A., Klemke, R.L., 2018. Pseudopodium-enriched  
1545 atypical kinase 1 mediates angiogenesis by modulating GATA2-dependent VEGFR2 transcription. *Cell*  
1546 *Discov.* 4, 26.  
1547  
1548 Wei, G., Meng, W., Guo, H., Pan, W., Liu, J., Peng, T., Chen, L., Chen, C.Y., 2011. Potent neutralization  
1549 of influenza A virus by a single-domain antibody blocking M2 ion channel protein. *PLoS One* 6, e28309.

1550  
1551 Weidle, U.H., Birzele, F., Tiefenthaler, G., 2018. Potential of Protein-based Anti-metastatic Therapy  
1552 with Serpins and Inter  $\alpha$ -Trypsin Inhibitors. *Cancer Genomics Proteomics*. 15(4), 225-238.  
1553  
1554 Weisel, J.W., Litvinov, R.I., 2013. Mechanisms of fibrin polymerization and clinical implications. *Blood*.  
1555 121, 1712–1719.  
1556  
1557 Wenthur, C., Daniels, J.S., Morrison, R., Engers, J.L., Niswender, C.M., Conn, P.J., Lindsley, C.W.  
1558 Development of a Second Generation mGlu3 NAM Probe. *Probe Reports from the NIH Molecular*  
1559 *Libraries Program* [Internet]. Bethesda (MD): National Center for Biotechnology Information (US);  
1560 2010-2012.  
1561  
1562 Wesolowski J, Alzogaray V, Reyelt J, Unger M, Juarez K, Urrutia M, et al., 2009. Single domain  
1563 antibodies: promising experimental and therapeutic tools in infection and immunity. *Med Microbiol*  
1564 *Immunol* 198, 157–74.  
1565  
1566 White, C.R., Datta, G., Giordano, S., 2017. High-Density Lipoprotein Regulation of Mitochondrial  
1567 Function. *Adv Exp Med Biol*. 982, 407-429.  
1568  
1569 Wieser, V., Tsibulak, I., Degasper, C., Welponer, H., Leitner, K., Parson, W., Zeimet, A.G., Marth, C.,  
1570 Fiegl, H., 2019. Tumor necrosis factor receptor modulator spermatogenesis-associated protein 2 is a  
1571 novel predictor of outcome in ovarian cancer. *Cancer Sci*. 110(3), 1117-1126.  
1572  
1573 Witalison, E.E., Thompson, P.R., Hofseth, L.J., 2015. Protein Arginine Deiminases and Associated  
1574 Citrullination: Physiological Functions and Diseases Associated with Dysregulation. *Curr. Drug Targets*.  
1575 16(7), 700-10.  
1576  
1577 Wu, H., Guang, X., Al-Fageeh, M.B., Cao, J., Pan, S., Zhou, H., et al., 2014. Camelid genomes reveal  
1578 evolution and adaptation to desert environments. *Nat Commun*. 5, 5188.  
1579  
1580 Yamamoto, N., Suyama, H., Yamamoto, N., 2008. Immunotherapy for Prostate Cancer with Gc Protein-  
1581 Derived Macrophage-Activating Factor, GcMAF. *Transl Oncol*. 1(2), 65-72.  
1582  
1583 Yamauchi, T., Kamon, J., Minokoshi, Y., Ito, Y.; Waki, H., Uchida, S., Yamashita, S., Noda, M., Kita, S.,  
1584 Ueki, K., et al., 2002. Adiponectin stimulates glucose utilization and fatty-acid oxidation by activating  
1585 AMP-activated protein kinase. *Nat. Med*. 8, 1288–1295.  
1586  
1587 Yamauchi, T., Kamon, J.; Ito, Y., Tsuchida, A., Yokomizo, T., Kita, S., Sugiyama, T., Miyagishi, M., Hara,  
1588 K., Tsunoda, M., et al., 2003. Cloning of adiponectin receptors that mediate antidiabetic metabolic  
1589 effects. *Nature*, 423, 762–769  
1590  
1591 Yang, J., Gao, J., Adamian, M., Wen, X.H., Pawlyk, B., Zhang, L., Sanderson, M.J., Zuo, J., Makino, C.L.,  
1592 Li, T., 2005. The ciliary rootlet maintains long-term stability of sensory cilia. *Mol. Cell. Biol*. 25, 4129–  
1593 4137.  
1594  
1595 Yang, T., Martin, P., Fogarty, B., Brown, A., Schurman, K., Phipps, R., Yin, V.P., Lockman, P., Bai, S.,  
1596 2015. Exosome delivered anticancer drugs across the blood-brain barrier for brain cancer therapy in  
1597 *Danio rerio*. *Pharm Res*. 32(6), 2003-14.  
1598  
1599 Yermakovich, D., Sivitskaya, L., Vaikhanskaya, T., Danilenko, N., Motuk, I., 2018. Novel desmoplakin  
1600 mutations in familial Carvajal syndrome. *Acta Myol*. 37(4), 263-266.

1601  
1602 Zhang, C., Du Pasquier, L., Hsu, E., 2013. Shark IgW C region diversification through RNA processing  
1603 and isotype switching. *J Immunol.* 191(6), 3410-8.  
1604  
1605 Zhang, Q., Fan, L., Hou F., Dong, A., Wang, Y.X., Tong, Y., 2015. New Insights into the RNA-Binding and  
1606 E3 Ubiquitin Ligase Activities of Roquins. *Sci Rep.* 5, 15660.  
1607  
1608 Zhang, N., Zhang, X.J., Song, Y.L., Lu, X.B., Chen, D.D., Xia, X.Q., Sunyer, J.O., Zhang, Y.A., 2016.  
1609 Preferential combination between the light and heavy chain isotypes of fish immunoglobulins. *Dev.*  
1610 *Comp. Immunol.* 61, 169-79.  
1611  
1612 Zhang, N., Zhang, X.J., Chen, D.D., Sunyer, O.J., Zhang, Y.A., 2017. Molecular characterization and  
1613 expression analysis of three subclasses of IgT in rainbow trout (*Oncorhynchus mykiss*). *Dev. Comp.*  
1614 *Immunol.* 70, 94-105.  
1615  
1616 Zhao, J., Zhao, J., Xu, G., Wang, Z., Gao, J., Cui, S., Liu, J., 2017. Deletion of *Spata2* by CRISPR/Cas9n  
1617 causes increased inhibin alpha expression and attenuated fertility in male mice. *Biol Reprod.* 97(3),  
1618 497-513.  
1619  
1620 Zhou, G., Yang, L., Gray, A., Srivastava, A.K., Li, C., Zhang, G., Cui, T., 2017. The role of desmosomes in  
1621 carcinogenesis. *Onco Targets Ther.* 10, 4059-4063.  
1622  
1623 Zhuo, L., Kimata, K., 2008. Structure and function of inter-alpha-trypsin inhibitor heavy chains.  
1624 *Connect. Tissue Res.* 49, 311-320.  
1625  
1626 Zhu, S., Zimmerman, D., Deem, S.L., 2019. A Review of Zoonotic Pathogens of Dromedary Camels.  
1627 *Ecohealth.* 2019 May 28. doi: 10.1007/s10393-019-01413-7. [Epub ahead of print]  
1628  
1629

1630 **Figure legends**

1631

1632 **Fig. 1. Extracellular vesicles (EVs) isolated from llama serum.** **A.** Nanoparticle tracking analysis  
1633 showing a poly-dispersed population of EVs in the size range of 30 to 576 nm, with main peaks at 38,  
1634 119, 167, 237, 323 and 403 nm. **B.** Llama serum EVs are positive for the EV-specific markers CD63 and  
1635 Flotillin-1 (Flot-1). **C.** Transmission electron microscopy (TEM) imaging of EVs isolated from llama  
1636 serum shows a polydispersed population; scale bar represents 100 nm.

1637

1638 **Fig. 2. Western blotting of deiminated proteins and PAD in llama serum.** **A.** Llama PAD homologues  
1639 were identified at the expected size of approximately 70-75 kDa using the human PAD2, PAD3 and  
1640 PAD4 isozyme specific antibodies respectively. Deiminated histone H3 (citH3), representative of  
1641 neutrophil extracellular traps (NETs), was verified in llama serum. **B.** Total deiminated proteins were  
1642 assessed by Western blotting in llama serum EVs, using the F95 pan-deimination specific antibody. **C.**  
1643 Immunoprecipitated deiminated proteins after F95-enrichment were assessed both in serum-EVs and  
1644 whole serum of llama by Western blotting. **D.** Venn diagram representing deiminated proteins  
1645 identified in total serum and serum-derived EVs by F95 enrichment and LC-MS/MS analysis. Overall,  
1646 43 proteins were identified in common with both samples, while 60 proteins were found deiminated  
1647 in serum only and 25 proteins were identified as deiminated in EVs only.

1648

1649 **Fig. 3. Protein-protein interaction networks of deiminated protein hits identified in whole llama**  
1650 **(*Lama glama*) serum.** Reconstruction of protein-protein interactions based on known and predicted  
1651 interactions using STRING analysis. Due to annotations for camelids not being present in STRING,  
1652 proteins are based on corresponding human protein identifiers. **A.** Coloured nodes represent query  
1653 proteins and first shell of interactors; white nodes are second shell of interactors. **B.** Biological GO  
1654 processes are highlighted for the same protein network as follows: red=response to stress;  
1655 blue=response to wounding; green=vesicle mediated transport; yellow=oxygen transport;  
1656 purple=regulated exocytosis; dark green=small molecule metabolic process. Coloured lines indicate  
1657 whether protein interactions are identified via known interactions (curated databases, experimentally  
1658 determined), predicted interactions (gene neighbourhood, gene fusion, gene co-occurrence) or via  
1659 text mining, co-expression or protein homology (see colour key for connective lines in A).

1660

1661 **Fig. 4. Protein-protein interaction networks of deiminated protein hits identified in EVs of llama**  
1662 **(*Lama glama*) serum.** Reconstruction of protein-protein interactions based on known and predicted  
1663 interactions using STRING analysis. Due to annotations for camelids not being present in STRING,

1664 proteins are based on corresponding human protein identifiers. **A.** Coloured nodes represent query  
1665 proteins and first shell of interactors. **B.** Biological GO processes are highlighted as follows:  
1666 red=response to stress; blue=cytoskeleton organisation; green=vesicle mediated transport. Coloured  
1667 lines indicate whether protein interactions are identified via known interactions (curated databases,  
1668 experimentally determined), predicted interactions (gene neighbourhood, gene fusion, gene co-  
1669 occurrence) or via text mining, co-expression or protein homology (see colour key for connective lines  
1670 in A).

1671

1672 **Table 1. Deiminated proteins identified by F95 enrichment and LC-MS/MS in total serum of llama**  
1673 **(*Lama glama*).** Deiminated proteins were isolated by immunoprecipitation using the pan-deimination  
1674 F95 antibody. The F95 enriched eluate was analysed by LC-MS/MS and peak list files were submitted  
1675 to in-house Mascot. Peptide sequence hits scoring with *Lama glama* (LAMGL) are included as well as  
1676 hits with other camelids (CAMFR=*Camelus ferus*; CAMDR=*Camelus dromedaries*; LAMGU=*Lama*  
1677 *guanicoe*; VICPA=*Vicugna pacos* (Alpaca)). Hits with uncharacterized proteins are omitted in the list.  
1678 For a full list of peptide sequences and m/z values see Supplementary Table 1. An asterisk (\*) indicates  
1679 that the protein hit is specific to whole serum only.

1680

1681 **Table 2. Deiminated proteins identified by F95 enrichment and LC-MS/MS in EVs isolated from**  
1682 **serum of llama (*Lama glama*).** Deiminated proteins were isolated by immunoprecipitation using the  
1683 pan-deimination F95 antibody, the F95 enriched eluate was analysed by LC-MS/MS and peak list files  
1684 were submitted to Mascot. Peptide sequence hits scoring with *L. glama* (LAMGL) are presented as  
1685 well as hits with other camelids (CAMFR=*Camelus ferus*; CAMDR=*Camelus dromedaries*;  
1686 LAMGU=*Lama guanicoe*). Hits with uncharacterised proteins are not listed. For a full list of peptide  
1687 sequences and m/z values see Supplementary Table 2. An asterisk (\*) indicates that the protein hit is  
1688 unique for EVs only.

1689

1690 **Supplementary Table 1. Deiminated proteins identified, including full list of all peptide sequences,**  
1691 **by F95 enrichment and LC-MS/MS in total serum of llama (*Lama glama*).** Deiminated proteins were  
1692 isolated by immunoprecipitation using the pan-deimination F95 antibody. The F95 enriched eluate  
1693 was analysed by LC-MS/MS and peak list files were submitted to in-house Mascot. Peptide sequence  
1694 hits scoring with *Lama glama* (LAMGL) are included as well as hits with other camelids  
1695 (CAMFR=*Camelus ferus*; CAMDR=*Camelus dromedaries*; LAMGU=*Lama guanicoe*; VICPA=*Vicugna*  
1696 *pacos* (Alpaca)). Hits with uncharacterized proteins are omitted in the list. Peptide sequences and m/z  
1697 values are listed. An asterisk (\*) indicates that the protein hit is specific to whole serum only.

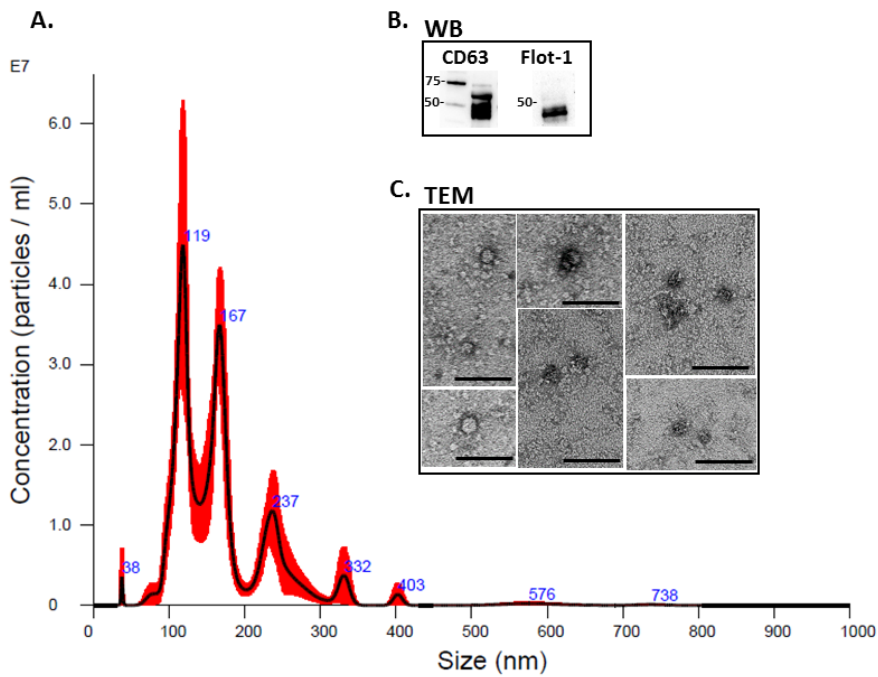
1698

1699 **Supplementary Table 2. Deiminated proteins, including all peptide sequences, identified by F95**  
1700 **enrichment and LC-MS/MS in extracellular vesicles isolated from serum of llama (*Lama glama*).**

1701 Deiminated proteins were isolated by immunoprecipitation using the pan-deimination F95 antibody,  
1702 the F95 enriched eluate was analysed by LC-MS/MS and peak list files were submitted to Mascot.  
1703 Peptide sequence hits scoring with *L. glama* (LAMGL) are presented as well as hits with other camelids  
1704 (CAMFR=*Camelus ferus*; CAMDR=*Camelus dromedaries*; LAMGU=*Lama guanicoe*). Hits with  
1705 uncharacterised proteins are not listed. Peptide sequences and m/z values are listed. An asterisk (\*)  
1706 indicates that the protein hit is unique for EVs only.

1707

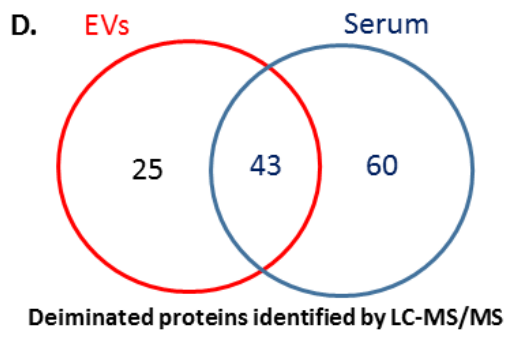
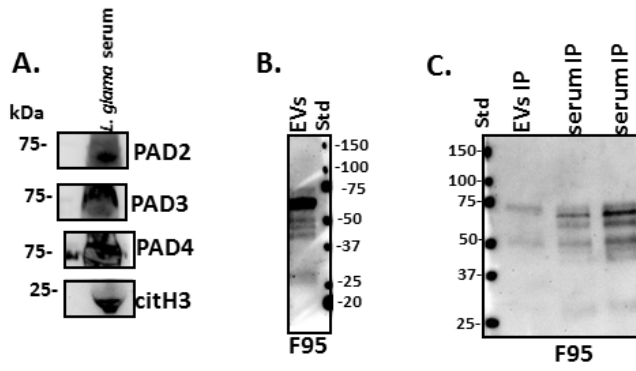
Fig.1



1708

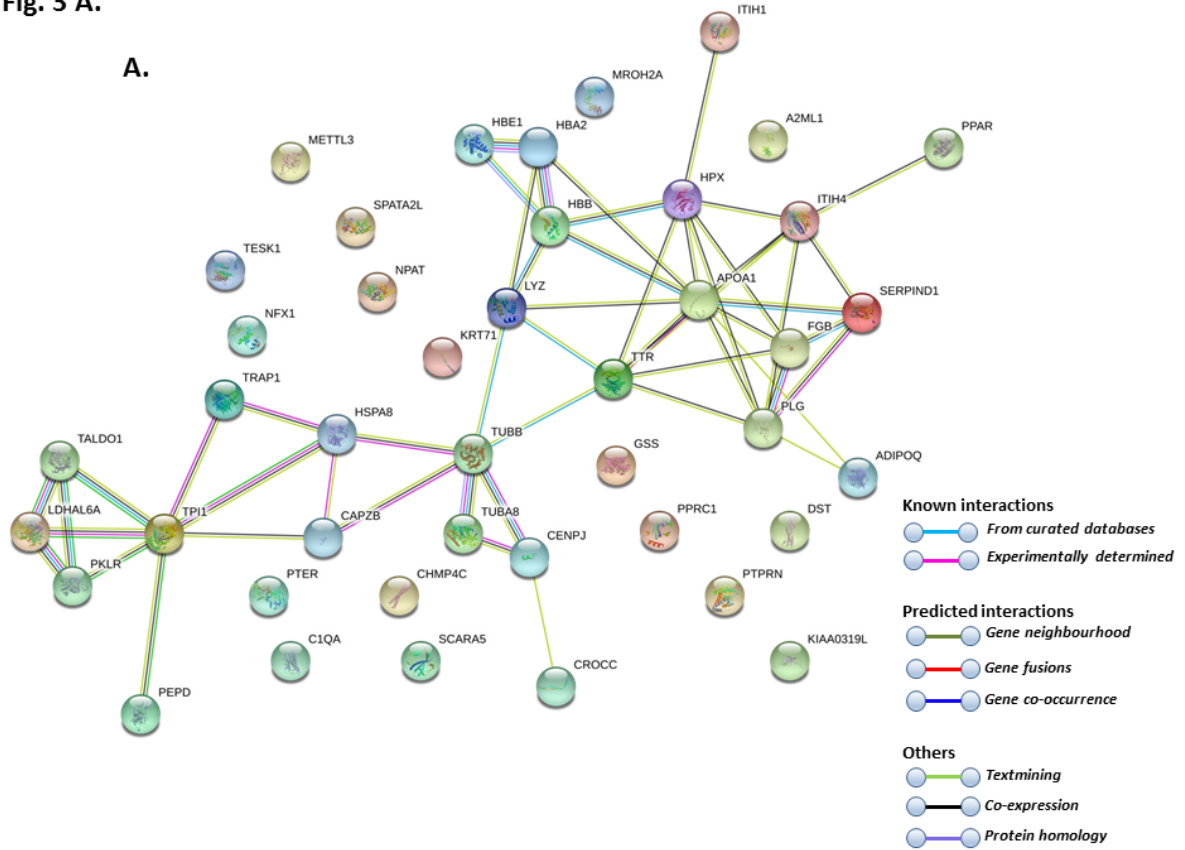
1709

Fig.2



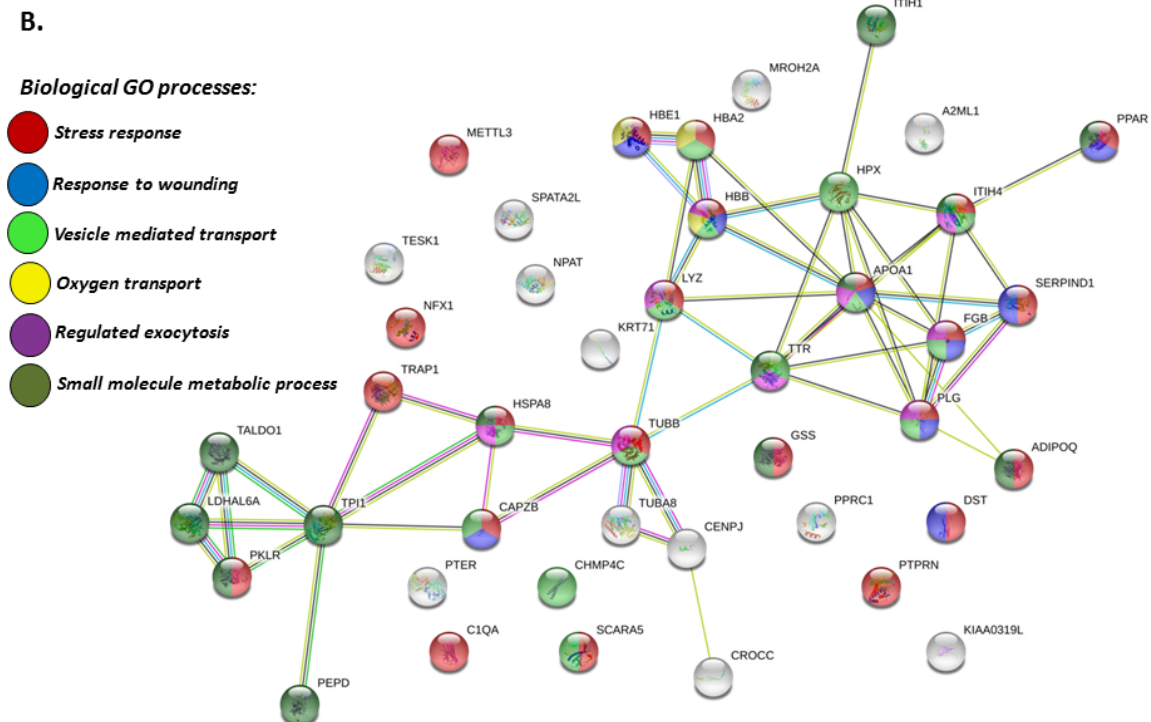
1710

Fig. 3 A.



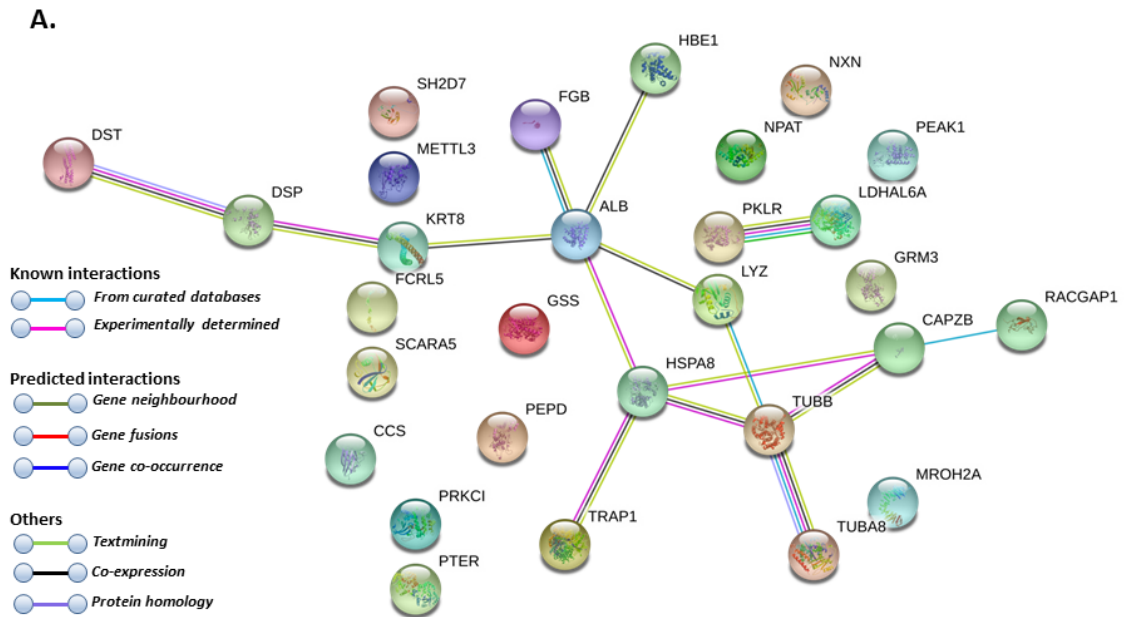
1711

Fig. 3B.



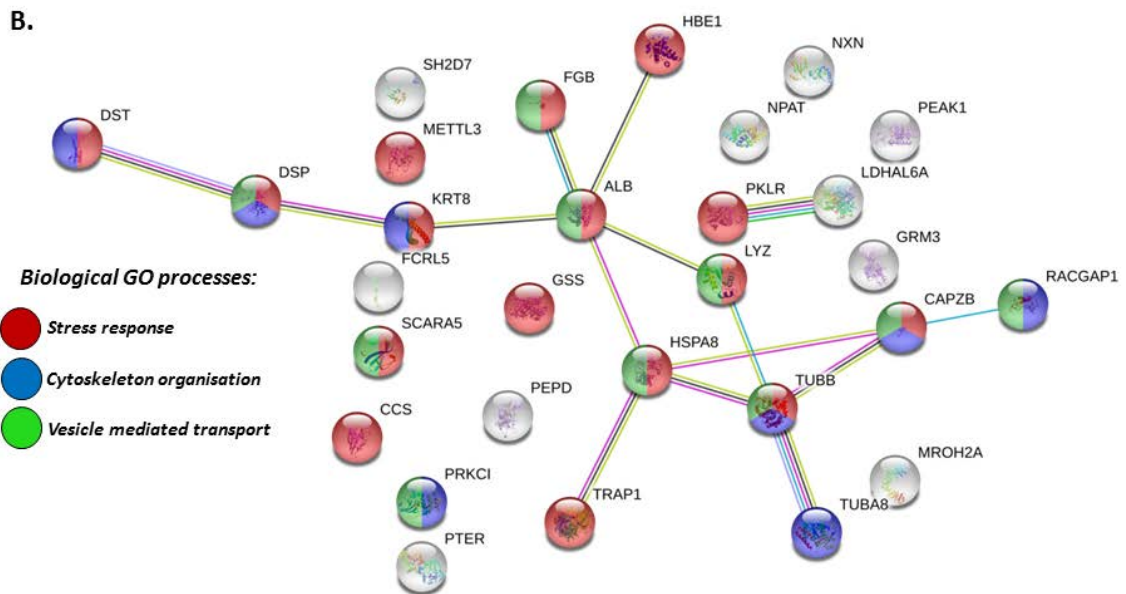
1712

Fig. 4A.



1713

Fig. 4B.



1714

1715 **Supplementary Table 1. Deiminated proteins identified, including full list of all peptide sequences, by F95**  
1716 **enrichment and LC-MS/MS in total serum of llama (*Lama glama*).** Deiminated proteins were isolated by  
1717 immunoprecipitation using the pan-deimination F95 antibody. The F95 enriched eluate was analysed by LC-  
1718 MS/MS and peak list files were submitted to in-house Mascot. Peptide sequence hits scoring with *Lama glama*  
1719 (LAMGL) are included as well as hits with other camelids (CAMFR=*Camelus ferus*; CAMDR=*Camelus dromedaries*;  
1720 LAMGU=*Lama guanicoe*; VICPA=*Vicugna pacos* (Alpaca)). Hits with uncharacterized proteins are omitted in the  
1721 list. Peptide sequences and m/z values are listed. An asterisk (\*) indicates that the protein hit is specific to whole  
1722 serum only.

Protein name (*unique for serum)	m/z	Peptide sequence	Score (p<0.05) <sup>†</sup>	Total score
*O97643_LAMGL <b>Fibrinogen A-alpha chain</b>	437.7734	R.QYLPLIK.M	26	282
	524.2692	K.EVSGSVSPGK.K	62	
	415.8943	K.GDKELLISNEK.V	38	
	513.5782	R.GDSVSHGAGSVPEPR.K	36	
	790.4611	K.QLEQVIGINLLPSR.D	69	
	697.8077	K.EVINSEGDGSDCGDTSLDLHHTFPSR.G	50	
*P01973 HBA_LAMGL <b>Hemoglobin subunit alpha</b>	409.7237	R.VDPVNFK.L	25	189
	521.2757	R.MFLGFPTTK.T	21	
	640.3666	K.FLANVSTVLTSK.Y	57	
	510.5830	K.IGGHAADYGAEALER.M	43	
	575.0433	K.AADHLDDLPSALSALSDLHAHK.L	43	
P68226 HBB_LAMGL <b>Hemoglobin subunit beta</b>	573.8375	R.LLVVYPWTR.R	31	166
	589.3436	K.VVAGVANALAHR.Y	52	
	664.8632	K.VKVDEVGGEALGR.L	45	
	705.8497	K.EFTPDLQAAYQK.V	38	
Q865W8_LAMGL <b>Beta actin</b>	566.7665	R.GYSFTTTAER.E	38	109
	895.9506	K.SYELPDGQVITIGNER.F	22	
	652.0263	R.VAPEEHPVLLTEAPLNPK.A	22	
	796.6590	R.TTGIVMDSGDGVTHTVPIYEGYALPHAILR.L	27	
AOA1W5VKM5_LAMGL <b>Anti-RON nanobody</b>	653.7847	K.SEDTAVYYCAK.D	44	117
	941.5050	-.EVQLVESGGGLVQPGGSLR.L	73	
*AOA1W5VKM7_LAMGL <b>Anti-RON nanobody</b>	608.7926	R.LSCAASGFTFR.A	38	111
	941.5050	-.EVQLVESGGGLVQPGGSLR.L	73	
*AOA1W5VKR8_LAMGL <b>Anti-RON nanobody</b>	423.7271	K.GLEWVSR.I	23	96
	941.5050	-.EVQLVESGGGLVQPGGSLR.L	73	
*AOA1W5VKQ9_LAMGL <b>Anti-RON nanobody</b>	425.2160	R.LSCVASGR.A	66	66
S9XDK9_CAMFR <b>Complement C3-like protein</b>	386.2036	K.EGIPEAR.Q	42	1575
	388.7369	K.GVFVLNK.K	21	
	400.7478	R.VGLVAVDK.G	39	
	417.2477	R.LPYSVVR.N	41	
	444.2330	R.NEQVEIR.A	47	
	449.7427	R.AVLYNYR.E	25	
	476.2484	K.FLNTATER.T	42	
	516.7754	K.LSINTQNSR.Q	53	
	531.7480	K.ADIGCTPGSGK.D	48	
	534.3140	K.VLLDGVQAPR.A	79	
	546.2920	K.DTCVGTLVVK.G	38	
	546.8186	K.NTLIYLDK.I	56	
	567.8348	R.HQQLVIPAK.S	40	
	584.2801	K.QNEDFTLTAK.G	39	
	673.3544	R.EVVADSVWVDVK.D	64	
	680.3649	K.QVLSSENTVLNR.A	92	
	685.8693	K.TIYTPGSTVLYR.I	60	
	720.8725	K.DYAGVFTDAGLALK.T	74	
	488.8977	K.ISHTQEDCLSFK.V	40	

	498.2757	<i>K.ELNLDVSIHLPSR.S</i>	56	
	787.9175	<i>K.FDLTVSLTPAPEPVK.K</i>	68	
	807.4440	<i>K.FDLTVSLTPAPEPVK.K</i>	58	
	842.3702	<i>K.VYSYYNLDETCTR.F</i>	59	
	844.8922	<i>K.AFLDCCEYITQLR.Q</i>	22	
	567.9807	<i>R.LPYSVVRNEQVEIR.A</i>	22	
	867.3949	<i>K.AADLSDQVPDTESETR.I</i>	25	
	581.2754	<i>R.SEETKQNEFTLTAK.G</i>	45	
	581.3295	<i>K.KFDLTVSLTPAPEPVK.K</i>	65	
	898.9662	<i>R.VELLYNPAFCSLATAK.K</i>	38	
	601.3332	<i>R.TGIPIVTSPIYQIHFTK.T</i>	44	
	932.4729	<i>K.EYVLPSEFVQVEPAEK.F</i>	36	
	936.9587	<i>R.SDLEDEIPEEDIISR.S</i>	22	
	765.0651	<i>R.HIPVVTQGSNVQSLTQDDGVAK.L</i>	44	
	639.8195	<i>K.QKPDGVFQEDGPIVHQEMIGGFK.N</i>	32	
S9WI87_CAMFR <b>Serum albumin</b>	386.7229	<i>K.AACL LPK.A</i>	34	972
	449.7441	<i>R.LCVLHEK.T</i>	28	
	460.2552	<i>K.LCTVASLR.E</i>	46	
	464.2503	<i>K.YLYEIAR.R</i>	32	
	469.7087	<i>K.DLGEDDFK.G</i>	38	
	538.2532	<i>R.NECFLQHK.S</i>	27	
	554.7310	<i>K.HVFEECK.D</i>	43	
	569.7529	<i>K.CCTESLVNR.R</i>	58	
	575.3115	<i>K.LVNEVTEFAK.T</i>	62	
	405.1956	<i>R.FKDLGEDDFK.G</i>	42	
	435.8773	<i>K.ECCEKPLLEK.S</i>	30	
	721.2823	<i>K.TCVADESAADC DK.S</i>	93	
	744.8028	<i>K.EYEATLEDCCAK.D</i>	71	
	746.3249	<i>K.YFCDNQETISSK.L</i>	59	
	746.7734	<i>R.ETYGEMADCCEK.Q</i>	60	
	516.2707	<i>K.LKECCEKPLLEK.S</i>	54	
	538.5977	<i>K.DVFLGMFLHEYAR.R</i>	46	
	623.2894	<i>K.TFTFHADLCSVSEPEK.Q</i>	66	
	668.6628	<i>K.LKPEPEALCTAFQEN EK.R</i>	34	
	540.7744	<i>K.LKPEPEALCTAFQEN EK.R.F</i>	52	
S9XAP9_CAMFR <b>Keratin, type I cytoskeletal 14-like protein</b>	404.2031	<i>R.LAADDFR.T</i>	55	522
	515.3008	<i>R.VLDELTLAR.A</i>	55	
	546.2613	<i>K.VTMQNLNDR.L + Deamidated (NQ)</i>	72	
	561.7933	<i>R.LEQEIATYR.R</i>	45	
	651.3333	<i>R.ALEEANADLEVK.I</i>	78	
	454.2382	<i>R.MSVEADINGLRR.V</i>	23	
	681.3488	<i>R.EVATNSELVQSGK.T</i>	93	
	685.3802	<i>K.ILTATVDNANIVLQIDNAR.L</i>	52	
	770.3600	<i>R.LLEGEDAHLSSSQFSSGSQSSR.D</i>	52	
S9Y6J1_CAMFR <b>Keratin, type II cytoskeletal 5 isoform 13-like protein</b>	405.7086	<i>R.QSSVSFR.S</i>	48	502
	453.7376	<i>R.FLEQQNK.V</i>	21	
	473.2593	<i>R.GRLDSELR.N</i>	41	
	508.2349	<i>K.HEISEMNR.M</i>	41	
	533.7618	<i>K.YEDEINKR.T</i>	57	
	602.3223	<i>K.WTLLQEQGTK.T</i>	46	
	621.7855	<i>R.TEAESWYQTK.L</i>	35	
	632.3512	<i>K.LALDVEIATYR.K</i>	76	
	649.8188	<i>R.TTAENEFVMLK.K + Oxidation (M)</i>	21	
	651.8621	<i>R.SLDLDSIIAEVK.A</i>	64	
	436.8894	<i>K.NKYEDEINKR.T</i>	55	
*S9X688_CAMFR	453.7376	<i>R.FLEQQNK.V</i>	21	462

<b>Keratin 6A-like protein</b>	469.7505 473.2593 503.2372 533.7618 578.2714 398.8752 604.8117 632.3512 651.8621	<i>R.SLYNLGGSK.S</i> <i>R.GRLDSELR.N</i> <i>K.LLEGEECR.L</i> <i>K.YEDEINKR.T</i> <i>R.DYQELMNVK.L + Oxidation (M)</i> <i>K.KYDEINKR.T</i> <i>R.TAAENDFVTLK.K</i> <i>K.LALDVEIATYR.K</i> <i>R.SLDLDSIIAEVK.A</i>	29 41 26 57 22 55 73 76 64	
<b>*S9YD43_CAMFR Complement component 4A-like protein</b>	485.2559 532.7665 557.8146 566.7924 577.8012 633.2790 653.3385 663.8513 670.3705	<i>R.VEYGFQVK.V</i> <i>R.FGLLGEDGEK.T</i> <i>K.VGDTINLNL.R.A</i> <i>K.STGLCVATPAR.V</i> <i>R.QGVNLFSSR.R</i> <i>K.NQDFQQTDR.S</i> <i>R.GSLEFPVGDVASK.V</i> <i>R.FVSSPFLDLSK.T</i> <i>K.LSININDLPGQR.L</i>	31 30 63 84 61 44 42 51 39	443
<b>*S9Y253_CAMFR Kininogen-2 isoform I</b>		<i>R.KALDLINK.G</i> <i>K.ATAQVVAGMK.Y + Oxidation (M)</i> <i>K.ESDCPVLSR.K</i> <i>K.ENSDFFASFR.V</i> <i>K.SGNQFVLYR.V</i> <i>K.LNAENNGNFYFK.I</i> <i>K.DSAQAATGECTVTVAK.R</i> <i>K.CNLYPGEDFVQPPGK.I</i>	31 30 74 52 78 45 48 21	380
<b>*TOMI13_CAMFR Alpha-2-macroglobulin-like protein</b>	401.2163 498.2343 595.3289 654.8455 442.5714 1092.0768 772.3862	<i>R.HVFSPSK.S</i> <i>K.IENCFANK.V</i> <i>K.ELTFYLIK.A</i> <i>R.AFEVNEYVLPK.F</i> <i>K.VTATPHSLCALR.A</i> <i>K.LQGGLNQSFPLSEEPILGR.Y</i> <i>K.SYVHLEPVAGTLACGQTQEV.R.A</i>	41 35 35 50 59 62 91	371
<b>S9XI90_CAMFR Keratin, type II cytoskeletal 75-like isoform</b>	453.7376 503.2372 508.2349 597.7917 604.8117 632.3512 651.8621 436.8894	<i>R.FLEQQNK.V</i> <i>K.LLEGEECR.L</i> <i>R.HEISEMNR.V</i> <i>K.YEELQQTAGR.H</i> <i>R.TAAENEFVSLK.K</i> <i>K.LALDVEIATYR.K</i> <i>R.SLDLDSIIAEVK.A</i> <i>K.VRYDDEINKR.T + Deamidated (R)</i>	21 26 41 68 32 76 64 29	357
<b>S9X494_CAMFR Keratin, type I cytoskeletal 42</b>	404.2031 515.3008 561.7933 651.3333 703.3495 1043.4957	<i>R.LAADDFR.T</i> <i>R.VLDELTLAR.A</i> <i>R.LEQEIATYR.R</i> <i>R.ALEEANADLEVK.I</i> <i>R.EVATNTEALQSSR.T</i> <i>R.GQVGGDVNVEMDAAPGVLSR.I</i>	55 55 45 78 22 32	285
<b>S9XBS9_CAMFR Ig gamma-3 chain C region</b>	433.7584 537.8010 561.2972 511.9165 810.8932 607.3409	<i>K.ALPAPIER.T</i> <i>K.APSVYPLTAR.C</i> <i>K.DTVSVTCLVK.G</i> <i>K.TFICDVAHPASSTK.V</i> <i>K.GFYPPDINVEWQR.N</i> <i>R.VVSVLPIQHQQDWLTGK.E</i>	37 49 30 29 54 64	263
<b>*S9XYY2_CAMFR Hemopexin</b>	482.7420 540.7608 546.7894	<i>K.VDGALCTTK.F</i> <i>K.FLGPNSCSAK.G</i> <i>K.KVDGALCTTK.F</i>	61 50 53	246

	603.8037 620.8141	<i>R.FDPVTGEVQSK.Y</i> <i>K.GGYTLVENYPK.R</i>	45 36	
AOA075T9L1_CAMDR <b>Dipeptidylpeptidase 4</b>	428.7481 458.2740 755.8279 493.9853	<i>K.AGAVNPTVK.F</i> <i>R.ISLQWIR.R</i> <i>K.WEYDYSVYTER.Y</i> <i>R.FRPAEPHFTSDGSSFYK.I</i>	50 36 56 34	174
S9XXW2_CAMFR <b>Fibrinogen beta chain</b>	490.7253 620.2627 646.8159	<i>R.QDGSVDFGR.K</i> <i>K.EDGGGWYNNR.C</i> <i>R.QGFGNIATNADGK.K</i>	68 45 58	172
*S9WDV3_CAMFR <b>Fibrinogen gamma chain isoform gamma-B</b>	597.7473 704.3240 740.6835	<i>R.DNCCILDER.F</i> <i>K.TSTADYSTFSVGPESDKYR.M</i> <i>K.EGFGHLSPTGNTEFWLGNEK.I</i>	70 56 43	169
*AOA1KOGY87_VICPA <b>Globin A1</b>	573.8375 589.3436 664.8632 705.8497	<i>R.LLVVYPWTR.R</i> <i>K.VVAGVANALAHR.Y</i> <i>K.VKVDEVGGEALGR.L</i> <i>K.EFTPDQAAYQK.V</i>	31 52 45 38	166
S9WB99_CAMFR <b>Histone H2B</b>	408.7322 477.3050 888.4086	<i>R.EIQTAVR.L</i> <i>R.LLLPGELAK.H</i> <i>K.AMGIMNSFVNDIFER.I + 2 Oxidation (M)</i>	45 31 69	146
S9XNF8_CAMFR <b>Xaa-Pro dipeptidase</b>	410.2396 557.3425 493.9340	<i>K.STLTVPR.L</i> <i>K.VPLALFALNR.Q</i> <i>R.VFKTDMEEVLVLR.Y</i>	42 45 56	142
*S9YS49_CAMFR <b>Putative E3 ubiquitin-protein ligase Roquin</b>	400.7165 420.2108 496.2475	<i>K.IPEATNR.R</i> <i>K.FDTISEK.T</i> <i>K.LGACDNTLK.Q</i>	42 31 59	132
*S9YGW7_CAMFR <b>Heparin cofactor 2</b>	418.2495 546.7880 727.4034	<i>R.VTIDLFK.H</i> <i>K.DYNLVEALR.S</i> <i>K.ALEAQLTPQVVER.W</i>	30 52 41	123
S9WPM4_CAMFR <b>Adiponectin</b>	478.7579 491.7873 533.7802	<i>K.AVLFTYDK.Y</i> <i>R.STVPNVPIR.F</i> <i>R.SAFSVGLETR.S</i>	32 31 52	115
A2V743_CAMDR <b>Beta actin</b>	566.7665 895.9506 652.0263 796.6590	<i>R.GYSFTTTAER.E</i> <i>K.SYELPDGQVITIGNER.F</i> <i>R.VAPEEHPVLLTEAPLNPK.A</i> <i>R.TTGIVMDSGDGVHTVPIYEGYALPHAILR.L</i>	38 22 22 27	109
*S9XP08_CAMFR <b>Inter-alpha-trypsin inhibitor heavy chain H1</b>	511.7794 540.2900 579.3171	<i>R.LTYEEVLR.R</i> <i>K.LDAQASFLSK.E</i> <i>K.AAISGENAGLVR.A</i>	38 48 23	109
S9XM15_CAMFR <b>Ferritin</b>	472.9072 569.3168	<i>R.ELAEKREGAER.L</i> <i>K.NLNQALLDLHALGSAR.A</i>	37 69	
T0NNK2_CAMFR <b>L-lactate dehydrogenase</b>	624.8058	<i>R.VIGSGCNLDSAR.F</i>	93	93
S9X3E8_CAMFR <b>Ig kappa chain V-II region RPMI 6410-like protein</b>	659.3199	<i>R.FTGSGSGDFTLK.I</i>	90	90
AOA0A0PAR2_CAMDR <b>Heat shock protein 90</b>	408.2604 757.3968	<i>R.ALLFVPR.R</i> <i>R.GVVDESDLPLNISR.E</i>	38 50	88
*S9XYF2_CAMFR <b>Heat shock cognate protein HSP 90-beta-like isoform 3</b>	415.2682 757.3968	<i>R.ALLFIPR.R</i> <i>R.GVVDESDLPLNISR.E</i>	38 50	87
S9XH24_CAMFR <b>Phosphotriesterase-related protein</b>	565.8065	<i>R.VLQEAGADISK.T</i>	83	83

S9XM68_CAMFR <b>Xaa-Pro dipeptidase isoform 3</b>	467.7714 489.2769	K.AIYEAVLR.S R.LADRIHLEELTR.I	33 41	73
S9WT57_CAMFR <b>Tubulin beta chain</b>	527.3079 623.3002	R.YLTVAEIFR.G R.ISEQFTAMFR.R + Oxidation (M)	27 46	73
*S9YV02_CAMFR <b>Non-specific protein-tyrosine kinase</b>	513.3091	K.IGGIGTVPVGR.V	69	69
*S9XC57_CAMFR <b>Plasminogen</b>	631.7936	K.QLGAGSVDECAR.K	63	63
*S9YL21_CAMFR <b>Apolipoprotein A-I</b>	463.2769 633.8224	K.VAPLGAELR.E K.VQPYLEDFQK.K	34 28	62
*S9WKZ8_CAMFR <b>Inter-alpha-trypsin inhibitor heavy chain H4</b>	573.2996	R.GESAGLVQATGR.K	62	62
S9WIA5_CAMFR <b>Glutathione synthetase</b>	436.7454	K.ILSNPNSK.G	61	61
T0MHN9_CAMFR <b>Pyruvate kinase</b>	680.3563	R.NTGIICTIGPASR.S	60	60
*S9Y4U4_CAMFR <b>Complement C1q subcomponent subunit C isoform 2</b>	798.3819	R.VITNPQGDYDTSTGK.F	58	58
S9WAX5_CAMFR <b>Unconventional myosin-Va isoform 2</b>	396.2074 444.2330	R.IIGANMR.T + Deamidated (NQ); Oxidation (M) K.NELNELR.K	29 30	57
S9WVY1_CAMFR <b>Actinin, alpha 1 isoform 6-like protein</b>	715.3859	R.TINEVENQILTR.D	56	56
S9XA40_CAMFR <b>Heat shock cognate protein</b>	627.3116	R.FEELNADLFR.G	55	55
*S9YFM0_CAMFR <b>Keratin, type II cytoskeletal 71</b>	617.8373	R.TAAENEFVLLK.K	52	52
A0A0U2KTX5_CAMDR <b>VHH5 (Fragment)</b>	498.7536	R.FTISTDNAK.N	52	52
S9XR87_CAMFR <b>Ig lambda chain C regions isoform 19-like protein</b>	592.9709	K.QDGTTVTQGVETTKPSK.Q	50	50
S9WGH8_CAMFR <b>Lysozyme</b>	700.8439	R.STDYGIFQINSR.Y	49	49
S9WMX2_CAMFR <b>Dystonin</b>	772.4020 1048.0221	R.ILTGNAVGLRNR.T + 2 Deamidated (NQ) R.VGQSLSLTCSTEQGVLAEK.L + Deamidated (NQ)	30 22	49
*S9X8K9_CAMFR <b>Transaldolase</b>	438.7245	R.VSTEVDAR.L	46	46
*TONM23_CAMFR <b>Rootletin</b>	544.3185 673.3367	K.AGTLQLTVER.L K.RLQEQRDLGR.Q + 2 Deamidated (NQ); 2 Deamidated (R)	26 21	45
S9W6I0_CAMFR <b>Ferritin</b>	438.7629	R.IFLQDIK.Q	45	45
S9WF34_CAMFR <b>Tubulin alpha chain</b>	543.3137	K.EIIDLVLDLDR.I	43	43
*S9YSI7_CAMFR	489.5794	K.TATPQQAQEVHEK.L	43	43

<b>Triosephosphate isomerase</b>				
*S9XSQ6_CAMFR <b>Vitamin D-binding protein-like protein</b>	903.0750	K.HQPQEFTYVEPTNDEICEAFR.K	40	40
*S9YMC0_CAMFR <b>Transcription factor 20 isoform 1</b>	416.2516 516.7796	K.TVGVIVSR.E + Deamidated (R) K.LKMSPGRSR.G + Deamidated (R)	20 20	40
*S9Y636_CAMFR <b>Receptor-type tyrosine-protein phosphatase-like N</b>	402.7397	R.LLQAGFR.E	39	39
*S9X6M4_CAMFR <b>Dyslexia-associated protein</b>	758.3907	K.GVRDSSYSLESSIELLKQDVVQLHAPR.Y + 2 Deamidated (NQ); 2 Deamidated (R)	37	37
T0MH94_CAMFR <b>Rabenosyn-5-like protein</b>	737.3970	R.TDEVRTLQENLR.Q	36	36
S9WJW3_CAMFR <b>N6-adenosine-methyltransferase subunit</b>	508.7724	K.QLDSLRRER.L	35	35
*A8IY99_LAMGU <b>Gamma-fibrinogen</b>	590.9761	K.AIQVSYNPAEPSKPNR.I	35	35
S9WRI7_CAMFR <b>Nuclear receptor coactivator 5 isoform 3-like protein</b>	450.2690	R.RDRSPIR.G	35	35
S9W421_CAMFR <b>Hemoglobin, epsilon 1</b>	664.8442	K.VNVEEAGGEVLGR.L	35	35
*S9W711_CAMFR <b>Charged multivesicular body protein 4c</b>	514.8088	K.RAALQALKR.K + Deamidated (NQ); Deamidated (R)	34	34
*S9X089_CAMFR <b>Ig lambda chain V-III region LOI-like protein</b>	550.3109	K.DSERPSGIPER.F	34	34
S9WUC8_CAMFR <b>Ig kappa chain V-II region RPMI 6410-like protein</b>	550.3109	R.LLIYYASTR.E	32	32
*S9WVI6_CAMFR <b>Complement C1q subcomponent subunit A</b>	667.3889	K.GLFQVVSGGTVLR.L + Deamidated (NQ)	32	32
*S9Y5S1_CAMFR <b>Transcriptional repressor NF-X1</b>	572.8298	K.ISRLDAELVK.Y + Deamidated (R)	32	32
*S9YC53_CAMFR <b>Alpha-1-antitrypsin-like protein</b>	454.2354	R.YPSSANLR.F	32	32
*S9Y3F6_CAMFR <b>Dual specificity testis-specific protein kinase 1</b>	564.8041	R.LPSNRGNTLR.E + Deamidated (R)	31	31
S9WKI8_CAMFR <b>HEAT repeat-containing protein 7B1</b>	421.7685	R.VGTLALIR.A	31	31

*S9WVS9_CAMFR <b>Peroxisome proliferator-activated receptor gamma coactivator-related protein 1</b>	430.2352	K.QAQKNLR.R + 2 Deamidated (NQ)	29	29
*S9XVK5_CAMFR <b>Transthyretin</b>	704.8226	K.AAETWEFASGK.T	29	29
*S9Y967_CAMFR <b>General transcription factor II, i isoform 4 isoform 1-like protein</b>	550.3373	K.INTKALQSPK.R	28	28
*TOMC04_CAMFR <b>Spermatogenesis-associated protein 2-like protein</b>	486.7591	R.QELLSQPR.D + Deamidated (NQ); Deamidated (R)	28	28
*S9YSZ6_CAMFR <b>Centromere protein J</b>	714.9224	K.AENTSLAKLRIGR.E	28	28

1723 †Ions score is  $-10 \cdot \log(P)$ , where P is the probability that the observed match is a random event. Individual ions  
1724 scores > 20 indicated identity or extensive homology ( $p < 0.05$ ). Protein scores were derived from ions scores as  
1725 a non-probabilistic basis for ranking protein hits. Cut-off was set at Ions score 20.  
1726

1727 **Supplementary Table 2. Deiminated proteins, including all peptide sequences, identified by F95 enrichment**  
1728 **and LC-MS/MS in extracellular vesicles isolated from serum of llama (*Lama glama*).** Deiminated proteins were  
1729 isolated by immunoprecipitation using the pan-deimination F95 antibody, the F95 enriched eluate was analysed  
1730 by LC-MS/MS and peak list files were submitted to Mascot. Peptide sequence hits scoring with *L. glama* (LAMGL)  
1731 are presented as well as hits with other camelids (CAMFR=*Camelus ferus*; CAMDR=*Camelus dromedaries*;  
1732 LAMGU=*Lama guanicoe*). Hits with uncharacterised proteins are not listed. Peptide sequences and m/z values  
1733 are listed. An asterisk (\*) indicates that the protein hit is unique for EVs only.

Protein name (*unique for EVs)	m/z	Peptide sequence	Score ( $p < 0.05$ ) <sup>†</sup>	Total score
AOA1W5VKM5_LAMGL <b>Anti-RON nanobody</b>	653.7846	K.SEDTAVYYCAK.D	22	164
	941.5044	-.EVQLVESGGGLVQPGGSLR.L	74	
Q865W8_LAMGL <b>Beta actin</b>	566.7667	R.GYSFTTTAER.E	85	85
	895.9502	K.SYELPDGQVITIGNER.F		
*S9XAP9_CAMFR <b>Keratin, type I cytoskeletal 14-like protein</b>	404.2033	R.LAADDFR.T	55	554
	515.3006	R.VLDELTAR.A	51	
	546.2614	K.VTMQNLNDR.L + Deamidated (NQ)	74	
	553.7849	R.ISSVLAGGSCR.A	54	
	561.7932	R.LEQEIATYR.R	56	
	651.3332	R.ALEEANADLEVK.I	78	
	681.3492	R.EVATNSELVQSGK.T	100	
	685.3798	K.ILTATVDNANIVLQIDNAR.L	41	
	770.3588	R.LLEGEDAHLSSSQFSSGSQSSR.D	46	
*S9X688_CAMFR <b>Keratin 6A-like protein</b>	469.7508	R.SLYNLGGSK.S	37	496
	473.2593	R.GRLDSELR.N	31	
	503.2371	K.LLEGEECR.L	42	
	533.7617	K.YEDEINKR.T	53	
	578.2716	R.DYQELMNVK.L + Oxidation (M)	35	
	398.8752	K.KYEDEINKR.T	61	
	604.8117	R.TAAENDFVTLK.K	79	
	619.7895	R.NMQDLVEDFK.K	21	
	632.3508	K.LALDVEIATYR.K	76	
	651.8625	R.SLDLDSIIAEVK.A	63	

S9Y6J1_CAMFR <b>Keratin, type II cytoskeletal 5 isoform 13-like protein</b>	405.7087 473.2593 533.7617 576.7803 602.3220 619.7895 621.7851 632.3508 651.8625 436.8895	R.QSSVSFR.S R.GRLDSELR.N K.YEDEINKR.T K.NKYEDEINKR.R K.WTLLQEQGTK.T R.NMQDLVEDFK.N R.TEAESWYQTK.L K.LALDVEIATYR.K R.SLDLDSIIAEVK.A K.NKYEDEINKR.T	23 31 53 27 44 21 43 76 63 58	438
S9WI87_CAMFR <b>Serum albumin</b>	449.7441 460.2554 464.2504 554.7310 569.7525 575.3110 721.2823 744.8029 746.3249	R.LCVLHEK.T K.LCTVASLR.E K.YLYEIAR.R K.HVFEECK.D K.CCTESLVNR.R K.LVNEVTEFAK.T K.TCVADESAADCCK.S K.EYEATLECCAK.D K.YFCDNQETISSK.L	27 43 34 46 58 48 79 64 32	430
*S9YN99_CAMFR <b>Keratin, type I cytoskeletal 17-like isoform</b>	404.2033 515.3006 561.7932 651.3332 681.3492 690.0522	R.LAADDFR.T R.VLDELTLAR.A R.LEQEIATYR.R R.ALEEANADLEVK.I R.EVATNSELVQSGK.T K.ILTATVDNANILLQIDNAR.L	55 51 56 78 100 77	417
*S9XI90_CAMFR <b>Keratin, type II cytoskeletal 75-like isoform</b>	503.2371 597.7917 604.8117 632.3508 651.8625 436.8895	K.LLEGEECR.L K.YEELQQTAGR.H R.TAAENEFVSLK.K K.LALDVEIATYR.K R.SLDLDSIIAEVK.A K.VRYDDEINKR.T + Deamidated (R)	42 69 36 76 63 32	318
S9X494_CAMFR <b>Keratin, type I cytoskeletal 42</b>	404.2033 515.3006 561.7932 651.3332 1043.4962	R.LAADDFR.T R.VLDELTLAR.A R.LEQEIATYR.R R.ALEEANADLEVK.I R.GQVGGDVNVEMDAAPGVDSL.R.I	55 51 56 78 28	269
S9XBS9_CAMFR <b>Ig gamma-3 chain C region</b>	433.7584 537.8009 561.2974 607.3406	K.ALPAPIER.T K.APSVYPLTAR.C K.DTVSVTCLVK.G R.VVSVLPIQHQDWLTGK.E	34 50 32 47	162
AOA075T9L1_CAMDR <b>Dipeptidylpeptidase 4</b>	428.7482 458.2738 755.8281	K.AGAVNPTVK.F R.ISLQWIR.R K.WEYYDSVYTER.Y	52 42 59	153
S9X684_CAMFR <b>Keratin, type II cytoskeletal 8</b>	632.3508 672.8415	K.LALDVEIATYR.K R.ASLEAAIADAEQR.G	76 61	136
S9WB99_CAMFR <b>Histone H2B</b>	408.7321 477.3053 888.4087	R.EIQTAVR.L R.LLLPGELAK.H K.AMGIMNSFVNDIFER.I + 2 Oxidation (M)	45 33 55	133
S9YQ51_CAMFR <b>Tubulin beta chain</b>	527.3073 623.3008 546.2816	R.YLTVAAI.FR.G R.ISEQFTAMFR.R + Oxidation (M) R.LHFFMPGFAPLTSR.G + Oxidation (M)	29 62 24	114
*S9WX81_CAMFR <b>Histone 1, H2ai isoform 3-like protein</b>	416.2502 425.7669 472.7691	K.STELLIR.K R.HLQLAIR.N R.AGLQFPVGR.V	34 25 31	89

*S9X8G9_CAMFR <b>Desmoplakin</b>	565.3085 636.3563	K.IEVLEEEELR.L R.QLQNIQATSR.E	56 33	88
A2V743_CAMDR <b>Beta actin</b>	566.7667 895.9502	R.GYSFTTTAER.E K.SYELPDGQVITIGNER.F	48 37	85
A0A0A0PAR2_CAMDR <b>Heat shock protein 90</b>	408.2603 757.3967	R.ALLFVPR.R R.GVVDESDLPLNISR.E	34 51	85
S9XA40_CAMFR <b>Heat shock cognate protein</b>	627.3118	R.FEELNADLFR.G	85	85
T0NNK2_CAMFR <b>L-lactate dehydrogenase</b>	624.8045	R.VIGSGCNLDSAR.F	81	81
S9XNF8_CAMFR <b>Xaa-Pro dipeptidase</b>	410.2398 493.9347	K.STLFVPR.L R.VFKTDMELEVL.R.Y	38 36	74
T0MHN9_CAMFR <b>Pyruvate kinase</b>	680.3557	R.NTGIICTIGPASR.S	71	71
S9WVY1_CAMFR <b>Actinin, alpha 1 isoform 6-like protein</b>	715.3860	R.TINEVENQILTR.D	60	60
*A0A0E3Z5I3_CAMDR <b>Superoxide dismutase</b>	845.1036	K.LTAVSVGVQSGWGWLGFNKEQGR.L	59	59
S9XHZ4_CAMFR <b>Phosphotriesterase-related protein</b>	565.8064	R.VLQEAGADISK.T	57	57
S9W9Y4_CAMFR <b>Ferritin</b>	569.3167	K.NLNQALLDLHALGSAR.A	57	57
S9XR87_CAMFR <b>Ig lambda chain C regions isoform 19-like protein</b>	592.9710	K.QDGTTVTQGVETTKPSK.Q	56	56
S9X3E8_CAMFR <b>Ig kappa chain V-II region RPMI 6410-like protein</b>	659.3194	R.FTGSGSGTDFTLK.I	50	50
S9WAX5_CAMFR <b>Unconventional myosin-Va isoform 2</b>	396.2075 565.3085	R.IIGANMR.T + Deamidated (NQ); Oxidation (M) K.LKNELELNR.K + Deamidated (NQ)	30 22	49
S9WF34_CAMFR <b>Tubulin alpha chain</b>	543.3137	K.EIIDLVLDLDR.I	44	44
*S9W806_CAMFR <b>Filamin-A isoform 1</b>	529.7776 681.3492	K.VAQPAITDNK.D + 2 Deamidated (NQ) K.GEITGEVRMPSGK.V + Deamidated (R)	23 20	43
*S9X6X3_CAMFR <b>Scaffold attachment factor B-like protein</b>	474.2696 543.3296	R.LSKEEKGR.S + Deamidated (R) K.ADTLLAVVKR.E	21 21	42
T0MH94_CAMFR <b>Rabenosyn-5-like protein</b>	737.3968	R.TDEVRTLQENLR.Q	40	40
*S9Y0S0_CAMFR <b>DNA-directed RNA polymerase subunit beta</b>	408.7425	K.TQISLVR.M	39	39
S9WJW3_CAMFR <b>N6-adenosine-methyltransferase subunit</b>	508.7720	K.QLDSLRRER.L	38	38

S9XM68_CAMFR <b>Xaa-Pro dipeptidase isoform 3</b>	467.7713	K.AIYEAVLR.S	38	38
*S9YV02_CAMFR <b>Non-specific protein-tyrosine kinase</b>	513.3086	K.IGGIGTVPVGR.V	38	38
S9WGH8_CAMFR <b>Lysozyme</b>	700.8445	R.STDYGIFQINSR.Y	32	32
S9WRI7_CAMFR <b>Nuclear receptor coactivator 5 isoform 3-like protein</b>	450.2691	R.RDRSPIR.G	32	32
S9W421_CAMFR <b>Hemoglobin, epsilon 1</b>	664.8441	K.VNVEEAGGEVLGR.L	32	32
*S9WI71_CAMFR <b>Metabotropic glutamate receptor 3</b>	552.2800	R.INEDRGIQR.L + 2 Deamidated (NQ); Deamidated (R)	32	32
*S9WB50_CAMFR <b>TSC22 domain family protein 3-like protein</b>	693.8827	R.EEVEILKEQIR.E + Deamidated (R)	31	31
S9WMX2_CAMFR <b>Dystonin</b>	772.4021	R.ILTGENAVGELRNR.T + 2 Deamidated (NQ)	31	31
S9WKI8_CAMFR <b>HEAT repeat-containing protein 7B1</b>	421.7683	R.VGTLALIR.A	31	31
S9WIA5_CAMFR <b>Glutathione synthetase</b>	436.7452	K.ILSNNPSK.G	31	31
*S9XC05_CAMFR <b>Telomere-associated protein RIF1 isoform 1</b>	503.7640	K.SSEKSVRGR.T + Deamidated (R)	31	31
AOAOU2KTX5_CAMDR <b>VHH5</b>	498.7538	R.FTISTDNAK.N	30	30
*TOMGG7_CAMFR <b>Nucleoredoxin</b>	650.3872	K.VVCRNGLLVIR.D + Deamidated (R)	30	30
*S9XET3_CAMFR <b>Rac GTPase-activating protein 1</b>	652.3622	R.VRSTLTRNTPR.R + Deamidated (NQ); 2 Deamidated (R)	30	30
S9XDK9_CAMFR <b>Complement C3-like protein</b>	417.2478	R.LPYSVVR.N	30	30
*S9XMI2_CAMFR <b>Pseudopodium-enriched atypical kinase 1</b>	913.8976	K.ENEPNHESLSGNNQEK.D + Deamidated (NQ)	29	29
*S9Y3S9_CAMFR <b>Core histone macro-H2A.1 isoform 2</b>	493.7978	K.QTAAQLILK.A + Deamidated (NQ)	29	29
S9XXW2_CAMFR <b>Fibrinogen beta chain</b>	490.7250	R.QDGSVDFGR.K	29	29
*S9YGX6_CAMFR <b>PAS domain-containing serine/threonine-protein kinase</b>	746.3763	K.TTEILVANDKACR.L + Deamidated (NQ)	29	29
*TONMU1_CAMFR <b>SH2 domain-containing protein 7</b>	487.7771	R.SKTEQLLR.D	28	28
*TOMIT6_CAMFR	420.2258	R.AHGREIR.K + Deamidated (R)	28	28

<b>Serine-tRNA ligase, mitochondrial</b>				
<b>*S9W449_CAMFR Fc receptor-like protein 5</b>	424.2454	<i>R.ASLEPGGGPR.G</i>	28	28

1734 †Ions score is  $-10 \cdot \log(P)$ , where P is the probability that the observed match is a random event. Individual ions  
1735 scores > 22 indicated identity or extensive homology ( $p < 0.05$ ). Protein scores were derived from ions scores as  
1736 a non-probabilistic basis for ranking protein hits. Cut-off was set at Ions score 20.  
1737